AMERICAN MUSEUM
Novitates

PUBLISHED BY THE AMERICAN MUSEUM OF NATURAL HISTORY
CENTRAL PARK WEST AT 79TH STREET, NEW YORK, NY 10024
Number 3483, 57 pp., 17 figures, 8 tables July 25, 2005

Amphicticeps and *Amphicynodon* (Arctoidea, Carnivora) from Hsanda Gol Formation, Central Mongolia and Phylogeny of Basal Arctoids with Comments on Zoogeography

XIAOMING WANG,[1] MALCOLM C. McKENNA,[2] AND DEMBERELYIN DASHZEVEG[3]

ABSTRACT

Amphicticeps shackelfordi and *Amphicynodon teilhardi* are two small carnivorans from the early Oligocene Hsanda Gol Formation of central Mongolia, and as basal arctoids (infraorder Arctoidea) in Asia, feature unique combinations of morphologies that offer insights into early diversification and zoogeography of the arctoids. Lack of adequate study of *Amphicticeps* and incomplete knowledge about *Amphicynodon*, however, prevented them from being figured in the discussions of arctoid relationships. New associated dental and cranial materials collected during recent expeditions in the 1990s substantially enrich our knowledge of the two genera and their stratigraphic positions, and serve as an impetus for a study of their phylogenetic relationships in the broad perspective of basal Arctoidea.

Hsanda Gol arctoids are represented by six small- to medium-sized species: *Amphicticeps shackelfordi* Matthew and Granger 1924, *A. dorog*, n.sp., *A. makhchinus*, n.sp., *Amphicynodon teilhardi* Matthew and Granger 1924,? *Cephalogale* sp., and *Pyctis inamatus* Babbitt, 1999. The three species of *Amphicticeps* apparently form an endemic clade confined to central Asia, whose zoogeographic origin is currently unknown. *Amphicynodon* has a much higher diversity in Europe than in Asia, and phylogenetically the Asian *A. teilhardi* seems to be nested within

[1] Division of Paleontology, American Museum of Natural History; Department of Vertebrate Paleontology, Natural History Museum of Los Angeles County, 900 Exposition Blvd., Los Angeles, California 90007; Institute of Vertebrate Paleontology and Paleoanthropology, Chinese Academy of Sciences (xwang@nhm.org).
[2] Division of Paleontology, American Museum of Natural History (m4pmck@indra.com).
[3] Geological Institute, Mongolian Academy of Sciences, Ulaanbaatar, Mongolia.

 ISSN 0003-0082

the European congeneric species, indicating an eastward dispersal for this group, linking the European ''Grande Coupure'' and the Asian ''Mongolian Reconstruction'' events.

To avoid excessive homoplasies in crown groups, we attempted a phylogenetic reconstruction based mostly on stem arctoids. Twenty genera of primitive arctoids occupying basal positions of nearly all major clades are selected for the analysis. The resulting tree, based on 39 characters, approximates the initial divergence of the arctoids. The traditionally dichotomous Arctoidea, formed by sister clades Ursida and Mustelida, is recovered in our analysis. Mustelida is also largely dichotomous with mustelid-like forms on one side and procyonid-like forms on the other. Despite its rather hypercarnivorous dentition, *Amphicticeps* is found on the Ursida side of the arctoids, although support for such a topology is relatively weak. *Amphicynodon* is a stem taxon of the Ursida and is a sister to an ursid–pinniped clade.

INTRODUCTION

Among the intriguing discoveries made during the Central Asiatic Expeditions by the American Museum of Natural History in the 1920s were several small carnivorans found in the rich deposits of Shand Gol (preferred spelling over ''Hsanda Gol'' of most previous literature) and Tatal Gol in the Mongolian People's Republic. The initial discovery of fossiliferous localities near Shand Gol (fig. 1) in 1922 led to a number of preliminary reports about a fauna that was almost entirely new to science (see Mellett, 1968, for a summary). *Amphicticeps shackelfordi* Matthew and Granger 1924, a small badger-sized carnivoran, was briefly reported as such and became part of a diverse Shand Gol ''fauna'' that serves as a regional standard in the mid-Tertiary of continental east Asia (Russell and Zhai, 1987, and references within).

At the time of its formal announcement, the holotype of *Amphicticeps shackelfordi* was the only specimen figured and briefly described, and was represented by a nearly complete skull (Matthew and Granger, 1924). It stood out as one of the best specimens among half a dozen small carnivorans initially reported from the Shand Gol and Tatal Gol localities. Although several mandibles of *Amphicticeps*-sized individuals were collected during the 1922 field season (additional materials were also collected in 1925), Matthew and Granger did not list the isolated jaw fragments, mentioning only the morphology of the lower carnassials, presumably partly because of a lack of a secure association of these mandibles with the holotype skull.

This lack of association is now remedied, more than half a century later, by naturally associated upper and lower jaws of *Amphicticeps shackelfordi* found by the Mongolian Academy of Sciences and the American Museum of Natural History joint expeditions (MAE) during the 1994 field season. The new MAE materials collected throughout the 1990s complement in important ways the original holotype skull by filling in gaps in our knowledge of the upper and lower teeth missing in the holotype, furnish additional materials that indicate the existence of two more species, and help to resolve some long-standing problems that have plagued paleontologists for many years.

Also among the newly collected materials are important additions to *Amphicynodon teilhardi* Matthew and Granger 1924, another basal arctoid that has a phylogenetic affinity with some congeneric species from European early Oligocene fissure fills in the Quercy region of France. *A. teilhardi* was originally based on a lower jaw fragment with m1–2, and our new materials combine to include much of the skull and lower jaw. With such improved knowledge about the anatomy of *Amphicticeps* and *Amphicynodon*, along with better documentation of the locality and stratigraphic data by the MAE field parties, a substantial contribution is now possible to resolve some long-standing systematic issues.

Matthew and Granger (1924: 4) considered *Amphicticeps* so out of place in the then existing understanding of primitive carnivorans that they originally regarded it as ''a highly progressive miacid'' rather than belonging to any existing family of carnivorans. Its puzzling array of mixed dental and basicranial morphology seems to suggest to recent authors (Schmidt-Kittler, 1981; Wolsan, 1993; Hunt, 1996b; Wang and Qiu, 2003a) a relationship of either musteloids or ursoids, two major clades of carnivorans that

Fig. 1. Map of early Oligocene localities (solid circles) of basal arctoids in Mongolian People's Republic and People's Republic of China. Map locations of fossil localities are based on Russell and Zhai (1987). *Amphicticeps* and *Amphicynodon* were reported from the Khatan-Khayrkhan locality in the Altai region of western Mongolia (Russell and Zhai, 1987: 324). However, no description of the materials was given and their occurrence in this locality needs to be confirmed.

include all living families of Arctoidea (Ursidae, Procyonidae, Mustelidae, Ailuridae, plus the Phocoidea [= Pinnipedia] clade). With its occurrence in the early Oligocene, a critical period of time when some European basal arctoids began to make their first appearance, *Amphicticeps* seems to have fallen somewhere in the initial diversification of the arctoids and is thus relevant in discussions of higher level relationships of the Arctoidea.

However, despite an exceptionally preserved holotype skull, *Amphicticeps* has not received more than a cursory mention or a few speculative remarks. A detailed description of its basicranial morphology, a region that features key anatomical innovations in various families of the Arctoidea (e.g., Hunt, 1974, 1977; Schmidt-Kittler, 1981; Cirot and Bonis, 1993; Wolsan, 1993; Wang, 1997), is still not available. With the new materials and revised stratigraphic framework in hand, the time has come to address the various issues outlined above. We aim to accomplish the following three objectives in this contribution: (1) to restudy the holotypes and to describe new materials of *Amphicticeps shackelfordi* and *Amphicynodon teilhardi*; (2) to place on record two new species of *Amphicticeps* from the Hsanda Gol Formation, as well as more fragmentary materials

of uncertain taxonomy; and (3) to conduct a phylogenetic analysis of the arctoids from Hsanda Gol Formation in relation to major clades of Arctoidea.

Institutional Abbreviations

AMNH	Department of Vertebrate Paleontology, American Museum of Natural History, New York
BSP	Bayerische Staatssammlung für Paläontologie und historische Geologie, Munich
F:AM	Frick Collection, Department of Vertebrate Paleontology, American Museum of Natural History, New York
FSP	Collections of Faculté des Sciences, Laboratoire de Géobiologie, Biochronologie et Paléontologie Humaine de l'Université du Poitiers, Poitiers
IVPP	Institute of Vertebrate Paleontology and Paleoanthropology, Chinese Academy of Sciences, Beijing
MAE	Collections of the joint Mongolian Academy of Sciences–American Museum of Natural History Paleontological Expeditions, currently housed in the American Museum of Natural History, New York
MM	Muséum d'Histoire naturelle de Montauban, Montauban
MNHN	Institut de Paléontologie, Muséum National d'Histoire Naturelle, Paris
NMB	Naturhistorisches Museum Basel, Basel
PIN	Institute of Paleontology, Russian Academy of Sciences, Moscow
PST	Paleontology–Stratigraphy Section of Mongolian Academy of Science, Ulaanbaatar
UCMP	University of California Museum of Paleontology, Berkeley
YPM-PU	Princeton University Collection of Peabody Museum of Natural History, Yale University, New Haven
ZPAL	Institute of Paleobiology, Polish Academy of Sciences, Warsaw

MATERIALS AND METHODS

Hsanda Gol materials collected during the American Museum Central Asiatic Expedition in the 1922 and 1925 seasons form an important basis of the present study. The Soviet Academy of Sciences 1946–1949 Expeditions obtained a significant collection of small carnivorans, particularly *Amphicynodon* (Janovskaja, 1970), housed in the PIN. Although we did not have full access to the PIN materials, casts of key specimens are available to us. The Polish–Mongolian Paleontological Expeditions in the 1960s also amassed a collection in Warsaw. Carnivores from the ZPAL collection were described by Lange-Badré and Dashzeveg (1989: 141), and only a few jaw fragments were relevant in the present study. New materials collected by the Mongolian Academy of Sciences and the American Museum of Natural History joint expeditions (MAE) add substantially to various anatomic components to be described below, and also furnish a modern stratigraphic context. In 1995–1997, a joint Austrian–Mongolian team also made a collection in the nearby Taatsiin (Tats) Gol area, particularly by screen washing for small mammals (Daxner-Höck et al., 1997; Daxner-Höck, 2000, 2001; Erbajeva and Daxner-Höck, 2001; Daxner-Höck and Wu, 2003) but large mammals were also collected (Vislobokova and Daxner-Höck, 2002). The carnivore materials are currently being studied by Nagel and Morlo (2001, 2003), who have kindly supplied us with two casts. Various groups of mammals from the new MAE collection are under study by specialists, a few of which have been published (Bryant and McKenna, 1995; Kellner and McKenna, 1996; Babbitt, 1999; Wang, 2001; Geisler, 2004).

The following specimens of North American primitive musteloids, referred to as Oligobuninae (Baskin, 1998a), are examined in this study: *Oligobunis crassivultus*: AMNH 6903, 6906, Turtle Cove Member of John Day Formation, early Arikareean; *Promartes* cf. *olcotti*: F:AM 27584, 27587, 27589, Marsland Formation, early Hemingfordian; *Zodiolestes daimonelixensis*: F:AM 27598, 27599, 27600, Harrison Formation, late Arikareean; *Megalictis ferox*: F:AM 25430, Marsland Formation, early Hemingfordian; AMNH 12880, upper part of Rosebud Formation, late Arikareean.

For European primitive musteloids, Wolsan's (1993) character matrix forms the principal database for comparison. Where possible, his observations are checked against casts or actual specimens of the following taxa available in the AMNH collection and elsewhere: *Simocyon primigenius*: IVPP V12162; *Pseudobassaris riggsi*: YPM-PU

11455; *Mustelavus priscus*: AMNH 129168, YPM-PU 13775; *Broiliana nobilis*: BSP 1937 II 13524 (cast); *Stromeriella franconica*: BSP 1937 II 13533 (cast); *Potamotherium valletoni*: AMNH 11003, AMNH 22520, and uncataloged basicranial materials from NMB. For most of the skull and dental characters, Wolsan's observations can also be verified by published descriptions: *Simocyon primigenius* in Beaumont (1964) and personal observations; *Angustictis* (*Plesictis mayri*) in Dehm (1950); *Bavarictis gaimersheimensis* in Mödden (1991); *Franconictis* (*Plesictis humilidens*) in Dehm (1950); *Mustelictis piveteaui* in Lange-Badré (1970); *Mustelictis olivieri* in Bonis (1997); *Plesictis genettoides* in Helbing (1930) and Dehm (1950); *Paragale huerzeleri* in Petter (1967); *Plesiogale angustifrons* in de Beaumont (1968b) and Helbing (1930). Basicranial morphologies of some of these musteloids are gleaned from works by de Beaumont (1968a), Schmidt-Kittler (1981), Cirot and de Bonis (1993), and Wolsan (1993), as well as from direct observations of the above specimens in the AMNH. A recent acquisition of a nearly complete skull of *Mustelavus* in the AMNH (still undescribed), complemented by earlier descriptions of its holotype (Scott and Jepsen, 1936; Clark, 1937), permits the inclusion of this primitive, presumably very basal musteloid in our analysis. A basal leptarctine mustelid, *Kinometaxia*, was recently found in the early Miocene Tabenbuluk area (Wang and Qiu, 2003b; Wang et al., 2004) and its inclusion in this analysis permits a better sense of the Mustelinae clade.

Relationships of basal ursoids have not been worked out in detail. We use *Cephalogale* as a basal form of the Ursidae (e.g., Beaumont, 1965; Ginsburg and Morales, 1995; Hunt, 1998c), and we examined the primitive species *C. minor* based on the recent FSP collection from the Pech du Fraysse locality of the Quercy district in late Oligocene (Paleogene biochronological level MP 28). A loosely defined Amphicynodontidae has been in circulation as a primitive group of ursoids that may have given rise to pinnipeds (Tedford et al., 1994; Baskin and Tedford, 1996; Hunt, 1996b, 1998c; Wang and Qiu, 2003a), and it generally includes *Amphicynodon*, *Pachycynodon*, and *Allocyon*. We rely on Cirot (1992) for a recent synthesis on *Amphicynodon*, supplemented by our own personal observations of the new FSP collection of specimens of this genus, particularly the well-preserved cranial and dental materials (FSP ITD 876, 312, 60, 569, 356) of *A. leptorhynchus* from Itardies, as well as our own casts of some critical specimens. We were able to study a nearly complete skull of *Pachycynodon boriei* in the FSP (uncataloged) collection and a right jaw (NMB QB 357). We also have access to casts of two mandibles of *P. filholi* (NMB QB 268 and 451). We examined UCMP 24106, holotype and only specimen of *Allocyon loganensis*.

STRATIGRAPHIC FRAMEWORKS

Little distinction was made in the stratigraphic relationships of the historical AMNH localities when the geology was being worked out by C. P. Berkey and colleagues. Nor was this a major concern at a time when the primary objective was to secure the best possible mammalian fossil collections. The concept of the Hsanda Gol Formation was originally proposed by Berkey and Granger (1923; more elaborated in Berkey and Morris, 1927) to encompass strata with Oligocene fossil mammals, but also included rocks as old as Cretaceous due to erroneous extrapolations of field geology. The Hsanda Gol Formation is now known to overlie the Eocene Kholobolchi and Elegen formations (Tsagaan Ovoo Formation of Höck et al., 1999) and underlie the Oligocene/Miocene Loh Formation (McKenna, 1995; Höck et al., 1999).

A complete revision of the biostratigraphy and chronology of the Shand Gol and Tatal Gol areas is underway (McKenna, 1995; McKenna et al., MS). Relocation of classic localities and improvements in the documentations of new collections help to establish a new stratigraphic framework. The importance of this contextual information becomes more apparent in light of revelations that more than one fossil-bearing horizon can be recognized (see also Höck et al., 1999), in contrast to the traditional practice of lumping all specimens from near Shand Gol and Tatal Gol as representing a single assemblage (Mellett, 1968).

Within the newly defined Hsanda Gol Formation, the reddish brown mudstones are di-

vided by a prominent basaltic lava into lithologically recognizable upper and lower parts. The lower Tatal Member includes sediments below the lava whereas the upper Shand Member includes strata above it (Dashzeveg, 1996). Faunally, two units can be differentiated, in contrast to the traditional assumption of a single faunal assemblage in the Hsanda Gol Formation, but the two faunal units do not exactly correspond to the two lithological members separated by the lava. Fossils from beneath the lava and those a few meters above it belong to the Ulaan Khongil fauna characterized by rodents such as *Cricetops dormitor*, *Karakoromys*, and *Selenomys*, whereas above it is the Zavlia fauna, which is characterized by *Yindirtemys* and *Tachyoryctoides* (McKenna, 1995). This scheme roughly corresponds to the rodent Biozones A and B of Höck et al. (1999: fig. 22), although their Biozone B extends to the top of the lava and their Hsanda Gol/Loh formation boundary is postulated to be time transgressive.

Absolute age for the lower of the two Hsanda Gol faunal levels is constrained by radioisotopic dates of the basaltic lava within the Hsanda Gol Formation. The lava yielded a whole-rock potassium–argon date of 31.2–32.0 Ma (Evernden et al., 1964: 193), which after correction (see Dalrymple, 1979), would be 32.0–32.8 Ma. Slightly younger dates of 28 ± 1.1 and 30 ± 1.1 Ma have been obtained by Gabuniya and Rubinshtein (1975). Most recently, Höck et al. (1999) obtained an $^{40}Ar/^{39}Ar$ age of around 31.5 Ma (with a range of 30.4–32.1 Ma) for their Basalt I within the Hsanda Gol Formation, and around 28 Ma (with a range of 27–29 Ma) for their Basalt II near the bottom of the overlying Loh Formation.

Following a recent shift of the terrestrial Eocene-Oligocene boundary in North America (Swisher and Prothero, 1990; Prothero and Swisher, 1992) and elsewhere in the world, Ducrocq's (1993) analysis of Paleogene Asian faunal turnover and Hunt and Tedford's (1993) study of fossil carnivorans suggest that the composite Hsanda Gol faunas correspond to the Early Oligocene instead of Middle Oligocene as traditionally recognized (e.g., Mellett, 1968; Kowalski, 1974; Li and Ting, 1983; Russell and Zhai, 1987; Lange-Badré and Dashzeveg, 1989; Wang, 1992). A broader faunal analysis by Meng and McKenna (1998) further proposed the existence of a ''Mongolian Remodeling'' corresponding to the European ''Grande Coupure'', although whether this is linked to climatic change is still being debated (e.g., Tsubamoto et al., 2004). Such a downwardly shifted chronological framework is consistent with the above radiometric dates and with the new North American Eocene–Oligocene boundary between the Chadronian and Orellan. The Orellan land mammal age was correlated by Mellett (1968) to the composite fauna collected from the Hsanda Gol Formation. In terms of the European continental stratigraphic framework, small carnivorans from the Hsanda Gol Formation, such as *Amphicynodon*, *Palaeogale*, *Stenoplesictis*, and so forth, are comparable to those in the early part of the Rupelian after the Grande Coupure event in MP21 (Schmidt-Kittler, 1989; Berggren et al., 1992; Lévêque, 1993).

The name Shand Gol is the preferred spelling over ''Hsanda Gol'' in much of the previous literature for a geographic feature. In the text below, we use Hsanda Gol Formation for formal reference to an established geologic unit, but use Shand Gol to refer to the geographic area in the vicinity of the Shand Gol drainage. Our usage of the Hsanda Gol area or Hsanda Gol carnivorans refers to the larger area that includes Shand Gol and Tatal Gol, as well as other localities in the Hsanda Gol Formation.

SYSTEMATIC PALEONTOLOGY

ORDER CARNIVORA BOWDICH, 1821

SUBORDER CANIFORMIA KRETZOI, 1943

INFRAORDER ARCTOIDEA FLOWER, 1869

PARVORDER URSIDA TEDFORD, 1976

SUPERFAMILY URSOIDEA FISCHER DE WALDHEIM, 1817

Amphicticeps Matthew and Granger, 1924

TYPE SPECIES: *Amphicticeps shackelfordi* Matthew and Granger, 1924.

INCLUDED SPECIES: *Amphicticeps shackelfordi* Matthew and Granger 1924, *A. dorog*, n.sp., and *A. makhchinus*, n.sp.

EMENDED DIAGNOSIS: *Amphicticeps* possesses the following derived characters that distinguish it from basal ursoids and musteloids such as *Amphicynodon*, *Pachycynodon*, *Cephalogale*, *Mustelavus*, *Amphictis*, *Bavarictis*, *Pseudobassaris*, *Mustelictis*, and *Broiliana*: broad and short rostrum, short infraorbital canal, enlarged M1 parastyle, small angle between labial borders of P4 and M1, reduced and lingually positioned M2, reduced m2, and extremely reduced or lost m3. It is primitive compared to *Kinometaxia*, *Paragale*, *Plesiogale*, and other mustelids in its possession of a carnassial notch on P4 and a shallow suprameatal fossa. In contrast to the North American oligobunines, *Amphicticeps* possesses a postprotocrista on the M1, lacks of a lingual notch on the m1 entoconid crest, and has reduced M2 and m2.

DISTRIBUTION AND AGE: Hsanda Gol Formation, Tsagan Nor Basin, eastern Valley of Lakes, central Mongolian People's Republic. Early Oligocene (see more comments in Geology and Age under *Amphicticeps shackelfordi*).

COMMENTS: Ever since its original description, *Amphicticeps shackelfordi* has remained something of an enigma in its phylogenetic relationships. Offering no formal classification, Matthew and Granger (1924: 4) initially remarked that ''it has the sharply reduced post-carnassial dentition of [stenoplesictoids] with the short, heavy precarnassial dentition of [cynodontoids]. It is not close to any one genus with which I [*sic*] have made comparisons and might be regarded as a highly progressive miacid rather than as a member of any of the existing families of fissiped Carnivora.'' Subsequent classifications also reflect this ambiguity; Simpson (1945: 110 and 115) listed it under both ''?Amphicynodontinae *incertae sedis*'' and ''?Stenoplesictinae *incertae sedis*'', whereas Piveteau (1961: 721) considered it as *incertae sedis* but compared it to *Cynodon* (= *Amphicynodon*). Without suggesting a taxonomic position for the genus, Bonis (1971) commented on its ''parallel'' resemblance to *Harpagophagus*, a genus based on a single left M1 and thought to be an amphicyonid.

In the first substantial discussion of *Amphicticeps* since its original description, Schmidt-Kittler (1981) pointed out the fundamentally arctoid basicranium of *Amphicticeps* and its musteloid-like molar reduction (transversely elongated M1) and short rostrum. However, he did not consider it a musteloid because of its shallow suprameatal fossa, a character especially emphasized in his analysis of musteloid phylogeny. The form of its M1 seemed to him to be another obstacle to recognizing it as a musteloid. Specifically, he regarded the somewhat swollen buccal border and a ''knoblike'' (*höckerartige*) lingual cingulum of the M1 as atypical of a musteloid. He therefore regarded *Amphicticeps* as a ''basal arctoid'' prior to the emergence of the musteloid clade. Wolsan (1993) compared its lingually located M2 with those of *Potamotherium*, but did not draw definite conclusions. Hunt (1996b, 1998c) suggested that *Amphicticeps* may be an amphicynodontid possibly ancestral to the North American *Allocyon* and *Kolponomos*, a suggestion that was followed by Wang and Qiu (2003a).

Among the small carnivorans from the Hsanda Gol Formation, *Amphicynodon teilhardi* (Matthew and Granger, 1924), founded on a few jaw fragments (see description below), is the only similar-sized arctoid that may potentially be confused with *Amphicticeps* (other Hsanda Gol carnivorans, such as *Stenoplesictis*, *Palaeogale*, and *Viverravus*, are easily distinguished on the basis of their far more trenchant carnassials that are typical of feliforms; Hunt, 1998b). With the benefit of the more complete materials for both *Amphicticeps* and *Amphicynodon*, these two primitive Shand Gol arctoids are contrasted in table 1 to facilitate identification.

Amphicticeps shackelfordi Matthew and Granger, 1924

Figures 2–7; Tables 2–4

HOLOTYPE: AMNH 19010, nearly complete skull with left and right P1–2, P4–M1, and alveoli of left and right C1, P3, and M2 (Matthew and Granger, 1924: figs. 4–5).

TYPE LOCALITY: Originally designated as from ''Hsanda Gol formation, Loh'' (Matthew and Granger, 1924: 4), AMNH 19010 (field no. 89) was collected from about 2 mi southwest of the Loh campsite, in Tsagan Nor Basin, eastern Valley of Lakes, Obor-

TABLE 1
Contrast of Two Genera of Small Primitive Arctoids in the Hsanda Gol Formation

	Amphicynodon	*Amphicticeps*
Rostrum	not shortened	shortened
Rostrum	narrow	broad
Distance from postorbital processes to postorbital constriction	short	long
C1	slender	long
M1 parastyle	reduced	robust
M2	labially positioned	enlarged
Lower premolars	slender	lingually positioned
m1 hypoconid	low crowned	high crowned
m1 talonid basin	crenulated	not crenulated
m2 protoconid/metaconid	widely separated	closely spaced
m3	always present	vestigial/absent

Khangay Province, in north-central Mongolia.

REFERRED SPECIMENS: AMNH 19017, partial left ramus with p2–m1 and alveoli of c1–p1 and m2, field no. 69, from Loh; AMNH 19127, partial right ramus with p3, m1, and alveoli of c1–p2, p4, and m2, field no. 84, from Loh; AMNH 19128, right ramal fragment with m1 and alveoli of c1–p4 and m2, field no. 92, from 2 mi southwest of Loh; AMNH 21695, left ramal fragment with m1 and alveoli of c1–p4, field no. 536, from 2 mi west of the ''Grand Canyon'' area, which is 10 mi west of Loh; AMNH 83610, left ramal fragment with p4–m2 and m3 alveolus, field no. 531, ''Grand Canyon''; AMNH 81336, left ramal fragment with m2 and m3 alveolus; AMNH 85749, right ramal fragment with m2–3, field no. 548; MAE BU.91.9187–90 (AMNH cast 129686), partial rostrum with right alveoli of C1–P2, right P3–M2, and left P3–M1, partial mandible with left p2, p4–m2, and alveoli of c1–p1 and p3, and right p1–m2 and root of m3, collected by Perlé Altangerel in 1994, field no. M-152, from 2 mi southwest of Loh; MAE SG.95.7518, right ramal fragment with p2, p4, and m1 (broken); MAE SG.95.8919, posterior skull fragments with top of the inion and left basicranial region, 45°17′49″N 101°37′13″E, collected by Khosbayar on 10 August 1995; and MAE M-217, isolated left m1, field no. M-217, from 2 mi southwest of Loh.

DISTRIBUTION: Early Oligocene of north-central Mongolia. An undescribed record was mentioned in the early Oligocene Khatan-Khayrkhan locality of Altai Province of Mongolia by Russell and Zhai (1987: 324).

GEOLOGY AND AGE: The above referred specimens of *Amphicticeps shackelfordi* come from three localities (some specimens lack a detailed locality record): (1) general vicinity of Loh for AMNH 19017 and 19127; (2) 2 mi southwest of Loh for AMNH 19010, AMNH 19128, MAE BU.91.9187–90, and MAE M-217; (3) general vicinity or 2 mi west of the Ulaan Khongil (''Grand Canyon'' or Tatal Gol) for AMNH 21695 and 83610.

While field studies are currently pursued by the on-going joint expeditions of the MAE and formal stratigraphic revisions will have to wait for that result (see Höck et al., 1999, for a recent summary), it is relevant to note here that the above three *Amphicticeps*-producing localities fall within a more restricted concept of the Hsanda Gol Formation close to the level of a discontinuous but approximately contemporary basaltic lava (Basalt I of Höck et al., 1999).

Historic collections are largely concentrated in the Ulaan Khongil fauna in the lower part of the Hsanda Gol Formation below the prominent basaltic lava and immediately above. *Amphicticeps* specimens from near the Loh campsite and 2 mi southwest of Loh (including the holotype) are darkly stained due to the percolation of ground water, and they all belong to the Ulaan Khongil fauna. AMNH 21695 and 83610 from near the ''Grand Canyon'' area, on the other hand, are light-colored and may belong to the Zavlia

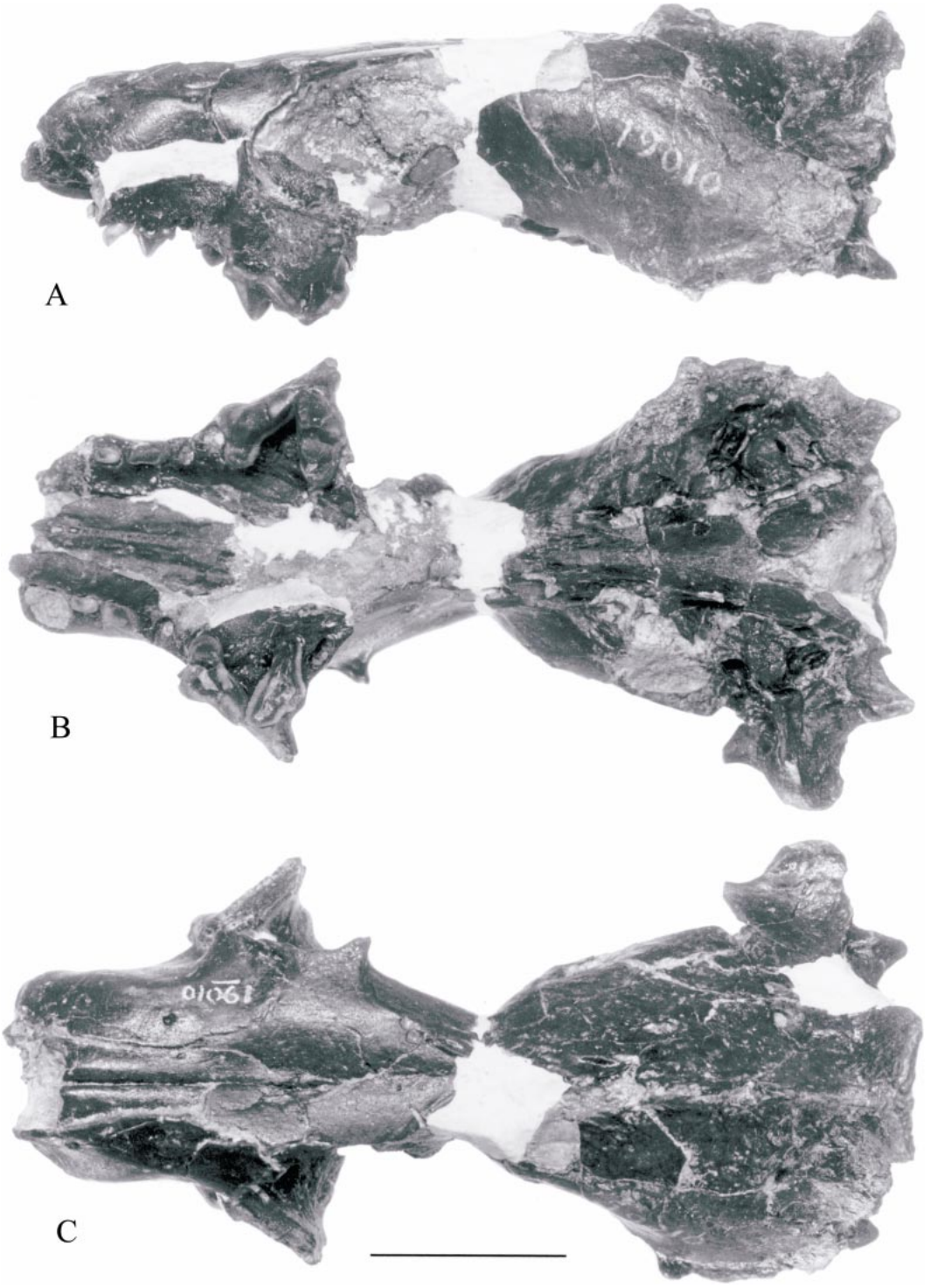

Fig. 2. Skull of *Amphicticeps shackelfordi*, AMNH 19010, holotype. **A,** lateral, **B,** ventral, and **C,** dorsal views. Scale = 20 mm.

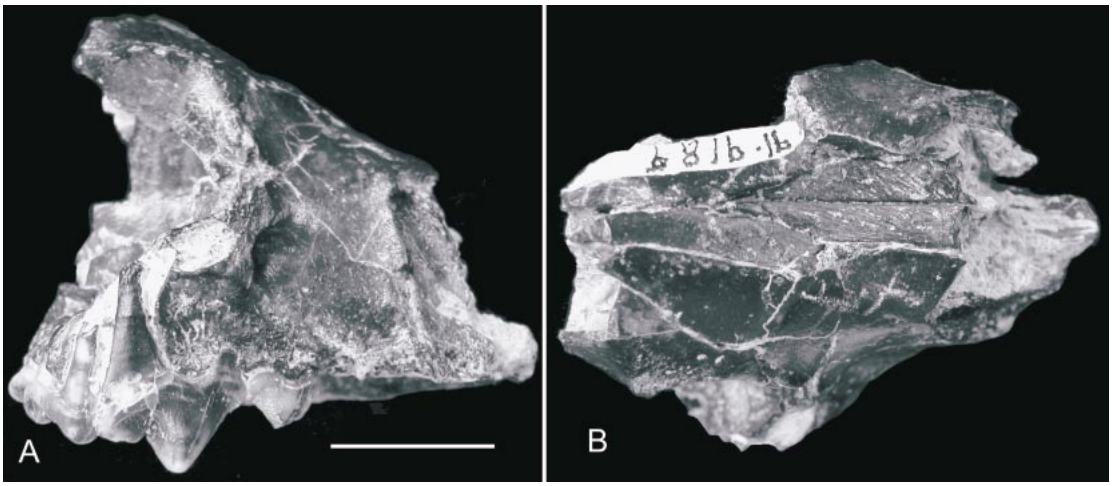

Fig. 3. Partial skull of *Amphicticeps shackelfordi*, referred specimen, MAE BU.91.9187–90. **A,** lateral and **B,** dorsal views. Scale = 10 mm.

fauna in the upper part of the Hsanda Gol Formation above the lava. This presumed younger age of AMNH 21695 and 83610 relative to the rest of the *A. shackelfordi* hypodigm is also consistent with the former's wider m1 and more prominent lingual cingulum on the m1 trigonid, tendencies that indicate a slightly more advanced stage of evolution for the species.

EMENDED DIAGNOSIS: *Amphicticeps shackelfordi* is distinguishable from the more derived *A. makhchinus* and *A. dorog* by its smaller size, smaller angle between the labial borders of P4 and M1, more enlarged M1 parastyle, larger M1 metaconule, more reduced anterior cingulum of M1, and more lingually located M2. In addition, the P4 protocone of *A. shackelfordi* is larger than in *A. dorog*, but is less well developed than in *A. makhchinus*.

DESCRIPTION: Matthew and Granger's (1924) original report of *Amphicticeps shackelfordi* consisted of a brief diagnosis only. A full description is furnished here for the holotype and the newly referred materials.

Skull (figs. 2–4): The holotype, AMNH 19010, is still the only nearly complete skull available, although additional referred cranial fragments supplement the holotype in a number of important ways. Its rostral part is slightly crushed, such that the left cheek region is uplifted by approximately 3 mm. The reconstructed skull illustrated by Matthew and Granger (1924: fig. 5) is mostly accurate in overall proportions except for a more posteriorly displaced mastoid process (relative to the nuchal crest) in the dorsal view.

For a small carnivoran, the skull is rather strongly built, with a short and broad rostrum. The incisor-bearing part of the premaxillary is broken off and only the posterior processes of the premaxillary between the nasal and maxillary are preserved; they extend slightly behind the level of the P2. The posterior tip of the nasal reaches nearly to the level of the postorbital process of the frontal. In keeping with the broad snout, the frontal shield is also wide, that is, there is a long distance between upper rims of the orbits. There is a small fossa above the antorbital rim on the frontal/maxillary suture, for the insertion of the levator nasolabialis, and this fossa is more prominent on the right side of the holotype. The postorbital process of the frontal is small but rather sharply pointed; that on MAE BU.91.9187–90 is more reduced. The distance between the postorbital constriction and the postorbital process is relatively elongated (the postorbital constriction is disjointed in the type but enough is preserved on the right side to indicate this elongation), and is approximately 12 mm, as is also seen in *Potamotherium* and *Paragale*. The temporal crests merge into the sagittal crest slightly behind the postorbital constriction. The braincase is not laterally expanded

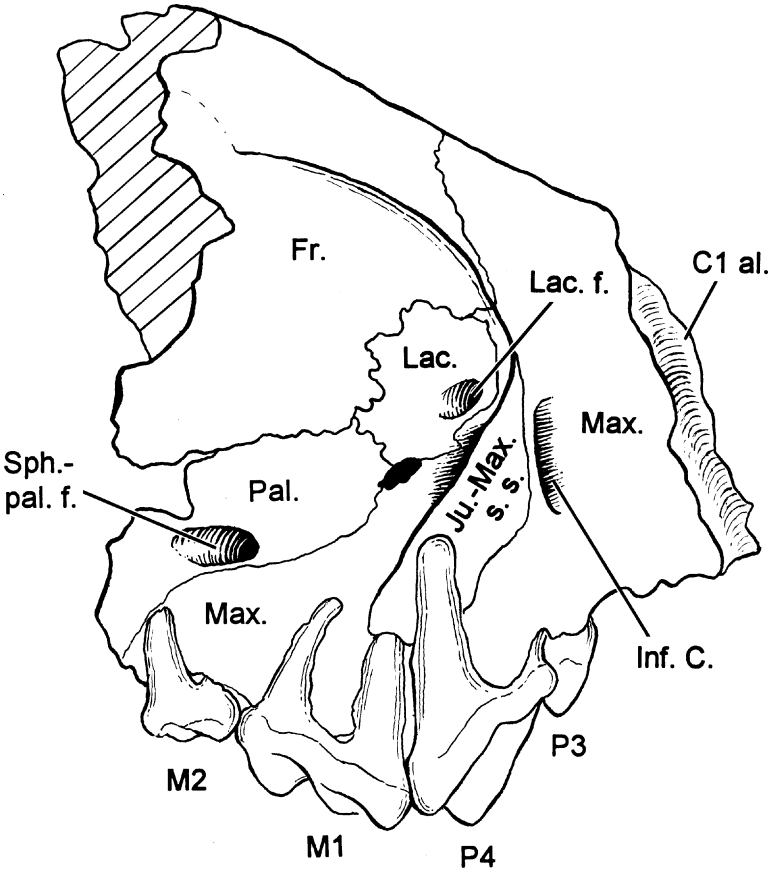

Fig. 4. Posterolateral view of the orbital region of *Amphicticeps shackelfordi*, MAE BU.91.9187–90, referred specimen. C1 al., partial alveolus of upper canine; Fr., frontal; Inf. C., infraorbital canal; Ju.-Max. s. s., jugal-maxillary suture surface; Lac., lacrimal; Lac. f., lacrimal foramen; Max., maxillary; Pal., palatine; Sph.-pal. f., sphenopalatine foramen.

near the postorbital constriction as in *Potamotherium* or nearly becoming so in *Paragale*. Although not very high, the sagittal crest is thick and robust; so is the nuchal crest. The temporal region of the skull has a rugose surface texture. In lateral view, the skull is somewhat shallow and has a rather flat forehead.

The anterior half of the right orbital region is well preserved on MAE BU.91.9187–90 (fig. 4). The infraorbital canal is short, about 3 mm long, and has a round cross section. Immediately above the canal is a small, rounded lacrimal bone forming the inner rim of the antorbital rim. The lacrimal foramen on the lacrimal bone opens posterodorsally. About 1 mm into the orifice for the lacrimal sac, there is a small foramen on the ventral floor that opens into the dorsal wall of the infraorbital canal. A slender process of the palatine meets the lacrimal and excludes orbital contact of the frontal with the maxillary. At the palatine–maxillary–lacrimal junction, there is a small, oval fenestra, probably due to lack of ossification at this stage of the ontogeny, although a fossa for inferior oblique muscle in hyaenids has been identified at the same triple junction (Werdelin and Solounias, 1991: fig. 26). The anterior process of the jugal is broken away in both AMNH 19010 and MAE BU.91.9187–90, leaving the jugal-maxillary suture surface well exposed in both specimens. From these sutures, it can be deduced that the anterior tip of the jugal stops just above the infraorbital canal and does not reach the lacrimal bone.

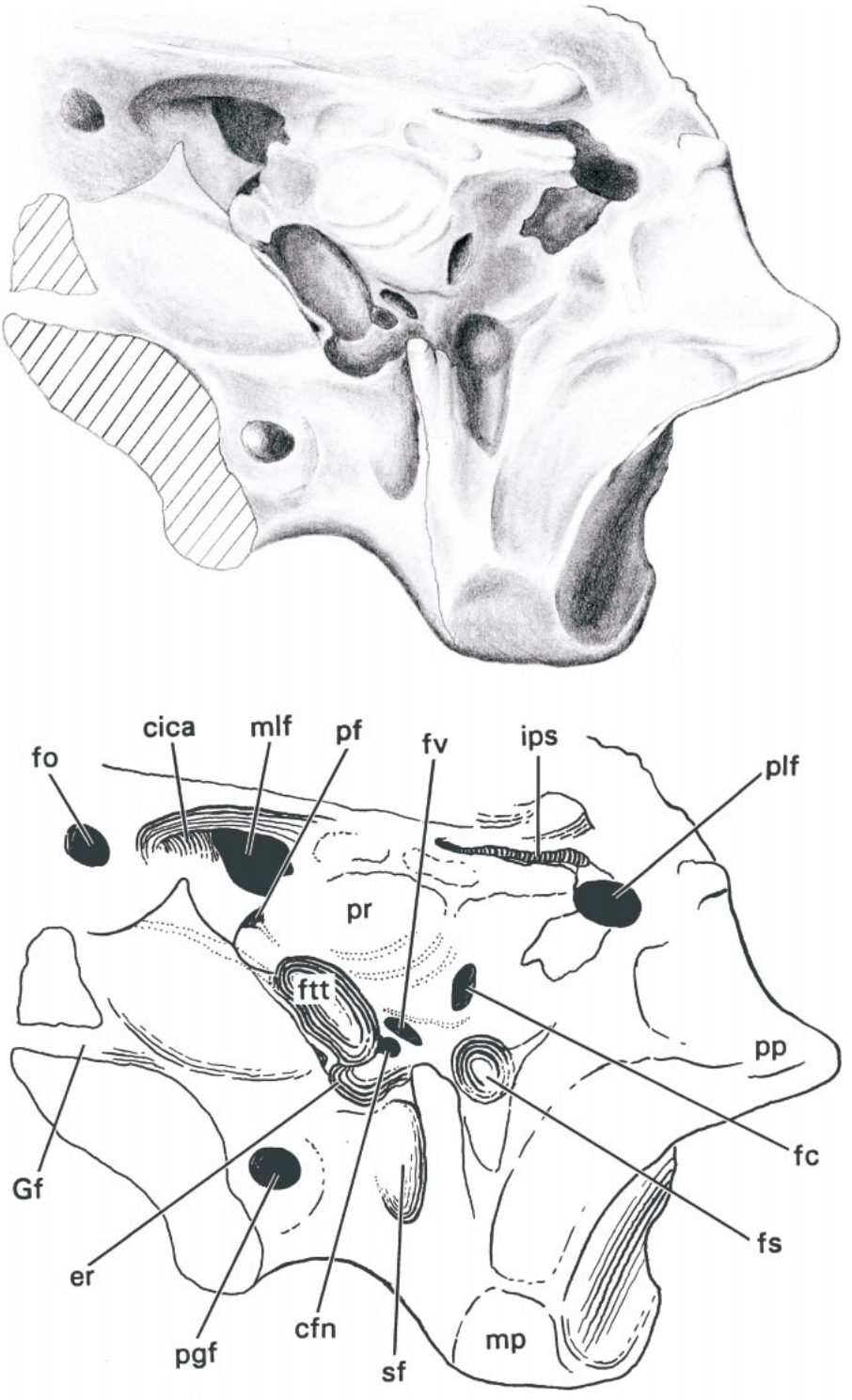
cica
mlf
pf
fv
ips
fo
plf
pr
ftt
pp
fc
Gf
fs
er
cfn
mp
pgf
sf

Basicranium (fig. 5): The occipital condyles are broken off on both sides of the holotype. The remaining basioccipital floor between the bullae is distinctly widened posteriorly, such that the lateral edges of the basioccipital form a 25° angle, in contrast to smaller angles in primitive arctoids such as *Amphictis* and to nearly parallel (0°) edges in canids. A small, rounded process for the attachment of the rectus capitis ventralis muscle lies close to the lateral edges of the basioccipital and is slightly in front of the posterior lacerate foramen. Both glenoid fossae are missing. On the left side, however, the medial segment of the postglenoid process is still preserved. Behind this broken process is a small postglenoid foramen, 1 mm in diameter.

The mastoid part of the petrosal is inflated, forming a prominent, laterally protruding mastoid process. The process has a smooth and flat lateral facet and is connected to the paroccipital process via a posterior ridge and to the lambdoidal crest via a more prominent dorsal blade. Such a blade can also be seen in most North American oligobunines. The mastoid tubercle (processus hyoideus) is formed by the petrosal. The posteriorly directed paroccipital process is broadly based because of its expanded wings on each side, but shows no sign of fusion with the bulla (not preserved) at the base. There is a low, longitudinally oriented ridge on the ventral surface of the paroccipital process.

In front of the mastoid process is an oval-shaped suprameatal fossa; its long axis is transversely oriented. The fossa is not fully enclosed toward the medial side, and is thus incompletely rimmed. Approximately 1.5 mm deep, the fossa is excavated into the squamosal bone, which forms the anterior wall of the mastoid process. The suprameatal fossa is primarily developed toward the caudal direction, and is excavated slightly toward the ventrolateral aspect such that it begins to be hidden by a thin bony rim, although the degree of excavation is far less than seen in some procyonids and mustelids.

Although both bullae are missing, the presence of an ectotympanic bulla is indicated by a clearly defined scar posterior to the postglenoid foramen and by a broad, smooth depression on the alisphenoid/squamosal suture (fused) area just medial to the postglenoid process. Such surface markings leave little doubt as to where the anterior crus of the ectotympanic ring was attached (also see the description under *Amphicticeps dorog* for the preserved ectotympanic). A broad facet facing anteroventrally between the posterior lacerate and stylomastoid foramina at the base of the paroccipital process is apparently the site of attachment of the posterior crus of the ectotympanic. The presence of an entotympanic, on the other hand, is indicated by a 2-mm-wide rugose area on the ventral surface of the promontorium immediately lateral to the petrosal/basioccipital juncture. It is not possible to ascertain whether a bony external auditory meatus was present. However, the rather distinct mark of the above mentioned ectotympanic attachment behind the postglenoid foramen suggests that the anterior crus of the ectotympanic does not wrap around to superimpose on the squamosal around the dorsal bony passage of the meatus to form a complete ring by the ectotympanic, as happens in many arctoids that have a tubular external bony auditory meatus.

The promontorium of the petrosal is prominently domed ventrally, particularly near the fenestra cochleae and fenestra vestibuli (oval and round windows). Its ventral surface is marked by at least two indistinct grooves (more clearly shown on the left side) that begin posteriorly at a small tubercle near the

←

Fig. 5. Ventrolateral view of the right side of the basicranium of *Amphicticeps shackelfordi*, AMNH 19010, holotype. The region near the postglenoid process is reconstructed from that of the left side. cfn, canal for facial nerve; cica, canal for internal carotid artery; er, epitympanic recess; fc, fenestra cochleae (fenestra rotunda); fo, foramen ovale; fs, fossa for stapedius muscle; ftt, fossa for tensor tympani muscle; fv, fenestra vestibuli (fenestra ovalis); Gf, Glaserian fissure; ips, inferior petrosal sinus; mlf, middle lacerate foramen; mp, mastoid process; pf, promontory foramen; pgf, postglenoid foramen; plf, posterior lacerate foramen; pp, paroccipital process; pr, promontorium; sf, suprameatal fossa.

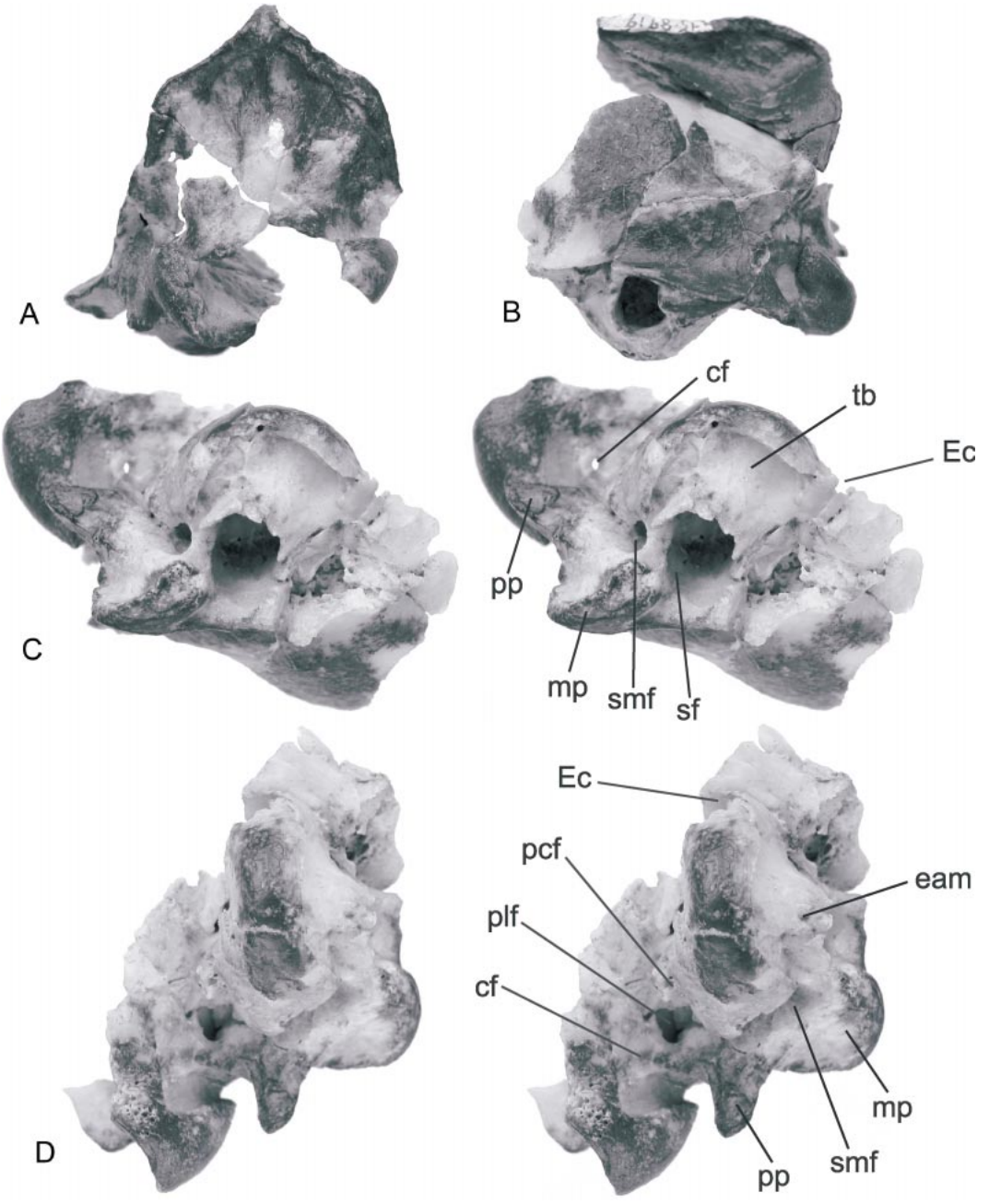

Fig. 6. *Amphicticeps shackelfordi*? MAE SG.95.8919, braincase and basicranial fragments. **A,** caudal view; **B,** lateral view; **C,** stereophotos of lateroventral aspect; and **D,** stereophotos of ventral view. cf, condyloid foramen; eam, external auditory meatus; Ec, Eustachian canal; mp, mastoid process; pcf, posterior carotid foramen; plf, posterior lacerate foramen; pp, paroccipital process; sf, suprameatal fossa; smf, stylomastoid foramen; tb, tympanic bulla.

entotympanic/promontorium contact facet. These grooves make small arches laterally at a level slightly in front of the fenestra cochleae and then turn medially toward the entotympanic/promontorium suture. Despite the superficial resemblance of the course of these grooves to the sulcus of the promontorial branch of the internal carotid artery and nerve in primitive caniforms (Wang and Tedford, 1994), its occupant is unlikely to be a promontorial artery, contrary to Cirot (1992: fig. 2), who postulated a promontorial artery in the primitive musteloid *Amphictis*, and to Schmidt-Kittler (1981), who implied the existence of an internal carotid artery on the promontorium of *Amphicticeps*. In taxa with a promontorial artery, there is usually a stapedial branch leading transversely toward the oval window. In *Amphicticeps* there is no such transverse sulcus medial to the oval window. Instead, there is a distinct groove along the ventral rim of the oval window. Such a longitudinal groove can also be found in *Promartes* and in living procyonids. In the case of the latter group, the soft structures that left the grooves are fine branches of the caroticotympanic artery and the accompanying caroticotympanic nerves (Story, 1951: fig. 83). The caroticotympanic artery, which is a minor component in the internal carotid artery, arises from the main internal carotid artery within the carotid canal, and after looping across the promontory, anastomoses with the tympanic arteries. The inferior tympanic artery and the tympanic nerve loop around the *posterior* edge of the round window instead the *anterior* position as in a promontory artery. The surface sulci on the promontorium of *Amphicticeps* are thus best reconstructed as left by an arterial and nervous configuration similar to that of extant procyonids, that is, no promontory artery is present. The main course of the internal carotid artery is assumed to be in the typical arctoid fashion enclosed within the medial bullar wall (see the description under *A. teilhardi* for further evidence of a medially positioned internal carotid artery).

At the posteromedial corner of the promontorium, there is a distinct posterior process protruding toward the posterior lacerate foramen. This process is broken off on the left side, showing pneumatic spaces beneath the bony surface.

The fossa for the tensor tympani is deep and located anteromedial to the epitympanic recess. There is a thin sheet of bone covering the canal for the facial nerve; some segments of this sheet are so thin that the bone is rather transparent along the nerve canal. The epitympanic recess is shallow, and walled by squamosal ventrolaterally and petrosal dorsolaterally.

Medial to the Eustachian canal at the level of the presumed anterior end of the entotympanic, the basisphenoid is deeply excavated into a large pit just anterior to the median lacerate foramen. This space marks the turnaround point of the internal carotid artery (cica of fig. 5; Wang and Tedford, 1994). The inferior petrosal vein is excavated into the lateral wall of the basioccipital but remains rather thin (approximately 1 mm in diameter) within a canal formed by the petrosal and basioccipital (ips of fig. 5; best seen near the posterior lacerate foramen). The caliber of the inferior petrosal vein is such that it is unlikely to be able to accommodate a double-looped internal carotid artery hypothesized to be present in many ursoids (Hunt, 1977; Hunt and Barnes, 1994).

The area anterior to the Eustachian canal is damaged on both sides of the skull, and it is not possible to ascertain the status of the alisphenoid canal except by indirect inferences. Schmidt-Kittler (1981: 784) stated, without elaboration, that *Amphicticeps* has an alisphenoid canal on each side of the skull. On AMNH 19010, only the anterodorsal roof of the foramen rotundum (shared with the anterior opening of the alisphenoid canal) is partially preserved on each side of the skull, and the ventral floor of the canal (if present) is missing. Further preparation on the better preserved left side of the holotype reveals a short segment of bone, about 2 mm in length, between the posterior aspect of the foramen rotundum and the foramen ovale. In *Canis* (Evans and Christensen, 1979) and *Ailurus* (Story, 1951), the maxillary artery enters the posterior opening of the alisphenoid canal (caudal alar foramen in Evans and Christensen, 1979) and emerges from the foramen rotundum (rostral alar foramen). In *Procyon* (which lacks the alisphenoid canal), on the

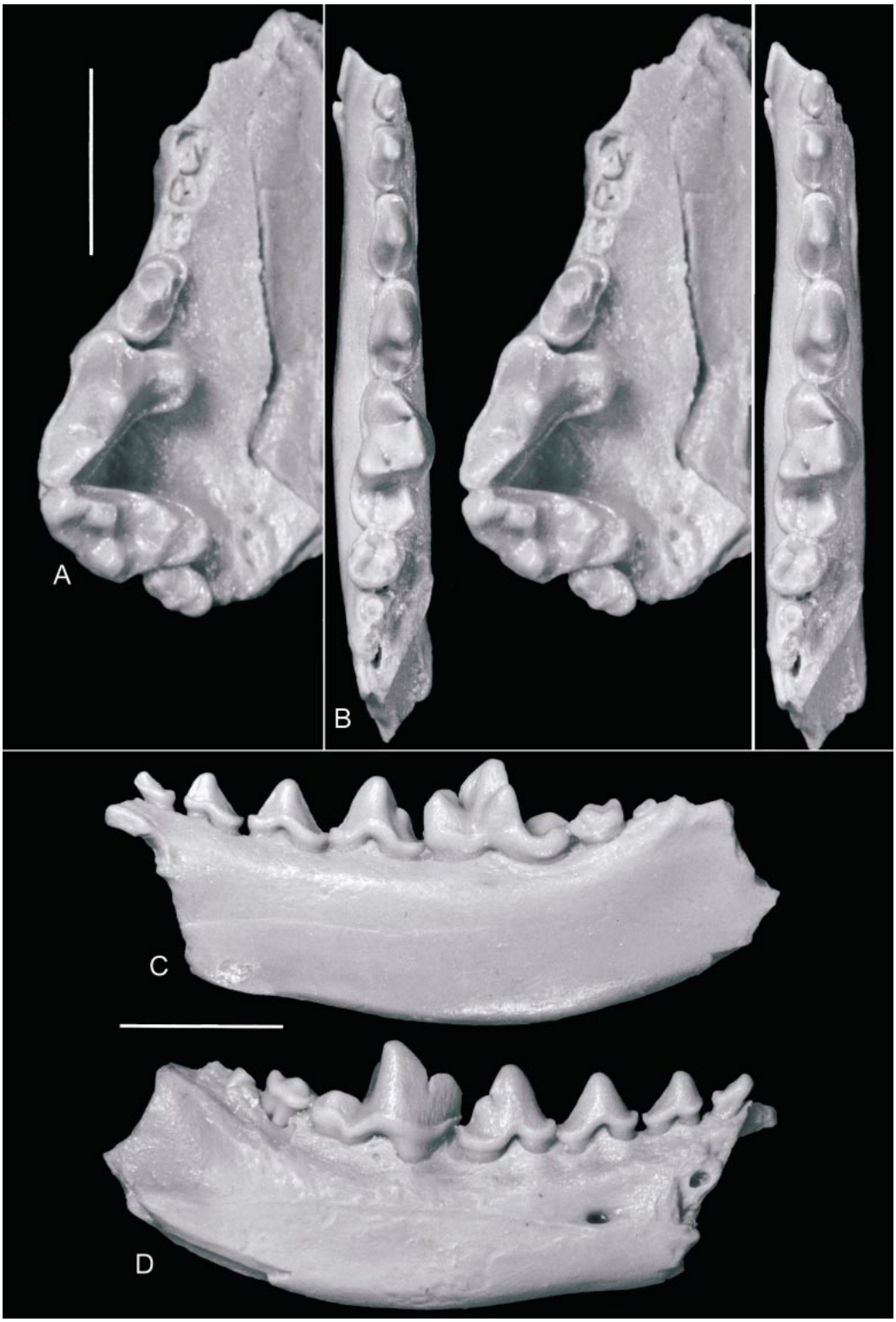
A
B
C
D

TABLE 2
Cranial Measurements of *Amphicticeps shackelfordi* and *Amphicynodon teilhardi* (in mm)

	Amphicticeps shackelfordi (AMNH 19010)	*Amphicynodon teilhardi* (PST 17/34)
Length of skull, inion to nasal tip	87.0	—
Breadth of rostrum across C (labial side)	22.6	13.8
Breadth of rostrum across P1 (lingual side)	13.8	9.3
Breadth of palate across left and right P4–M1	35.5	26.3
Breadth of frontal across postorbital processes	29.0	18.3
Breadth of postorbital constriction	13.3	13.1
Distance between postorbital constriction and postorbital process	12.2	7.0

other hand, only a small branch of the internal maxillary artery, the medial meningeal artery, enters the foramen ovale (Story, 1951: fig. 82). On AMNH 19010, the bony bridge flooring the orbital fissure and roofing the alisphenoid canal forms a half-pipe structure on the ventral view, possibly because of a broken ventral floor for the alisphenoid canal. A tiny foramen is present on the medial wall of the alisphenoid canal at the level of the presumed posterior entrance of the canal, as is also seen in *Amphicynodon teilhardi*. While structural damages do not permit us to state with certainty the existence of a posterior opening of the alisphenoid canal, we agree with Schmidt-Kittler that an alisphenoid canal is likely present.

Bulla of MAE SG.95.8919 (fig. 6): We tentatively refer a left bulla and associated posterior-most portion of the skull, MAE SG.95.8919, to *Amphicticeps shackelfordi*. Although the bullar size and overall basicranial morphology seems to be compatible with the holotype, there are a number of differences that prevent us from being certain of our reference. Furthermore, in the absence of associated dental materials in MAE SG.95.8919, it is prudent to describe this bulla separately in order to highlight the conflicting morphologies in the basicranial area from those in the holotype.

MAE SG.95.8919 consists of a crushed posterolateral aspect of the skull, preserving much of the left bulla as well as the occipital condyles and the top of the skull. Although much of the bony relationships between various elements are intact, crushing has distorted some areas so that full restoration of their original relationships is no longer possible.

The top of the braincase is well preserved, including about 25 mm of the posterior-most segment of the sagittal crest and a complete nuchal crest. The sagittal crest is 7 mm high at its deepest point just in front of the nuchal crest. The posterior segment of the sagittal crest on the holotype is missing, but based on the height of its nuchal crest, seems to be slightly lower than that in MAE SG.95.8919. The temporal foramen at the suture of parietal and supraoccipital is more posteriorly located than in the holotype. The profile of the nuchal crest, viewed from the caudal end, is also different from that of the holotype; instead of a rather flat top in the holotype, MAE SG.95.8919 has a rather pointed inion with a more steeply sloped nuchal crest on either side. The nuchal crest is also slightly thinner than in the holotype.

The most prominent difference between MAE SG.95.8919 and the holotype is in the size and lateral extrusion of the mastoid processes, although the overall construction of the mastoid process in MAE SG.95.8919 is

←

Fig. 7. *Amphicticeps shackelfordi*, MAE BU.91.9187–90, referred specimen, photographs of polyester cast. **A,** occlusal view of upper teeth, stereophotos; **B,** occlusal view of lower teeth, stereophotos; **C,** medial and **D,** lateral views of lower jaw. Scales = 10 mm.

TABLE 3
Measurements of Upper Teeth of *Amphicticeps* (in mm)

	shackelfordi		*dorog*			*makhchinus*
	AMNH 19010	MAE BU.91.9187-90	AMNH 85224	MAE SG.9799	MAE SG.9194	MAE 93-213
Length of C1 (alveola)	6.8	—	—	—	—	—
Width of C1 (alveola)	4.5	—	—	—	—	—
Length of P1	2.8	—	—	—	—	—
Width of P1	1.6	—	—	—	—	—
Length of P2	4.7	—	—	—	—	—
Width of P2	2.6	—	—	—	—	—
Length of P3	—	5.4	6.4	—	—	—
Width of P3	—	3.0	4.0	—	—	4.7*
Labial length of P4	9.7	9.5	—	—	11.0	12.7
Lingual length of P4 (protocone to metastyle)	10.8	10.7	—	—	11.7	14.4
Anterior breadth of P4	6.9	6.6	—	—	7.7	10.6
Labial length of M1	7.1	6.7	—	7.9	8.1	10.3
Max. transverse width M1	10.5	9.7	—	10.6	11.4	14.2
Longitudinal length of M2	—	2.6	—	—	—	—
Max. transverse width M2	—	4.0	—	—	—	—
Alveolar distance P1–M2	28.9	26.0	—	—	—	—

* Indicates an estimate.

similar to that in the holotype. A laterally expanded mastoid forms a conspicuous, rounded (in dorsal view) crest continuous from the lambdoidal crest. In lateral view, the outline of the mastoid process is roughly triangular. A posteroventral facet for attachment of the obliquus capitis cranialis muscle (Antón et al., 2004) is the largest surface of the process, and this facet is less posteriorly oriented than in the holotype. The depth of

TABLE 4
Measurements of Lower Teeth of *Amphicticeps shackelfordi* (in mm)

	AMNH 19017	AMNH 19127	AMNH 19128	AMNH 21695	AMNH 81336	AMNH 83610	AMNH 85749	MAE BU.91. 9787-90	MAE SG.95. 7518	MAE SG.97. 3576	MAE M-217
Length of p1	—	—	—	—	—	—	—	2.8	—	—	—
Width of p1	—	—	—	—	—	—	—	1.5	—	—	—
Length of p2	4.0	—	—	—	—	—	—	3.9	4.6	—	—
Width of p2	2.2	—	—	—	—	—	—	2.4	2.4	—	—
Length of p3	5.0	4.5	—	—	—	—	—	5.0	—	—	—
Width of p3	2.5	3.0	—	—	—	—	—	2.9	—	—	—
Length of p4	—	—	—	—	—	6.3	—	6.1	6.2	—	—
Width of p4	—	—	—	—	—	3.7	—	3.6	3.0	—	—
Length of m1	8.7	8.5	9.2	9.2	—	9.2	—	9.2	—	9.8	9.4
Trigonid length of m1	5.4	5.4	5.6	6.0	—	6.2	—	6.1	—	6.0	6.3
Trigonid width of m1	4.2	4.4	4.8	4.6	—	4.5	—	4.8	4.4	4.2	5.1
Talonid width of m1	3.7	3.8	4.4	4.2	—	4.0	—	4.3	—	4.5	4.9
Length of m2	—	—	—	—	3.9	3.5	4.3	3.8	—	—	—
Width of m2	—	—	—	—	3.7	3.1	3.6	3.4	—	—	—
Diameter of m3 alveola	—	—	—	—	—	—	2.0	1.5	—	—	—
p1–m2 (alveolar)	28.7*	27.3	31.5*	—	—	—	—	30.1	—	—	—

* Indicates an estimate.

the mastoid process in MAE SG.95.8919 is also significantly less than in the holotype, resulting in a smaller area of the lateral facet of the mastoid for attachment of the sternomastoideus muscle. Overall, one gets the impression that the much enlarged and laterally extruded mastoid process in the holotype is mostly related to the increased size and leverage of the m. obliquus capitis cranialis, and thus presumed more powerful head rotation (Antón et al., 2004), although ontogenetic variation may also be responsible for such differences.

Associated with its smaller mastoid process, the paroccipital process in MAE SG.95.8919 is also narrower in ventral view—the broader process in the holotype is apparently the result of a proportional lateral expansion due to its greatly expanded mastoid process. Otherwise, the paroccipital process is of the same general construction, with a dorsally convex and ventrally flat process that is completely posteriorly oriented without any hint of a ventral bending toward the bulla. Such a ''free'' paroccipital process, without hugging the bulla, is often a primitive condition for all caniforms (e.g., see Wang, 1994; Wang and Tedford, 1994; Wang et al., 1999).

The bulla is more or less intact with the exception of a crack on the ventrolateral aspect. The lateral half of the ectotympanic ring is slightly caved in by approximately 1 mm along this crack. Other than such a distortion, the bulla seems to maintain its original proportions. The form of the bulla is quite inflated for a basal arctoid, more so than the modern ursid ''type A'' bulla (Hunt, 1974). The axis along the ventralmost rim of the bulla forms a slight angle with the parasagittal axis of the skull, in contrast to the canid condition of mostly parallel bullar axes. Composition of the bullar elements is difficult to ascertain due to extensive fusions and fine cracks on the bullar surface. An extremely subtle groove seems to run from the base of the paroccipital process across the posterior aspect of the bulla, crossing slightly behind the ventral floor of the bulla and reaching toward the anterior carotid foramen (the anterior extent of this groove is less well defined because surface marks are becoming less clear). This narrow band of slightly roughened area may be one possible interpretation of the rostral entotympanic–ectotympanic contact, although such an interpretation is highly speculative and other alternatives are just as likely. The posterior carotid foramen is located on the anterior rim of the large posterior lacerate foreman.

Toward the medial aspect of the bulla, the basioccipital–basisphenoid region is fractured, and anatomic relationships are difficult to interpret. The nearly vertical medial wall of the bulla is buttressed by a thickened lateral wall, up to 6 mm in depth, of the basioccipital. The lateral surface of this lateral wall of the basioccipital is essentially flat and hugs the medial wall of the bulla, although there is a narrow gap between these two walls toward the posterior aspect of their contact. The medial wall of the basioccipital lacks a prominent invagination for the embayment of the inferior petrosal sinus seen in many ursoids such as ursids, amphicyonids, and basal pinnipeds (e.g., Hunt, 1977; Hunt and Barnes, 1994). The above mentioned gap between the lateral wall of the basioccipital and the medial wall of the bulla-petrosal seems too small to accommodate an enlarged inferior petrosal sinus. On the medial side of the lateral basioccipital wall a small canal is embedded within the basioccipital bone. This canal, probably for a nutrient blood vessel, emerges anteriorly into the braincase slightly behind the level of the anterior carotid foramen.

The external auditory meatus is quite well developed for a basal arctoid. The ventral lip of the meatus is 3–4 mm long, much longer than those in European basal arctoids such as *Amphicynodon leptorhynchus* (FSP ITD 312) and *Amphictis ambiguus* (FSP PFRA 28). Areas inside the meatus were prepared. A suprameatal fossa is vaguely developed on the posterodorsal aspect of the meatal wall of the squamosal. Such a weak fossa is in contrast to that in the holotype, on which it is not only substantially deeper but also better defined by a sharp rim along its lateral and ventral aspects. The fossa in MAE SG.95.8919 is also less well developed than in *Amphicynodon teilhardi* (see description below). The postglenoid process is broken off, exposing the canal for the retroarticular vein, which is of relatively small caliber.

Mandible (fig. 7B–D): Discovery of the associated upper and lower jaws of MAE BU.91.9187–90 allows us confidently to refer several ramal fragments to *Amphicticeps*. Nonetheless, our knowledge of the angular process and the ascending ramus is still incomplete.

The mandible is short, thick, and deep, with an average thickness of 6.0 mm and depth of 11.0 mm (both measured at the level of the talonid basin of m1; $N = 5$). On AMNH 19127, the remaining ascending ramus suggests a rather erect anterior border, forming a 125° angle with the horizontal ramus. There are two mental foramina, one below the anterior edge of the p2 and another between the two roots of the p3.

Teeth (figs. 2, 7): No upper incisor is preserved. Only the root of right I3 is partially intact on AMNH 19010. A robust upper canine can be inferred from the large alveoli on both sides of the holotype. Immediately behind the canine is a small, single-rooted P1 with a single main cusp. The double-rooted P2 also has a single main cusp, which is surrounded by a weak cingulum on the lingual side. This cingulum thickens on the posterior end and shows an incipient development of a cingular cusp. Both P3s are missing on the type, but are well preserved in MAE BU.91.9187–90. Like P2, P3 is single cusped, although its cingulum is stronger than that on P2. The upper carnassial, P4, is transversely broad due to a lingually extended protocone, which is near the anterolingual corner of the tooth. The apex of the P4 protocone is relatively low and formed by a raised lingual cingulum. This crestlike protocone contrasts with that of the North American oligobunines, which have a primitively tall, cusplike protocone (i.e., the apex is not associated with the cingulum). A low crest is present on the labial aspect of the protocone. There is a narrow cingulum on the labial side, which continues in front of the tooth and thickens slightly to become an indistinct parastyle. A carnassial notch is present.

M1 is transversely elongated, and its labial border forms a steep angle, averaging 112°, with that of the P4. The M1 parastyle is strong, rising to nearly the same height as the paracone. In MAE BU.91.9187–90, there is a faint notch (absent in the holotype) separating the parastyle from the paracone. The paracone is much higher than the metacone. The preprotocrista is low and lacks a protoconule on the holotype but is swollen slightly at the base of the paracone to indicate an indistinct protoconule in MAE BU.91.9187–90. The postprotocrista is clearly present and is oriented somewhat posteriorly. The postprotocrista ends at the posterior border of the M1 rather than at the base of the metacone. The lingual cingulum is moderately developed. It is rather low as compared to the protocone, and is thickest along the posterolingual border of the M1. The cingulum quickly tapers off anterior and posterior to the protocone, in contrast to a well-developed posterior ridge bordering a deep talon basin in the oligobunines. M2 is double-rooted and is located lingually such that its lingual border is at the same level as that of M1 whereas its labial border only reaches the middle of M1. The oval-shaped M2 has a prominent paracone toward the labial margin, and a posterolingually located, but much smaller, metacone at the posterior border of the tooth. A crestlike protocone is near the middle of the tooth, and is surrounded lingually by a lingual cingulum.

No lower incisors or canines are preserved on the holotype or referred specimens. The lower premolars are as robust as their upper counterparts. The p1 is single rooted and has a single main cusp. A cingulum is present around the anterior and posterior borders of p2–p3, which are single cusped. The p4, however, has a small posterior accessory cusp behind the main cusp. The p4 cingulum nearly completely surrounds the tooth except the region between the roots on the labial side. The m1 is rather broad (transversely) and its trigonid is short. The trigonid cusps are low and blunt, and the metaconid is not greatly reduced. The lingual border between the paraconid and metaconid is slightly concave to give a somewhat sigmoid appearance in occlusal view. Most individuals have a labial cingulum on the trigonid, whereas the lingual cingulum is more reduced. But the lingual cingulum is usually present at the level of the carnassial notch and may extend along the entire trigonid as in AMNH 21695, which occurs stratigraphically higher than the rest of the sample. The talonid of m1 is

narrower than the trigonid, and consists of a dominant hypoconid bordered lingually by a low entoconid crest much like a cingulum. The anterior hypoconid crest, the cristid obliqua, is oriented parasagittally. There is a weak cingulum on the labial side of the hypoconid. The entoconid crest does not have a notch at the base of the trigonid as in *Potamotherium* and the oligobunines. The double-rooted m2 is shortened and nearly quadrate in outline. The protoconid and metaconid are large and distinct. There is no paraconid anterior to the protoconid and metaconid; in its place there is a low, triangular platform. The greatly reduced talonid consists of a small hypoconid along the posterolabial border of the tooth. The entoconid takes the form of a narrow cingulum. A narrow cingulum is also present along the labial border of m2. The presence of a tiny m3 is indicated by a small root in MAE BU.91.9187–90, but it is absent in other individuals (definitely in AMNH 19127 and probably in AMNH 19017).

COMPARISON: Although Matthew and Granger's (1924) diagnosis of *Amphicticeps shackelfordi* indicated the presence of lower jaws, they did not elaborate the exact nature of the specimens, nor did they illustrate a lower jaw of this species. Four lower jaws were probably available at the time of their study (specimens that were collected during the 1922 season), and what Matthew and Granger had in mind were probably AMNH 19017 and 19128 because these two jaw fragments possess an m1 but are missing the m2, a combination that matches their descriptions. Their descriptions of the lower teeth, although very brief, must have been important in their attempt to delineate various species. In particular, their contrasts between lower carnassials of *Amphicticeps* and *Amphicynodon* (their *Cynodon*) must have been based on these referred lower jaws.

With the naturally associated upper and lower jaws of MAE BU.91.9187–90, our confidence in the references of isolated lower dental materials to *Amphicticeps shackelfordi* is considerably increased. In light of the new materials, Matthew and Granger's (1924: 4) comparisons about the lower carnassials having ''a narrower and shorter heel with more distinct hypoconid crest'' relative to those of *Amphicynodon* are still correct and their concept of the hypodigm still valid. However, specimens from the 1922 collection lack an m3, which naturally led Matthew and Granger to conclude that absence of this last molar is one of the main distinctions between *Amphicticeps* and *Amphicynodon*.

Our new discovery that MAE BU.91.9187–90 has an unmistakable m3 adds a new wrinkle to the interpretation of this character. As pointed out in the above descriptions about specimens that have preserved the posterior dental battery, an m3 is definitely absent in AMNH 19127 and is probably absent as well in AMNH 19017. Given the tiny size of the m3 in MAE BU.91.9187–90, it is quite possible that individuals, such as AMNH 19217, could have had an m3 in an earlier part of their life, which was later broken and fully healed without leaving traces of its root, a situation common in carnivores with small p1s (personal obs.). Whatever the actual situation with AMNH 19217, taken at the face value of existing materials, 30%–50% of individuals have retained an m3, although our sample size is obviously too small to allow a true statistical sense of the ratios. A similar situation is better documented in the loss of the M3 in the basal canid *Hesperocyon gregarius*, in which about 7% of the Chadronian individuals still retain a small, nonfunctional M3 and by Orellan time all have lost it (Wang, 1994: 30). However, the actual ratio may not be an important point in the present analysis. The important phylogenetic implication is that *Amphicticeps* represents a small clade that in its most basal species, *A. shackelfordi*, is on its way to losing its last molars, and this loss is yet another independent disappearance of this molar among carnivorans.

It is also worth noting that AMNH 21695, the only referred specimen of *A. shackelfordi* from the Zavlia fauna well above the level of the persistent basalt, is also the most robust individual known, both in terms of ramal construction and width of the m1. In addition, it is the only individual with a nearly complete cingulum on the lingual side of the trigonid, and its premolar alveoli indicate an individual with a relatively shorter rostrum compared to individuals from the Ulaan Khongil fauna below or immediately above the lava. The reliability of these features as

indications of a later stage of evolution of the species remains to be verified by further samples from the Zavlia fauna.

MAE SG.95.8919 offers the only bulla for Hsanda Gol carnivorans, and despite its less than certain taxonomic status, is of considerable importance in our understanding of the basal arctoids. That it belongs to the basal arctoids is certain. Of the main two arctoid lineages in the Shand Gol that are likely candidates, *Amphicynodon teilhardi*, the only species so far known for the genus in Mongolia, is too small for MAE SG.95.8919. Species of *Amphicticeps*, on the other hand, encompass a size range that is consistent with that of MAE SG.95.8919. More specifically, the holotype of *A. shackelfordi* has the same bulla size (judging from the attachment sites for the bulla) and general basicranial morphology as the MAE SG.95.8919. We thus cautiously place MAE SG.95.8919 in *A. shackelfordi*.

Overall, the holotype of *Amphicticeps shackelfordi* has a more robust construction than in MAE SG.95.8919, particularly in its thicker nuchal crests and larger and more laterally extruded mastoid process. These proportional differences may seem conspicuous, but probably are all attributable to a stronger development of the head–neck musculatures in the holotype. Even more extreme lateral expansions of the mastoid process can be seen in *Allocyon*. In the absence of contradicting evidence, we tentatively treat such differences as variations due to sexual dimorphisms in *Amphicticeps*. If our treatment is correct, the variations in the size of the suprameatal fossa are also considerable.

Amphicticeps dorog Wang, McKenna, and Dashzeveg, new species
Figure 8; Tables 3, 5

HOLOTYPE: MAE SG.9194, right maxillary fragment with P4–M1 and M2 alveolus.

TYPE LOCALITY: Tsagan Nor Basin, eastern Valley of Lakes, Obor-Khangay Province, Mongolian People's Republic. Top of Tatal Member, Hsanda Gol Formation, early Oligocene.

REFERRED SPECIMENS: AMNH 21656, left ramal fragment with m2 broken and m3 alveolus, field no. 538; AMNH 21672, left ramal fragment with m1–2, from ''Grand Canyon'', field no. 531; AMNH 84211, right ramal fragment with m1–2, field no. 532; AMNH 85217, left ramal fragment with m1 and alveoli of p2–4, field no. 538; AMNH 85223, isolated left m1, field no. 538; AMNH 85224, left maxillary fragment with P3, field no. 538; AMNH 85233, isolated left m1, field no. 538; MAE SG.91.9192, left ramal fragment with c broken and p2–4, from locality MAE 91–82, Tatal Gol, below lava in Tatal Member; MAE SG.95.8655, left ramus fragment with p3; MAE SG.97.3576, isolated right m1; and MAE SG.9799, left maxillar fragment with M1.

ETYMOLOGY: Mongolian: *dorog*, badger.

DIAGNOSIS: *Amphicticeps dorog* differs from *A. shackelfordi* in its possession of the following derived characters: larger size and more robust dentitions and jaws, lower and more crestlike P4 protocone, more prominent P4 anterior cingulum, more reduced M1 parastyle, relatively larger and more labially located M2, relatively shorter m2, and loss of m3. It is readily distinguishable from *A. makhchinus* in its smaller size, less lingually and posteriorly expanded P4 protocone crest, more labially oriented M1 postprotocrista, and less lingually expanded lingual cingulum of M1.

DESCRIPTION: Our knowledge of this new species is still limited to isolated maxillar and mandibular fragments and cheek teeth.

Upper teeth (figs. 8A, C): Only a single isolated P3 (AMNH 85224) is available and it has a simple main cusp and a well-developed cingulum. The P4 on the holotype is relatively wide due to a rather lingually expanded protocone. The protocone is low and its apex is located along the lingual margin and is continuous with the lingual cingulum through crests on either sides of the cusp. There is also a low ridge on the labial side of the protocone that ends at the base of the paracone. A cingulum is strongly developed around the entire P4, and the anterior cingulum is especially strong to the point of almost forming a parastyle. The labial cingulum is better developed than the lingual cingulum. The paracone is broad based and has a distinct anterior ridge leading down from the apex to the base. There is a well-developed carnassial notch.

The most distinguishing feature of the M1 is its transverse elongation, mostly due to a large paracone and parastyle. The paracone is the tallest cusp of the tooth, and is substantially larger and taller than the metacone. A large parastyle is formed by a prominent elevation of the labial cingulum surrounding the paracone. In contrast, the labial cingulum around the metacone is much narrower and lower. The metacone is on the posterolingual aspect of the paracone. The protocone is about the same height as the metacone. A distinct pre- and postprotocrista converge at the apex of the protocone and form a sharp V-shaped crest. No protoconule or metaconule is present. The lingual cingulum surrounds the protocone but is asymmetrical—its posterolingual corner behind the protocone is more swollen than its anterolingual corner.

No M2 is preserved. The double-rooted alveoli on the holotype suggest an M2 that is probably transversely elongated, as is M1, but probably anteroposteriorly short because of a short m2 and the absence of an m3 (see below). The location of the labial root indicates an M2 that is not lingually shifted as in *Amphicticeps shackelfordi*.

Lower teeth (figs. 8B, D, E, F): Although no associated upper and lower jaws are available, our references of isolated lower jaws are mostly based on their intermediate sizes, corresponding to size differences of upper teeth of different species of *Amphicticeps*, and on their dental morphologies that are consistent with those of the upper teeth. Fragmentary lower jaws, such as in AMNH 21672, indicate a robust mandible of deep and thick horizontal ramus.

Lower premolars are best preserved in MAE SG.91.9192, which has p2–4. Both p2 and p3 are similar, with a simple main cusp and an indistinct anterior cingular cusp, although the latter is larger and less asymmetrical in lateral view. A narrow cingulum surrounds much of the crown of these premolars. The p4 has added a moderate posterior accessory cusp as well as a posterior cingular cusp. Its anterior cingular cusp is also better developed than those of anterior premolars. The p4 cingulum also becomes more distinct.

The m1 trigonid is relatively short and its shearing blade bends lingually. The protoconid is the largest and tallest cusp. The metaconid and paraconid are of approximately the same height. The metaconid is lingual to, and slightly posterior to, the protoconid. The labial cingulum is narrow, and a short and indistinct lingual cingulum is present between the paraconid and metaconid. The tall trigonid is in contrast to a low talonid, which is dominated by a large (at the base), but relatively low hypoconid. The hypoconid is crestlike. It is rather labially located at its posterior end and stops anteriorly at the base of the protoconid, almost directly below the apex of the protoconid. The entoconid is no more than a low crest, directed posteriorly at an angle with the long axis of the tooth. The entoconid crest is decorated with fine wrinkles along its top edge. An indistinct labial cingulum surrounds the talonid but no cingulum is present on the lingual side.

The m2 is single rooted, very short, and almost equal in its length and width. The trigonid is formed by two low cusps, the protoconid and metaconid, which are set apart from each other. The two cusps are located almost on the lingual and labial borders of the tooth. A hypoconid is barely distinguishable on the talonid. A vague cingulum is developed on the anterior half of the tooth. The m3 is absent.

COMPARISON: Even on the basis of the fragmentary materials at hand, the transitional nature of this species seems readily apparent—*Amphicticeps dorog* is in many ways an intermediate form between the more primitive *A. shackelfordi* and more derived *A. makhchinus*. Average length of the upper carnassials is 15% longer than that of *A. shackelfordi* but 16% shorter than that of *A. makhchinus*. In the lower carnassial length, *A. dorog* is 22% longer than that of *A. shackelfordi*. Such size differences are comparable to those among modern sympatric species of some desert canids (Dayan et al., 1989, 1992), which offer a quantitative criterion for identification of fragmentary materials. These overall size differences, in addition to the fact that the two species cluster by themselves without intermediate individuals to bridge the gap, strongly suggests a separate species for *A. dorog*.

Qualitative morphological differences also

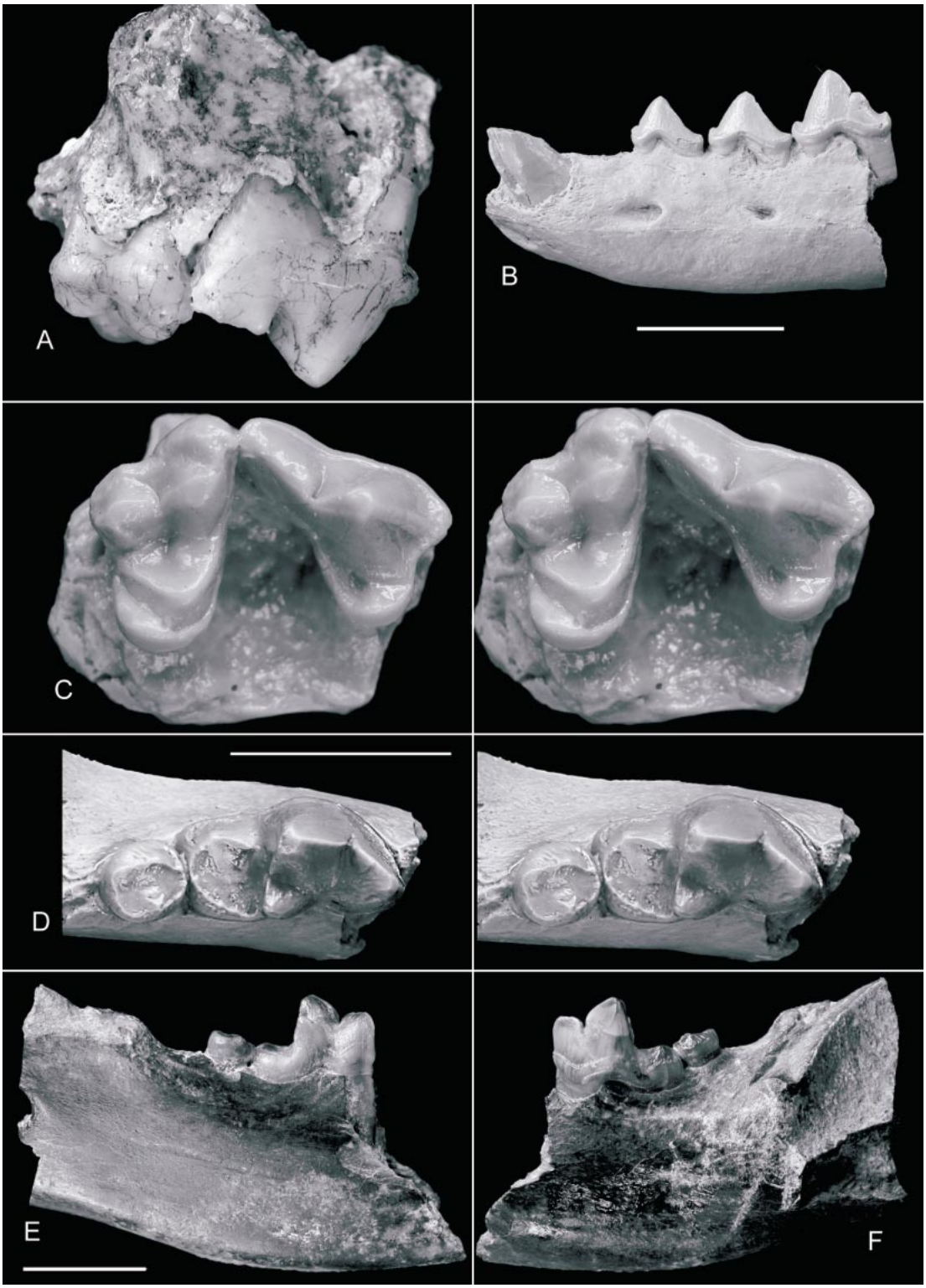
A
B
C
D
E
F

TABLE 5
Measurements of Lower Teeth of *Amphicticeps dorog* (in mm)

	AMNH 21672	AMNH 84211	AMNH 85217	AMNH 85223	AMNH 85233	MAE SG.91.9192	MAE SG.95.8655
Length of p2	—	—	—	—	—	5.3	—
Width of p2	—	—	—	—	—	2.6	—
Length of p3	—	—	—	—	—	5.9	5.5
Width of p3	—	—	—	—	—	2.9	3.0
Length of p4	—	—	—	—	—	7.0	—
Width of p4	—	—	—	—	—	3.7	—
Length of m1	10.5	10.5	11.2	11.8	11.4	—	—
Trigonid length of m1	6.9	6.5	7.2	7.8	7.7	—	—
Trigonid width of m1	5.6	4.6	5.3	6.0	4.8	—	—
Talonid width of m1	4.9	4.5	—	5.7	5.0	—	—
Length of m2	4.2	3.8	—	—	—	—	—
Width of m2	3.9	3.9	—	—	—	—	—

indicate a transitional form for *Amphicticeps dorog*. In the following characters *A. dorog* is almost exactly intermediate between *A. shackelfordi* and *A. makhchinus*: the crestlike P4 protocone, the development of the P4 anterior cingulum, the size of the M1 parastyle, the development of the posterior lingual cingulum of M1, and the angle between the labial borders of the P4 and M1.

Amphicticeps makhchinus Wang, McKenna, and Dashzeveg, new species
Figure 9; Table 3

HOLOTYPE: MAE 93–213 (AMNH cast 129862), right maxillary fragment with P4–M1, partial P3, and alveolus of M2. Collected by James M. Clark on 16 August 1993.

TYPE LOCALITY: MAE 93–213 was found in the Tatal Gol (Ulaan Khongil or ''Grand Canyon'') locality, 45°17′50″N, 101°37′16″E, Tsagan Nor Basin, eastern Valley of Lakes, Obor-Khangay Province, Mongolian People's Republic.

GEOLOGY AND AGE: MAE 93–213 was collected from the main exposure of the Tatal Gol locality, below the level of the lava, in the Tatal Member of the Hsanda Gol Formation, early Oligocene.

REFERRED SPECIMENS: Holotype only.

DIAGNOSIS: As the largest and possibly the most derived species of the genus, *Amphicticeps makhchinus* is distinguished from the other two species of the genus, *A. shackelfordi* and *A. dorog*, in its larger size, a broadened P3 with an extra lingual root, a low and lingually expanded P4 protocone crest, a slightly more reduced M1 parastyle, an enlarged M1 metaconule, and a more expanded M1 lingual cingulum.

ETYMOLOGY: Mongolian: *makhchinus*, meat eater, carnivore.

DESCRIPTION: *Amphicticeps makhchinus* is the least known of the three Hsanda Gol species of the genus. We are limited to two and a half teeth on the fragmentary right maxillary of the holotype. The maxillary clearly shows a shortened infraorbital canal, implying a shortened rostrum. Attached to this maxillary fragment is the anterior-most part of the jugal. The well-delineated jugal-maxillary suture indicates that the anterior jugal process stops at the antorbital rim and

←

Fig. 8. *Amphicticeps dorog*, n.sp. **A,** lateral view of upper teeth, MAE SG.9194, holotype; **B,** lateral view of anterior ramal fragment, MAE SG.91.9192; **C,** occlusal view of upper teeth, MAE SG.9194, holotype, stereophotos; **D,** occlusal (stereophoto), **E,** lingual, **F,** labial views of lower jaw fragment, AMNH 21672. Scales = 10 mm; top scale is for **B,** middle scale for **A, C–D,** and lower scale for **E** and **F.**

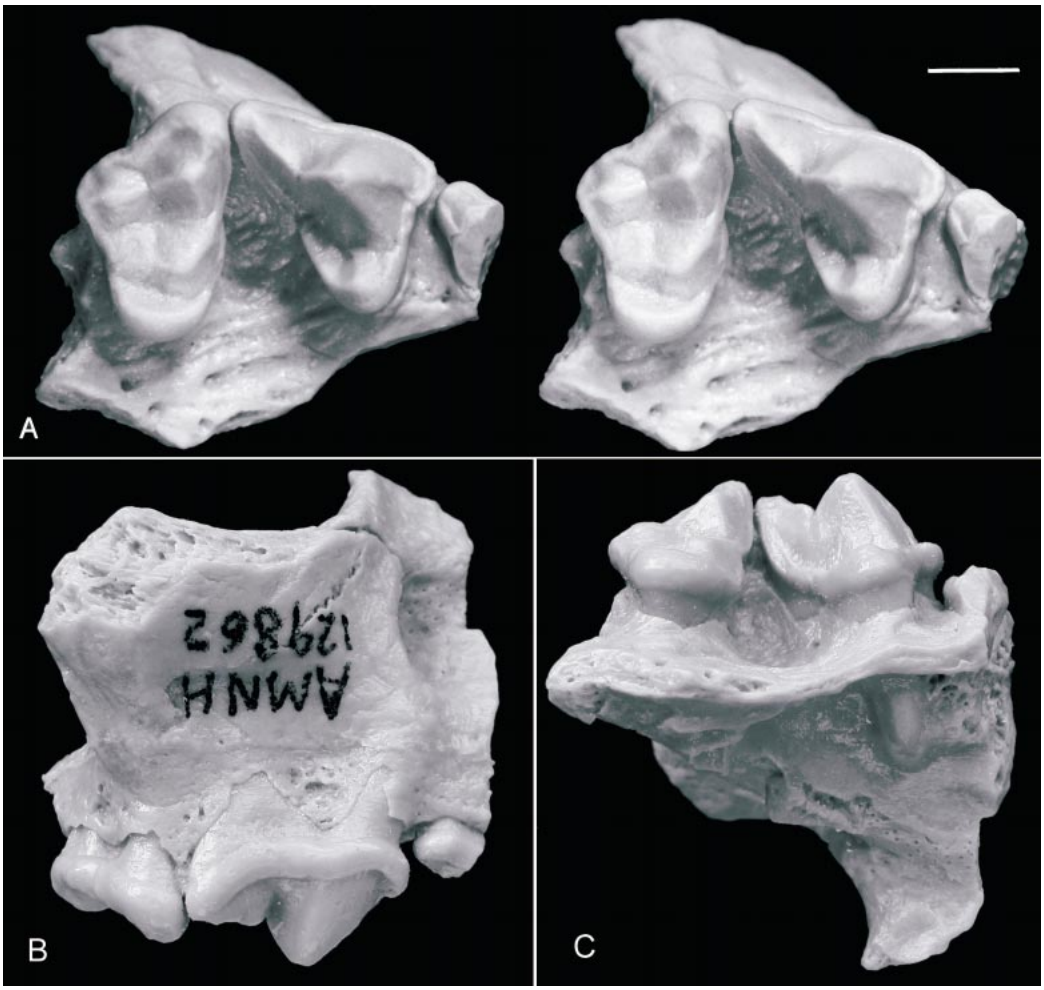

Fig. 9. *Amphicticeps makhchinus*, n.sp, MAE 93–213, holotype, photographs of a polyester cast (AMNH 129862). **A,** occlusal view of upper teeth, stereophotos; **B,** lateral view of upper teeth and maxillary; and **C,** lingual view of upper teeth and maxillary. Scale = 5 mm.

is probably not in contact with the lacrimal or frontal as in other species referred to this genus.

Only the posterior half of the P3 is preserved, which has a well-developed cingulum. The P3 has a significantly broadened lingual side and appears to have an extra lingual (third) root, in contrast to the double-rooted condition in other species of *Amphicticeps*. The P4 is typical of the genus, with a complete cingulum surrounding the entire tooth. The anterolabial corner of the cingulum is the strongest, but it does not elevate to form a parastyle. Like that of other species of *Amphicticeps*, the P4 protocone is composed of a raised lingual cingulum. However, the protocone is more expanded toward the lingual side than in the other species of the genus. As in the other two species of *Amphicticeps*, there is a low crest on the labial side of the protocone. The broad-based paracone has an anterior ridge leading up to the cingulum.

Overall proportions of the M1 have an anteroposteriorly broadened appearance for a basal ursoid. The parastyle is large and rises above the paracone, but does not reach to the same degree of expansion as seen in *A.*

shackelfordi and is more similar to that of *A. dorog*. Likewise, the cingulum adjacent to the metacone shows no sign of reduction as in *A. shackelfordi*. Consequently, the angle between the labial borders of the P4 and M1 remains a relatively large 124°, 15° greater than in *A. shackelfordi* but almost identical to that in *A. dorog*. A distinct pre- and postprotocrista are present, the latter being slightly more posteriorly directed than in *A. shackelfordi* and *A. dorog*. There is no protoconule (paraconule) and the metaconule is only indicated by a vague platform (probably suffered from some wear) slightly raised above the surrounding areas. The M1 internal cingulum is broad and thick, much more expanded than in *A. shackelfordi*. An anterior spur of this cingulum is present near the base of the preprotocrista. M2 is missing. Its partial roots, however, indicate a transversely broadened M2 whose lingual border is more internal than that in the M1. Its labial border is flush with that of M1, similar to that in *A. dorog* but in contrast to a lingually shifted M2 in *A. shackelfordi*.

COMPARISON: *Amphicticeps makhchinus* is the largest species of the genus so far known. It is 16% larger than *A. dorog* and 32% larger than *A. shackelfordi* (based on measurements of P4 labial length). It is 62% larger than *Amphicynodon teilhardi*. Besides its large size, *A. makhchinus* is also the most hypocarnivorous species in the genus. Dental features that indicate such hypocarnivory include an enlarged but low-crowned P4 protocone, a reduction of M1 parastyle, expansion of M1 lingual cingulum, a reduced angle between lingual borders of P4 and M1, and an enlarged M2.

Dental morphology of *Amphicticeps makhchinus* is reminiscent of certain ursids, particularly a basal ursid such as *Cephalogale*, so far known mostly in the Oligo-Miocene of Eurasia and North America. In particular, the French early Oligocene Quercy fissure fills produced some of the most primitive forms (e.g., *Cephalogale minor*). Similarities between *A. makhchinus* and *Cephalogale* include an enlarged grinding part of the dentition (M1–2) at the expense of the shearing part (P4). More specifically, *A. makhchinus* has a low, shelflike P4 protocone and a quadrate outline on M1, features often seen in *Cephalogale*. However, structural details of these features tend to argue against a true homology in the hypocarnivorous dentitions shared between *A. makhchinus* and *Cephalogale*. For example, the P4 protocone in all ursids (including *Cephalogale*) is formed by a swollen lingual cingulum, often in the form of a crest instead of a conical cusp, that has receded far back from the anterior border of the tooth, in contrast to an essentially conical protocone located on the anterolingual corner of P4 in *A. makhchinus*. Another derived character for the Ursidae is a posteriorly oriented postprotocrista of M1. This is a highly consistent feature among all known ursids. Such a condition is lacking in *A. makhchinus* (although wear in this region in the holotype of *A. makhchinus* renders our observation less certain). Finally, all ursoids, including the commonly acknowledged basal ursoids such as *Amphicynodon*, have a highly reduced parastyle and lingual cingulum on M1, in sharp contrast to a still relatively prominent parastyle in *A. makhchinus*.

Conversely, everything about *Amphicticeps makhchinus* is consistent with other species of *Amphicticeps*, despite its modest deviations toward the direction of hypocarnivory. Our inclination to assign it to *Amphicticeps* is further helped by the transitional nature of *A. dorog* between *A. shackelfordi* and *A. makhchinus*—in just about every aspect of its dental morphology *A. dorog* bridges the gap between the extremes in *A. shackelfordi* and *A. makhchinus*. In the final analysis, given what we know, it is easily conceivable that a series of three endemic species of *Amphicticeps* form a clade in the early Oligocene of central Asia.

Amphicynodon Filhol, 1881

COMMENT: Cirot and Bonis (1992) recently revised the taxonomy of the genus *Amphicynodon* and furnished a cladistic relationship for included species. However, their diagnosis of the genus is almost entirely based on primitive characters (Cirot and Bonis, 1992: 105): ''arctoide primitive; crâne alongé et bas, bulle ossifiée, fosse supraméatale superficielle, canal de l'alisphénoide present,'' which essentially describe the morphotypical condition for a basal arctoid but shed no light

of whether or not the genus forms a natural clade. As such the concept of *Amphicynodon* remains a grade of small, primitive arctoids that are not easily placed in other genera of carnivorans of similar ages.

Ten species of *Amphicynodon* were recognized by Cirot and Bonis (1992; see Baskin and Tedford, 1996, for a possible North American species). With the exception of *A. teilhardi* and *A. mongoliensis* (see below), all are from Europe and most are produced from the classic Quercy fissure fills. As defined by Cirot and Bonis, their concept of *Amphicynodon* offers a measure of morphological consistency, despite primitive status of most of their features. The limited scope of their phylogenetic analysis (within the genus), however, does not permit a sense of overall relationships among basal arctoids, nor does it address the question of to what extent the genus might be paraphyletic, given that certain derived forms (such as *Pachycynodon* and *Cephalogale*) may have arisen from within the genus. Such questions are difficult to address because most of the species of *Amphicynodon* are still represented by fragmentary jaws and teeth only. A comprehensive analysis of basal arctoids at the species level is not feasible. Our Mongolian materials, though significantly improved over those available for previous studies, are still not as complete as their European counterparts.

Amphicynodon teilhardi (Matthew and Granger, 1924)

Figures 10–14; Tables 2, 6, 7

Cynodon (*Pachycynodon*) *teilhardi* Matthew and Granger, 1924: 9, fig. 6D.

Amphicynodon teilhardi (Matthew and Granger): Mellett, 1968: 11; Lange-Badré and Dashzeveg, 1989: 139; Cirot and Bonis, 1992: 119, fig. 13; Dashzeveg, 1996: 3.

Cynodictis mongoliensis Janovskaja, 1970: 73, figs. 2–6.

Amphicynodon mongoliensis (Janovskaja): Cirot and Bonis, 1992: 119.

HOLOTYPE: AMNH 19007, left ramal fragment with m1–2 and m3 alveolus.

TYPE LOCALITY: Loh, in Tsagan Nor Basin, eastern Valley of Lakes, Obor-Khangay Province, in north-central Mongolian People's Republic. In Tatal Member (''lower red beds'') of Hsanda Gol Formation, early Oligocene.

REFERRED SPECIMENS: AMNH 19014, right ramal fragment with p1–3, field no. 73; AMNH 19129, left ramal fragment with m1, from 10 mi west of Loh, ''Grand Canyon''; AMNH 21628, left maxillary fragment with P2–4, field no. 532; AMNH 21673, left ramal fragments with p2, m1–3, and alveoli of c–p1, field no. 531, ''Grand Canyon''; AMNH 84198, isolated left m1, field no. 531, ''Grand Canyon''; AMNH 84212, left ramal fragment with m2–3 and m1 alveolus, field no. 532; MAE SG.8162, left ramus with p2–m1 (broken); MAE SG.9198–201, basicranium and maxillary fragments with left P2 and P4–M2 (AMNH cast 129861), and right M1–2, from loc. MAE M-174, 2 mi southwest of the Loh, on east side of a ridge, 45°16′14″N, 101°46′02″E, found not far above a brown sandstone layer, a local equivalent of the basalt lava (MAE M-174 is still within the Ulaan Khongil fauna that contains most specimens of *Amphicticeps shackelfordi* in Shand Member); MAE SG.9193, right maxillary fragment with P4–M2, from locality MAE 95-M-50, the Main Camp Locality, Tatal Gol, in Tatal Member; MAE SG.95.7488, left ramal fragment with broken p4 and m1; PST 17/34, anterior half of skull with complete right upper incisors, broken left and right canines, and complete left and right P2–M2, from Tatal Gol (Ulaan Khongil); PIN 475–3016, holotype of *Cynodictis mongoliensis* (Janovskaja, 1970: figs. 2–3), partial skull with complete left and right upper teeth and left ramus with p2–m3, from Tatal Gol (fig. 14); PIN 475–1388, partial palate with P3–M2 (Janovskaja, 1970: fig. 4); ZPAL MgM III/96, right ramal fragment with p3–m2 and m3 alveolus, Tatal Gol (Lange-Badré and Dashzeveg, 1989: 139); and ZPAL MgM III/97, left ramal fragment with p3–m1, Tatal Gol.

DISTRIBUTION: Early Oligocene of north-central Mongolian People's Republic. Dashzeveg (1996: fig. 1) reported that *Amphicynodon teilhardi* occurs in both the lower Tatal Member and upper Shand Member of the Hsanda Gol Formation. An undescribed record was reported in the early Oligocene Khatan-Khayrkhan locality of Altai Province

of Mongolia by Russell and Zhai (1987: 324).

EMENDED DIAGNOSIS: As the only known species from Asia, *Amphicynodon teilhardi* differs from all European species of the genus, except *A. velaunus*, in its shortened m2, along with a correspondingly reduced M2, in contrast to a primitively long m2 and large M2 in most European species. *A. teilhardi* primitively retains a distinct posterior accessory cusp on p4, which is lost or extremely reduced in the European *A. gracilis*, *A. speciosus*, and *A. velaunus*. *A. teilhardi* further differs from European *A. typicus*, *A. gracilis*, and *A. crassirostris* in its relatively low hypoconid of m1 with wrinkled enamel, in contrast to a trenchant talonid in the latter three species.

DESCRIPTION: PST 17/34 offers the best cranial morphology among all materials. Although it is missing the posterior one-third of the skull, the remaining skull of PST 17/34 is nearly perfectly preserved and offers fine details of bony and dental structures. Another cranial fragment, MAE SG.9198–201, is less complete on the anterior part (consisting of a heavily crushed partial rostrum plus left orbital region) but preserved a partial left basicranium. In addition, we are in possession of a cast of a partial skull and mandible from the collection of the Russian Paleontological Institute, PIN 475–3016 (holotype of *Cynodictis mongoliensis*). In combination, much of the skull, except the posterodorsal portion, is known.

Skull (figs. 10, 11): The overall proportion of the skull is less specialized than that of *Amphicticeps*. The rostrum is not shortened and broadened and the temporal region is not elongated, as in the latter. The premaxillaries form a thin blade on either side of the nasal opening. The entire premaxillary is preserved. The posterior process of the premaxillary does not touch the anterior process of the frontal, and ends near the posterior tip of the canine root at the level of P1. Both nasals are broken anteriorly, and their posterior tips end at roughly the same level as the maxillary-frontal suture. The frontal process inserts between the nasal and maxillary and ends anteriorly at the level of the P2 main cusp. The frontal is slightly domed, in contrast to a flat forehead in *Amphicticeps*. The postorbital process is small and does not have the distinct protrusion seen in *Amphicticeps*. The orbit is relatively large and is of approximately the same size as that of *Amphicticeps*, which has a much larger skull. The distance between the postorbital process and postorbital constriction is 7 mm on PST 17/34 and 9 mm on MAE SG.9198–201, significantly shorter than the 12 mm of *Amphicticeps*, and thus has a far shorter temporal region than the latter. Furthermore, the postorbital constriction is not so narrow as in *Amphicticeps*. The temporal crests are very indistinct, and they converge more slowly toward the sagittal crest than in *Amphicticeps*. In PST 17/34, the temporal crests do not fully converge at the posterior edge of the broken skull, and the sagittal crest, if present, is not preserved.

In lateral view, the orbital region is best preserved on the right side of PST 17/34 (fig. 11). It is complemented by the partially preserved left orbital region of MAE SG.9198–201. The orbital mosaic is quite similar to that of *Amphicticeps* in several respects: a short infraorbital canal, presence of a shallow fossa in front of the antorbital rim (less developed in PST 17/34), a small, nearly rounded lacrimal bone with a lacrimal foramen near its anterior aspect, anterior process of jugal in contact with the lacrimal, and other topographic relationships among individual bony elements. Perhaps of phylogenetic significance is the shorter postorbital area between the postorbital process and postorbital constriction.

In ventral view, the incisive foramen (palatine fissure) is short and located at the level of the anterior aspect of the upper canine. A tiny foramen is present along the midline suture at the junction of the premaxillary and maxillary (foramen palatine medialis of Story, 1951), as is commonly seen in arctoids. The maxillary–palatine suture is mostly fused and difficult to recognize. The palatine foramen is somewhat behind the level of the P4 protocone. The posterior border of the palatine bone is anterior to the posterior border of the M2 and is distinctly indented by a semicircular notch on either side of the midline suture.

The width of the rostrum across P1s (measured on the lingual edge of the alveolus) measured 9.4 mm in PST 17/34. That for

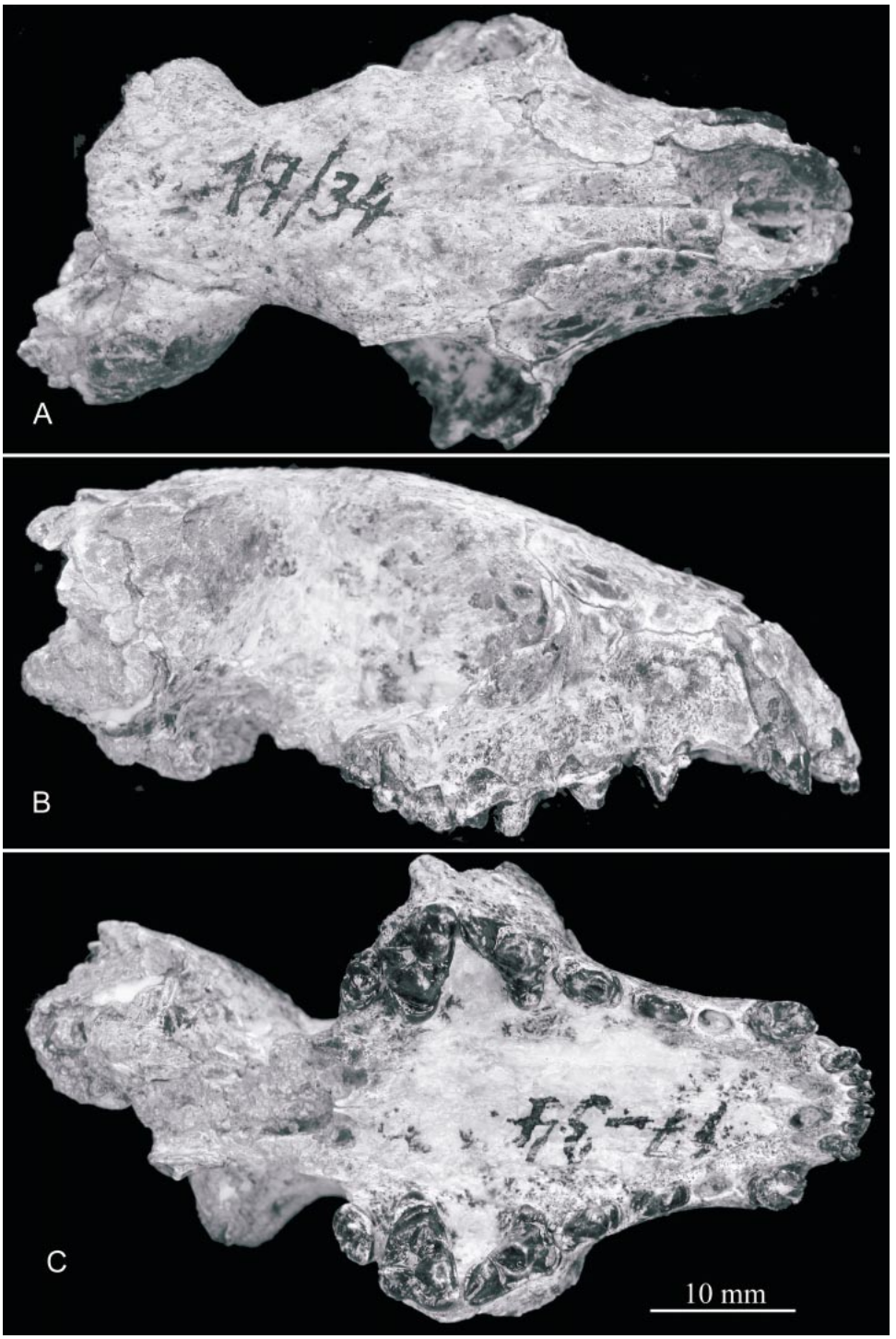

Fig. 10. *Amphicynodon teilhardi*, PST 17/34, referred specimen. **A,** dorsal, **B,** lateral, and **C,** ventral views of skull.

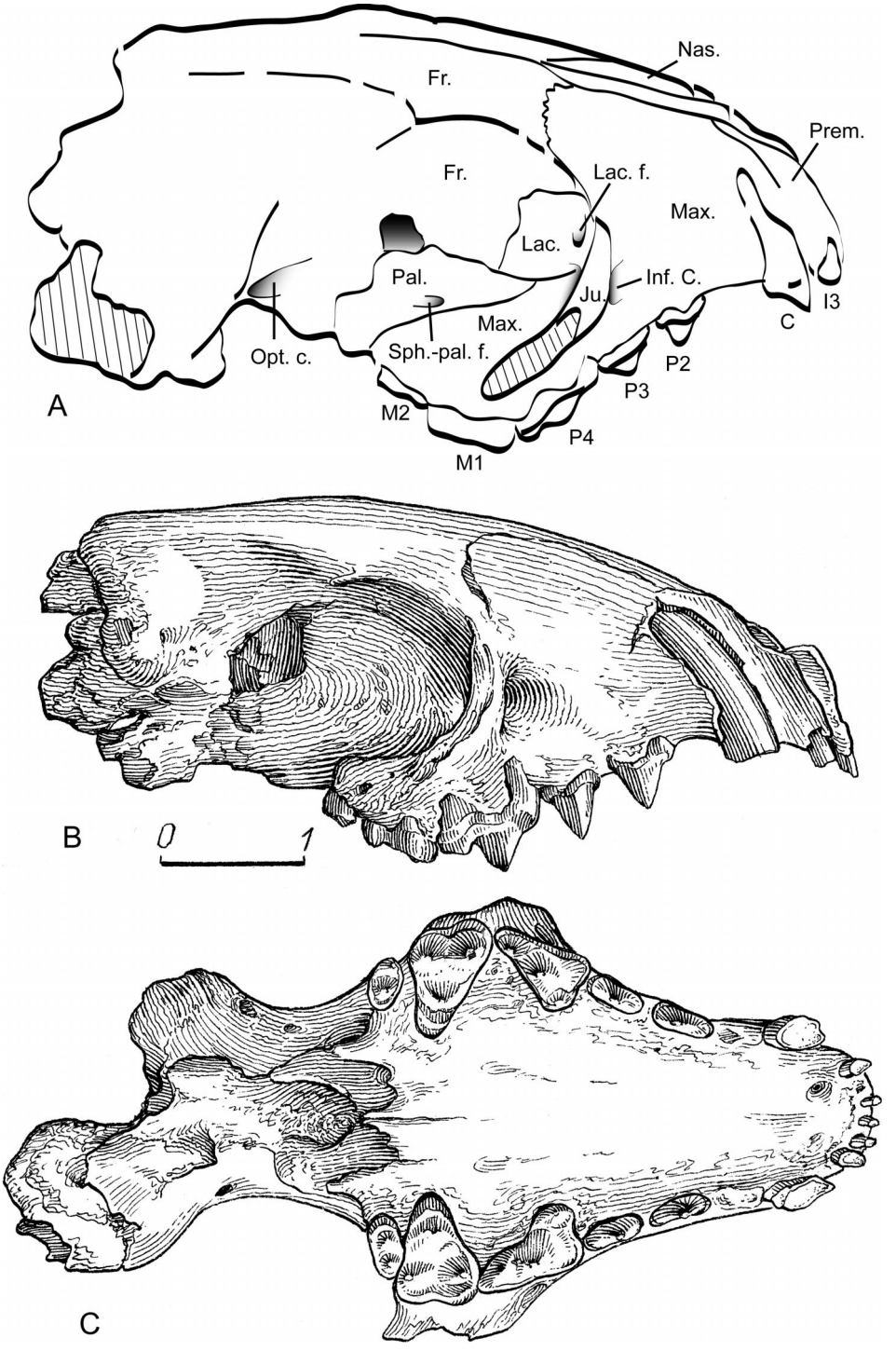

Fig. 11. Dorsolateral aspect of skull in *Amphicynodon teilhardi* (PST 17/34), showing anatomy of the orbital region. Abbreviations are the same as in figure 4, except for Nas, nasal and Prem, premaxillary.

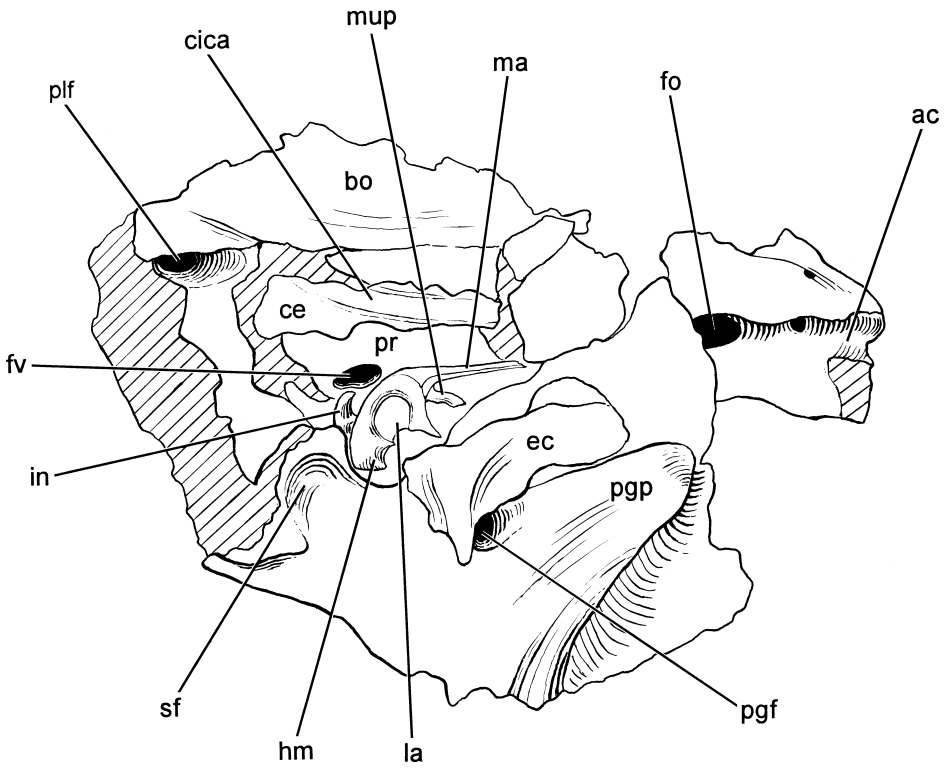

Fig. 12. Ventrolateral view of the left side of the basicranium of *Amphicynodon teilhardi*, MAE SG.9198–201. Cross-hatched areas indicate unprepared matrix. ac, alisphenoid canal; bo, basioccipital; ce, caudal entotympanic; cica, canal for internal carotid artery; ec, ectotympanic; fo, foramen ovale; fv, fenestra vestibuli (fenestra ovalis); hm, head of malleus; in, incus; la, lamina; ma, manubrium; mup, muscular process; pgf, postglenoid foramen; pgp, postglenoid process; plf, posterior lacerate foramen; pr, promontorium; sf, suprameatal fossa.

the laterally crushed rostrum on MAE SG.9198–201 measured 11 mm (restored from distorted left and right halves). These compare with 15.2 mm for the same measurement in *Amphicticeps shackelfordi*—the rostrum of *Amphicynodon teilhardi* is on average 49% narrower than the former. Given a size difference of 22% for the average length of P4 between these two species, the width of the rostrum in *A. teilhardi* is also relatively narrower than that of the type species. See additional cranial measurements (table 2) for PST 17/34.

Basicranium (fig. 12): The fragmentary materials of MAE SG.9198–201 offer the only information about the basicranium of *Amphicynodon teilhardi*. Although heavily crushed dorsoventrally, the left side of the basicranium of MAE SG.9198–201 preserves several key anatomical features absent in *Amphicticeps*. The overall basicranial morphology of *Amphicynodon teilhardi* is somewhat similar to that of *Amphicticeps*. The most obvious similarities are the presence of a shallow suprameatal fossa and a laterally expanded squamosal blade for the dorsal roof of the external auditory meatus. Much of the posterior half of the mastoid

→

Fig. 13. Teeth and lower jaw of *Amphicynodon teilhardi*. **A,** lateral view of upper teeth, PST 17/34; **B,** occlusal view of upper teeth, PIN 475–1388; **C,** occlusal view of upper teeth, PST 17/34,

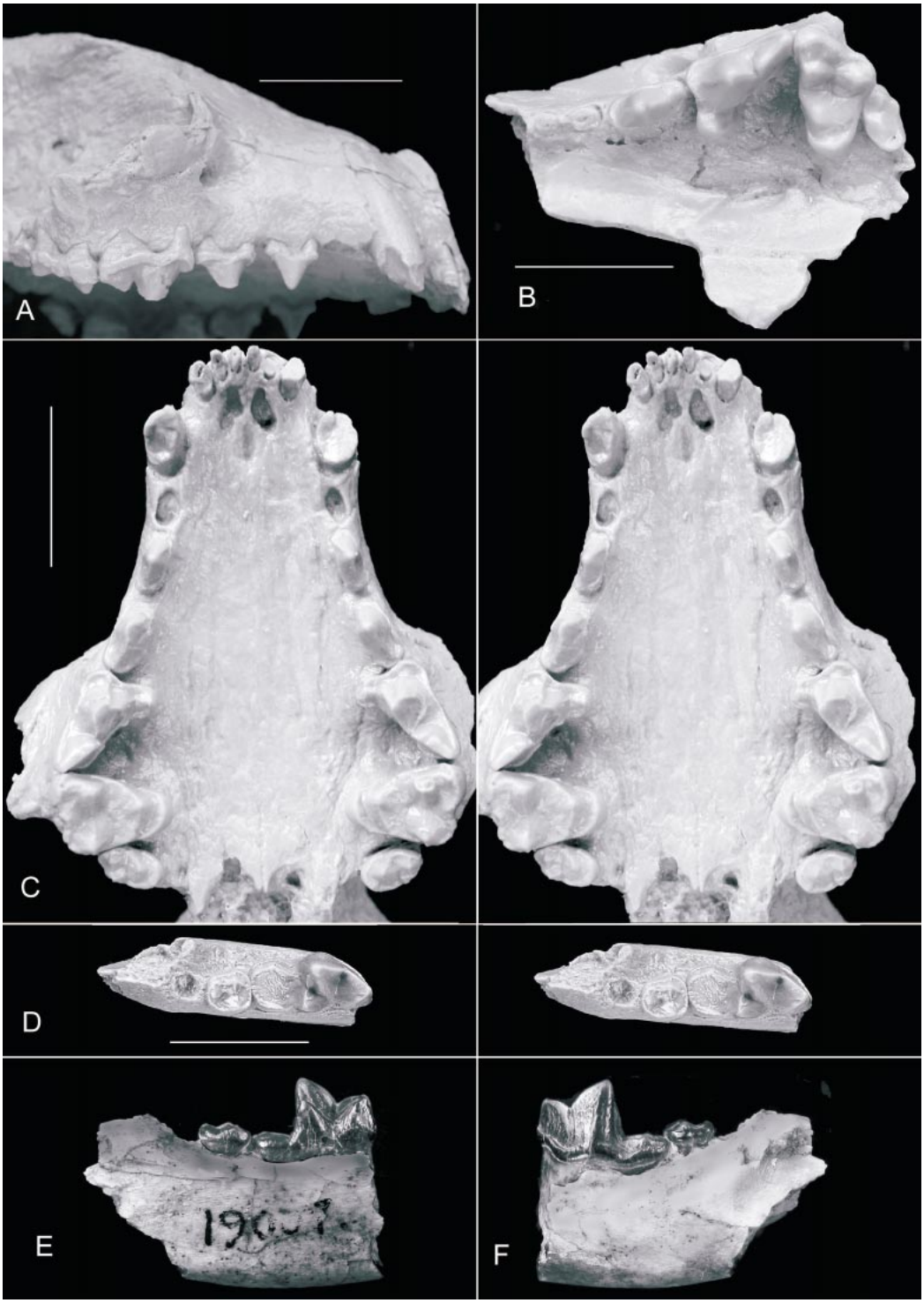

stereophotos; **D,** occlusal view of lower teeth, AMNH 19007, holotype, stereophotos; **E,** lingual, and **F,** labial views of lower jaw, AMNH 19007, holotype. All, except **E** and **F,** are photographs of a polyester cast. Scales = 10 mm.

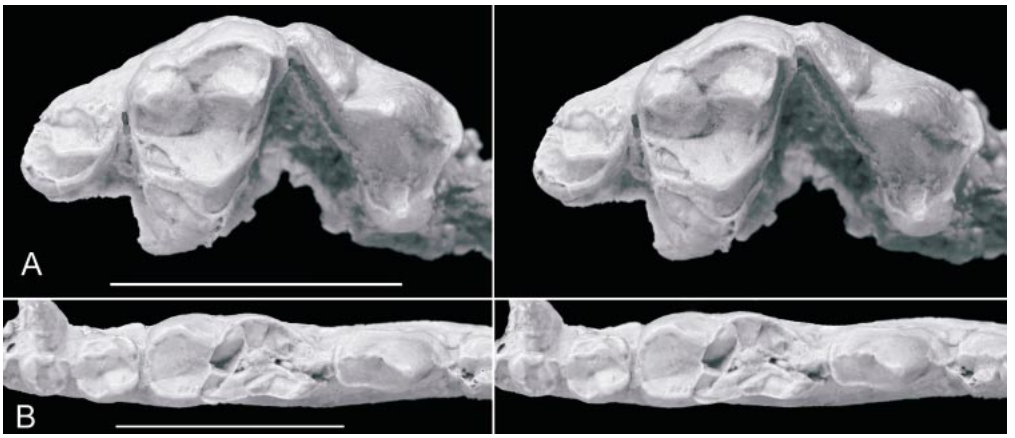

Fig. 14. Stereophotos of a cast of PIN 475–3016 (holotype of *Cynodictis mongoliensis* Janovskaja, 1970). **A,** occlusal view of upper teeth and **B,** occlusal view of lower teeth. Scales = 10 mm.

process is lost. However, the process is less laterally protruded than in *Amphicticeps*, judged from a more vertically oriented lateral wall of the braincase that forms a 90° angle with the horizontal squamosal shelf, in contrast to *Amphicticeps*, in which far more inclined lateral braincase walls (in posterior view) almost continue into the mastoid process. The suprameatal fossa is slightly less well developed than in *Amphicticeps*. In particular, its lateral half is not so deeply excavated into the squamosal as in *Amphicticeps*, and it does not have so clear-cut a lateral rim as in the latter.

The basisphenoid area is fragmented, and the ventral floor of the alisphenoid canal is broken off. However, enough is preserved in the area surrounding the foramen rotundum to indicate the presence of a canal, that is, the presence of a deep groove on the alisphenoid that probably forms its posterior opening. A small foramen opens into the me-

TABLE 6
Measurements of Upper Teeth of *Amphicynodon teilhardi* (in mm)

	AMNH 21628	MAE SG.91.9198-201	MAE SG.9193	PST 17/34	PIN 475-1388	PIN 475-3016
Length of C1	—	—	—	4.9	—	3.7
Width of C1	—	—	—	2.7	—	2.9
Length of P1	—	—	—	—	—	2.9
Width of P1	—	—	—	—	—	1.7
Length of P2	4.4	4.0	—	3.9	—	3.7
Width of P2	2.3	1.9	—	1.7	—	2.0
Length of P3	5.0	—	—	4.6	5.4	4.8
Width of P3	2.9	—	—	2.7	2.7	2.6
Labial length of P4	8.0	8.0	7.8	7.4	7.6	7.7
Lingual length of P4 (protocone to metastyle)	9.2	9.1	8.9	8.2	9.4	8.9
Anterior breadth of P4	5.8	5.9	5.3	4.9	5.4	5.4
Labial length of M1	—	5.6	5.3	5.8	6.2	6.0
Max. transverse width M1	—	8.6	7.9	8.2	8.8	—
Longitudinal length of M2	—	2.1	2.4	2.3	2.5	2.5
Max. transverse width M2	—	3.7	3.7	4.4	4.5	4.3
Alveolar distance P1–M2	—	—	—	25.7	—	—

TABLE 7
Measurements of Lower Teeth of *Amphicynodon teilhardi* (in mm)

	AMNH 19007	AMNH 19129	AMNH 21673	AMNH 84212	AMNH 84198	AMNH 19014	MAE SG. 8162	MAE SG.95. 7488	ZPAL MgM III/96	ZPAL MgM III/97	ZPAL MgM III/98
Length of p1	—	—	—	—	—	—	—	—	—	—	—
Width of p1	—	—	—	—	—	—	—	—	—	—	—
Length of p2	—	—	4.4	—	—	4.3	—	—	—	—	—
Width of p2	—	—	2.2	—	—	2.3	—	—	—	—	—
Length of p3	—	—	—	—	—	4.8	4.5	—	—	—	—
Width of p3	—	—	—	—	—	2.6	2.3	—	—	—	—
Length of p4	—	—	—	—	—	—	5.2	—	5.5	5.5	5.5
Width of p4	—	—	—	—	—	—	2.7	—	2.6	2.5	2.9
Length of m1	8.6	7.9	8.7	—	8.9	—	—	8.0	7.7	—	—
Trigonid length of m1	5.4	4.9	5.3	—	5.4	—	—	5.1	—	—	—
Trigonid width of m1	4.1	3.6	4.2	—	4.0	—	—	3.6	3.8	—	—
Talonid width of m1	3.8	3.3	3.9	—	4.1	—	—	3.6	—	—	—
Length of m2	3.0	—	3.3	3.9	—	—	—	—	2.8	—	—
Width of m2	3.2	—	3.4	3.9	—	—	—	—	2.6	—	—
Length of m3	—	—	2.2	2.0	—	—	—	—	—	—	—

dial wall of the canal at the level of its posterior opening.

The postglenoid process is large, forming a long ventral hook for articulation with the condyle of the mandible. At the posterior base of the postglenoid process, behind the postglenoid foramen, there is a triangular piece of ectotympanic still firmly attached to the basicranium. Part of the anterior ectotympanic ring for attachment of the tympanic membrane is also preserved. The ectotympanic does not extend laterally far beyond the postglenoid foramen, indicating no or a very short bony external auditory meatus. On the medial side, along the suture between promontorium and basioccipital, several broken pieces of the entotympanic are still preserved and cover the internal carotid canal. The ventral flooring of the canal, presumably formed by the caudal entotympanic, forms a gentle curve in a typical primitive arctoid fashion, leading toward the middle lacerate foramen. The presence of this medially positioned carotid canal further confirms our conclusion that there is no promontorial artery in *Amphicynodon* and *Amphicticeps*, despite of the sulci on ventral surface of the promontorium in the holotype of *Amphicticeps shackelfordi* (see description under that species). No sulcus is visible on the promontorium of *A. teilhardi*.

The promontorial part of the petrosal has been pushed dorsally toward the brain cavity, and its ventral surface is unnaturally rotated into a vertical orientation. The ventral promontorial surface has thus become laterally facing and is partially hidden beneath the lateral edge of the basioccipital. The postmortem crushing of the promontorium into the brain cavity, however, is apparently beneficial for the preservation of a nearly complete malleus and incus, which occupy the space originally occupied by the promontorium.

The malleus lies on its medial side with the lateral surface (for attachment of the tympanic membrane) of the manubrium facing ventrally. The malleus has a rather slender construction but is of large size—the head to manubrium tip (broken) measures 5.8 mm. The lateral process is inconspicuous. The muscular process (for insertion of m. tensor tympani) is broken near its base and its main body sticks out between the anterior process and the manubrium instead of its original position, pointing away from the plane of tympanic membrane. This slightly dislocated muscular process is very large and has a broad distal end, which contrasts with the much reduced condition in living ursids (Segall, 1943). The neck is slender and forms a smooth curve between the head and the manubrium. The head is not enlarged as in pin-

nipeds (Wyss, 1987). The sharp-tipped anterior process completes the anterior rim of a circular lamina. Much of the incus is buried beneath the head of the malleus. Only the processus brevis is fully exposed.

Upper teeth (figs. 13A–C, 14): Most of the upper dentition is now known. Upper incisors in PST 17/34 are all broken and the crown morphology is no longer preserved. The roots indicate progressively enlarged incisors from I1 to I3, with the I3 almost twice as large as the I1. All incisor roots are mediolaterally compressed. The left and right I3s in PIN 475–3016 are preserved and are slightly precumbent in lateral view, as is also the case in PST 17/34. The upper canines on both sides are also broken in PST 17/34, preserving only the roots. The canine roots are oval in cross section. The canines in PIN 475–3016 are present. The canine crowns are smooth surfaced and their tips curve backward slightly.

The cheek teeth are evenly spaced with short alveoli between all premolars in PST 17/34 but slightly more tightly spaced in PIN 475–3016, in contrast with crowded premolars of *Amphicticeps* due to its shortened rostrum. P1 is only seen in PIN 475–3016, and is single rooted. It has a simple main cusp and an indistinct cingulum anteriorly and posteriorly. The P2s are single cusped and are more slender than that of *Amphicticeps*. A rather tall and erect main cusp has a posterior ridge and an anterolingual ridge. The anterior and posterior cingula are slightly more distinct than in the P1s, but there is no cingular cusp on either end. The cingulum is continuous on the lingual side and discontinuous on the labial side. The main distinction between P3 and P2, besides a larger size and more prominent cingulum in the P3, is a slight swelling on the posterolingual cingulum of the tooth, but there is no extra root beneath this swelling. The morphology of P4 is similar in overall construction to that of *Amphicticeps*, except for a much smaller protocone. A distinct cingulum surrounds the entire tooth. The anterior cingulum is particularly well developed, as is the parastyle. However, the parastyle is not cusplike but more like a wide cingulum. As in *Amphicticeps*, the anterior border of the P4 protocone is slightly ahead of the parastyle. The protocone apex is clearly continuous with the lingual cingulum. The cuspidate protocone has an indistinct ridge on the labial side of the cusp. The paracone has a distinct anterior ridge reaching up to the parastyle, and a less distinct anterolingual ridge that reaches to the base of the protocone. A deep carnassial notch separates the paracone from the metastylar blade.

The overall construction of M1 is less hypercarnivorous than that of *Amphicticeps*. The M1 parastyle is substantially reduced as compared to those of *Amphicticeps*, even for the least developed M1 parastyle in *A. makhchinus*. A vague notch separates the parastyle and paracone. The labial cingulum is slightly swollen around the paracone in PIN 475–3016 and around the right M1 of PST 17/34, similar to the swellings in *Amphicticeps shackelfordi*. The labial cingulum near the metacone is not so reduced as in *Amphicticeps*; this is especially so in MAE SG.9193. Together, the smaller parastyle and less reduced labial cingulum along the metacone give M1 a more quadrate look. The labial borders of P4 and M1 form an angle of 127°, 18° larger than in *Amphicticeps shackelfordi*. The differences in size and height between paracone and metacone are also relatively smaller than in *Amphicticeps*. There is a well-developed preprotocrista and postprotocrista. There is no protoconule, except a slight swelling in PST 17/34, which is absent in the Russian specimens. The postprotocrista is essentially posteriorly oriented, particularly so in PST 17/34, leaving a broad valley between the postprotocrista and metacone. A metaconule is only vaguely suggested by a low and indistinct swelling at the posterior end of the postprotocrista and by a slight notch toward the posterior end of the postprotocrista. The internal cingulum (hypocone) surrounds the entire protocone, although its anterior segment is narrower. This anterior extension in front of the protocone, less well developed in MAE SG.9193, has a narrow spur near the base of the preprotocrista.

M2 has the same distinct shape as in *Amphicticeps*, reaching the same stage of reduction and acquiring the same peculiar cusp pattern as in the latter, although this tooth tends to vary more than does M1. A large

paracone is located at the labial border of the tooth, whereas the metacone is reduced to a faint cusp at the posterior border (that in PST 17/34 is more distinct). The protocone is relatively large and is in the middle of the tooth, followed lingually by a broad cingular shelf. The main feature to be distinct from that of *Amphicticeps* is its less lingually shifted position. Instead of being flush with the lingual border of the M1 as in *Amphicticeps shackelfordi*, the lingual border of M2 in *Amphicynodon* is slightly lateral to the M1 lingual border.

Lower teeth (figs. 13D–F, 14): Lower jaws figured by Janovskaja (1970: figs. 3, 5, 6) substantially improved the knowledge of *Amphicynodon teilhardi* over the original topotype series. The following descriptions of the ramus are based on figures published by Janovskaja. Her dental illustrations, however, lack sufficient details for useful comparisons, and have exaggerated the length of the m2 (see table 7 and comparison below), a critically important feature of this species. Our dental descriptions are mainly based on a cast of the PIN 475–3016, as well as more fragmentary materials from the AMNH.

The horizontal ramus is relatively slender compared to that of *Amphicticeps*. The ascending ramus has a rather erect anterior border. The angular process is slender and pointed. No lower incisor is preserved. The lower canine hooks backward slightly. The lower premolars are relatively more slender than those of *Amphicticeps*. The p1 is not preserved. The p2 has a simple main cusp and a very vague cingulum. The p3 begins to have a tiny posterior accessory cusp and a slightly more distinct cingulum. The p4 posterior accessory cusp is further enlarged, and its cingulum surrounds the entire tooth. The anterior cingulum has a hint of developing into an anterior cingular cusp, and the posterior cingulum is also slightly elevated.

The m1 trigonid is tall crowned. The metaconid is approximately the same height as the paraconid. The metaconid is on the lingual side of the protoconid, not trailing behind the protoconid as seen in most ursids. A cingulum is present on the entire labial margin of m1 but is only vaguely present on the lingual side of the paraconid. The m1 talonid is low, especially the hypoconid. The hypoconid is largely crestlike and is oriented at a slight angle from the anteroposterior axis of the tooth. Anteriorly, the hypoconid crest ends at the base of the protoconid just below its apex. The entoconid consists of a low ridge, rather like a cingulum. Together with the hypoconid, the entoconid encloses a broad basin on the talonid. The talonid cusps are decorated with fine wrinkles. The m2 is small and distinctly short; its length and width are nearly identical. No paraconid is visible. A protoconid and metaconid are of equal height and positioned on the borders of the tooth, such that a central valley essentially runs through the length of the tooth. A small cristid connects between the protoconid and metaconid in the holotype but is absent in PIN 475–3016. On the talonid, the hypoconid is far better developed than the entoconid, which is absent in the holotype. A small m3 is present in all specimens that preserve this part of the jaw. It is formed by a small, rounded, peglike structure with a surrounding cingulum but without a distinct cusp pattern.

COMPARISONS: The topotype series of *Amphicynodon teilhardi* consists of a few jaw fragments and lower teeth without upper teeth. Based on such meager materials, Matthew and Granger (1924: 8) were initially ambivalent in their assignment of this species to *Cynodon* (*Amphicynodon* of current usage): ''This species can be referred only provisionally until better specimens are available. It appears to fall within *Pachycynodon* rather than the typical *Cynodon*, by Teilhard's key to the Phosphorite genera,'' in reference to Teilhard de Chardin's (1915) monographic revision on Quercy carnivorans that dealt with these genera. The first major breakthrough in the state of knowledge of this species came by a crushed but associated skull and lower jaw (PIN 475–3016; fig. 14) along with a few more specimens collected by the 1946–1949 Expeditions of the Soviet Academy of Sciences. The Russian collection was described as a new species, *Cynodictis mongoliensis*, by Janovskaja (1970). While describing three additional jaw fragments collected by the Polish–Mongolian Paleontological Expeditions in the 1960s, Lange-Badré and Dashzeveg (1989: 141), however, argued that ''there are no signifi-

cant morphological or biometrical differences between *C. mongoliensis* and *A. teilhardi* and those that exist represent no more than intraspecific variation.'' More recently, Cirot and Bonis (1992), in their phylogenetic analysis of the species of *Amphicynodon*, chose to leave *Amphicynodon mongoliensis* as a valid species, and in their cladogram, placed it next to *A. teilhardi* as the sister-species forming an Asiatic clade.

Although we are unable to examine the three jaw fragments in the ZPAL collection (Lange-Badré and Dashzeveg's measurements for the holotype of *A. teilhardi* are apparently an underestimate), we have access to casts of two PIN specimens in the topotype series of *C. mongoliensis*. With the addition of even better materials from the MAE collections, we are in a position to evaluate morphological variations of at least 20 specimens (see table 7). Although the increased sample size naturally leads to a slight increase in variations, the coefficient of variation for most dental measurements generally falls between 5% and 8%, a range not uncommon for small carnivorans (e.g., Wang et al., 1999). The only exceptions are for the upper canines, which tend to be more dimorphic among arctoids, and the m2s, which have the least occlusal constraint because of their flat grinding surfaces. Cirot and Bonis (1992: 119 and fig. 16) noted the rather long m2 in *A. mongoliensis*, apparently on the basis of Janovskaja's (1970: fig. 3) illustration of the holotype, and assigned this presumed long m2 as an autapomorphy for the species. Our own examination of a plaster cast of PIN 475–3016 shows no elongation of the m2 (fig. 14). In fact, our own measurements on the cast indicate a shorter length than the width for the m2 (3.0 mm in length and 3.2 mm in width), in sharp contrast to an elongated m2 shown in Janovskaja's figure. It seems clear that the m2 length in Janovskaja's illustration was exaggerated (the lack of morphological details in her illustration of the m2 further undermines the reliability of her published line arts). In our examinations of the rest of the dentitions, we failed to detect any substantial difference, either in size or shape, between the Russian collection and the rest of the samples. We thus fully agree with Lange-Badré and Dashzeveg that *Cynodictis mongoliensis* is synonymous with *Amphicynodon teilhardi*. The combined materials from AMNH, PIN, ZPAL, and MAE allow more confident assignments of fragmentary specimens and, as a result, increased morphological cohesion of this species.

Lange-Badré and Dashzeveg (1989: 141) chose to compare the Mongolian form with three Quercy species of *Amphicynodon*: *A. typicus*, *A. leptorhynchus*, and *A. gracilis*. They concluded that *A. teilhardi* was closer to *A. leptorhynchus* or *A. typicus* than to *A. gracilis*. Characters that were cited to indicate such a relationship include the wrinkled enamel and a reduced m2 paraconid. A revision of the systematics and phylogeny of *Amphicynodon* by Cirot and Bonis (1992: 119 and fig. 16), on the other hand, recognized 10 valid species, 8 European and 2 Asian, and suggested a relationship almost opposite to that suggested by Lange-Badré and Dashzeveg. Cirot and Bonis placed *A. teilhardi* (along with *A. mongoliensis*; see comments above) as the sister-taxon to the terminal clade formed by *A. gracilis* and *A. cephalogalinus*, whereas *A. leptorhynchus* and *A. typicus* are further down the tree in more basal positions. A critical synapomorphy cited in support of above relationship was a ''trigonide de M/1 disjoint'' shared by *A. teilhardi*, *A. gracilis*, and *A. cephalogalinus* (Cirot and Bonis, 1992: fig. 16, node 10). In their remarks on *A. teilhardi* (Cirot and Bonis, 1992: 119), this character was explained as an open trigonid due to a reduction and a posterior position of the metaconid of m1 (''un trigonide ouvert en raison de la réduction et de la position reculée du métaconide''). Lange-Badré and Dashzeveg's character, a reduced m2 paraconid, was pushed further down the tree by Cirot and Bonis and was shared by *A. velaunus*, *A. leptorhynchus*, *A. teilhardi*, *A. gracilis*, and *A. cephalogalinus*. While it is beyond our scope to reevaluate species relationships of *Amphicynodon*, we note that Cirot and Bonis's character of a disjoint m1 trigonid is not readily apparent in their illustrations of three of the four species of *Amphicynodon* that are supposed to share it. On the other hand, their illustration of *A. leptorhynchus* (Cirot and Bonis, 1992: fig. 3), a species that was supposed to possess a primitive condition for

this character, shows a more posteriorly displaced m1 metaconid than in any other species. Our own examination of some of Cirot and Bonis' materials in the Université de Poitiers, which form the partial basis of their systematic revision, fails to substantiate the validity of this character. Such a character, if it does exist, must be quite subtle at this stage of its evolution. In our observations, the presence and absence of an m2 paraconid does seem to be a valid character that unites some species of *Amphicynodon*, including *A. teilhardi*.

As for the generic status of the Mongolian species, Lange-Badré and Dashzeveg (1989: 141) rejected the initial suspicion by Matthew and Granger (1924) that the Hsanda Gol form was closer to the European *Pachycynodon* than to *Amphicynodon*: ''*C. teilhardi* belongs unquestionably to the genus *Amphicynodon*. It differs from *Pachycynodon* in the situation of the metaconid on m1, in the open basin, in the wrinkled enamel, in the reduced paraconid and entoconid in m2 and in the ratios of the talonid and trigonid on m2.'' Cirot and Bonis (1992) more explicitly placed *A. teilhardi* among the rest of the European species of the genus. In light of the entire dentition available in this study, *A. teilhardi* falls within the overall parameters of the genus. However, since *Amphicynodon*, as a basal ursoid, was long suspected to have given rise to other clades (e.g., Teilhard de Chardin, 1915), it is likely a paraphyletic genus in a strict cladistic sense—various species may ultimately be shown to be more closely related to other clades. Until a comprehensive, species-level phylogenetic analysis is done, current concepts of *Amphicynodon* remain largely gradational. See table 1 for more contrasts of morphological differences between *Amphicticeps* and *Amphicynodon*.

?*Cephalogale* sp.
Figure 15A–C

REFERRED SPECIMEN: MAE SG.97.5396, left ramal fragment with m2.

COMMENTS: MAE SG.97.5396 (fig. 15A–C) is clearly not assignable to the Hsanda Gol ursoids discussed above. The size of the m2 indicates an animal of the size of *Amphicticeps dorog*, but it does not have the extremely shortened m2 of the latter. Indicating its primitive status, MAE SG.97.5396 has a paraconid platform in front of the protoconid, and the paraconid is separate from the protoconid by a weak notch. A paraconid is absent in the Hsanda Gol *Amphicticeps* and *Amphicynodon*. Furthermore, the protoconid and metaconid are not widely separate from each other, as in both of the above genera. The morphological condition in MAE SG.97.5396 evokes that of a more primitive carnivoran, and the fact that it has an m3 alveolus tends to suggest a basal arctoid among known lineages in this period of time.

In size and overall proportions, MAE SG.97.5396 is closest to a recently described small arctoid, *Pachycynodon tedfordi* Wang and Qiu, 2003, from the early Oligocene Saint Jacques locality of Chinese Inner Mongolia (see further comments below about its generic status). Unfortunately, the m2 on the Chinese specimen is too worn to permit detailed comparisons.

PARVORDER MUSTELIDA TEDFORD, 1976

SUPERFAMILY MUSTELOIDEA FISCHER DE WALDHEIM, 1817

Pyctis inamatus Babbitt, 1999

COMMENTS: *Pyctis inamatus* was named on the basis of a left jaw fragment with p3 (broken)–m1 and partial m2 alveolus from the Tatal Gol area in a ''red claystone unit, SW of Maikant, 16.9 m above the lava layer in the Shand Member'' (Babbitt, 1999: 791). With an m1 length of approximately 11 mm, *Pyctis* is somewhat smaller than *Amphicticeps makhchinus* (arctoids tend to have a somewhat shorter P4 than m1; the reverse is true between *Pyctis* and *A. makhchinus*) but falls in the range of *A. dorog* (see measurements in tables 3, 5). *Pyctis* is highly hypercarnivorous with an extremely trenchant m1 talonid, which has a single, centrally located hypoconid, along with the complete loss of m1 metaconid. This dental pattern is almost exactly opposite to that in *A. makhchinus*, which tends toward the hypocarnivorous direction. *Pyctis* is also more hypercarnivorous than *A. dorog*, which still retains a substantial m1 metaconid and entoconid. Another important difference between *A. dorog* and

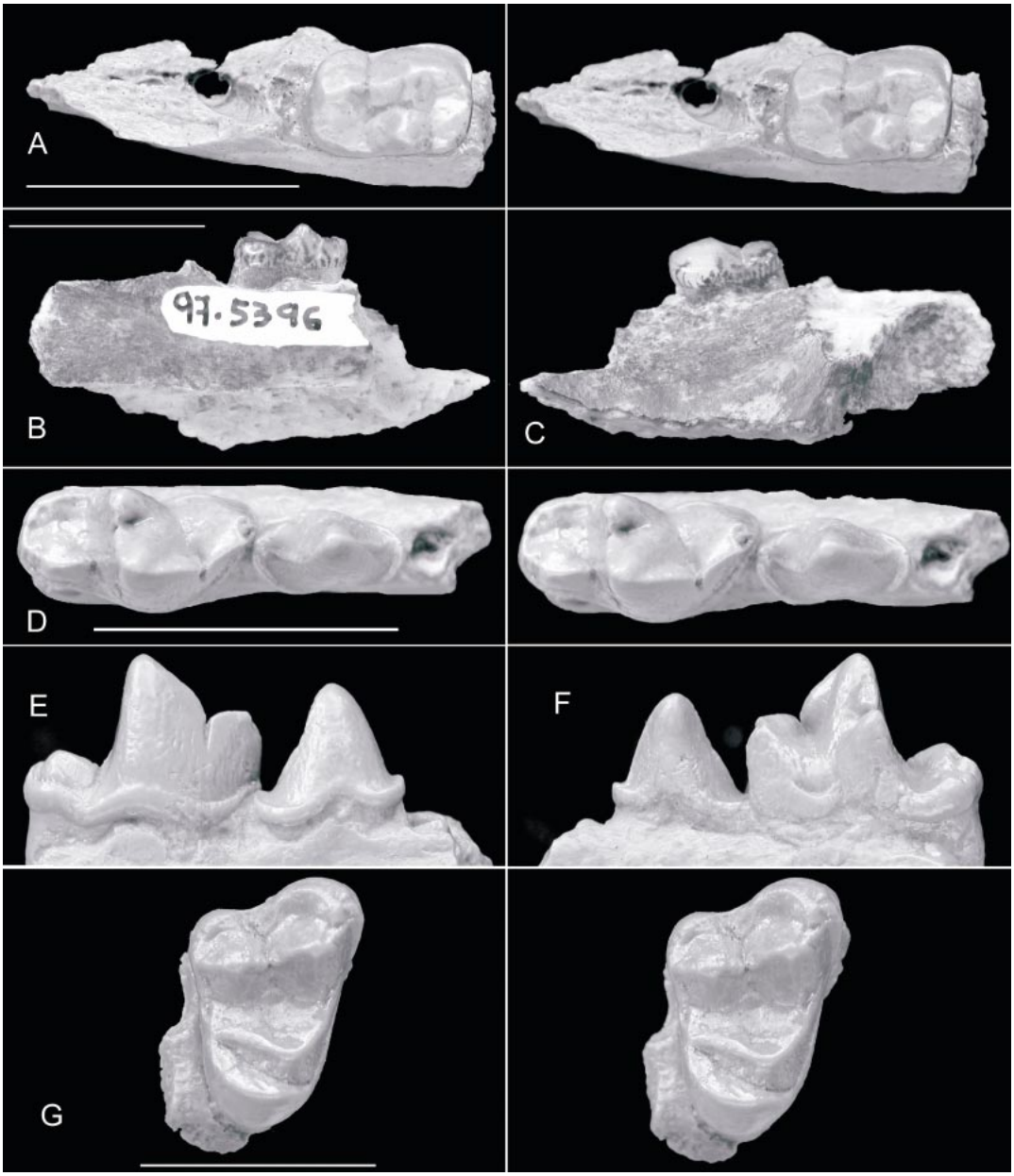

Fig. 15. **A,** stereophotos of occlusal view of left m2, **B,** labial view of jaw, and **C,** lingual view of jaw of MAE SG.97.5396, ?*Cephalogale* sp. **D,** stereophotos of occlusal view of right m1–2, **E,** labial view of jaw, and **F,** lingual view of jaw of IVPP V10527.1, ?*Amphicticeps* sp. **G,** stereophotos of right M1, ?*Amphicticeps* sp. Scales = 10 mm.

Pyctis is the presence of a posterior accessory cusp on the p4 of the former, which is lacking in the latter.

Babbitt (1999) compared *Pyctis* with some basal mustelids from the early Miocene of Europe, such as *Plesiogale* and *Paragale*, and she also made comparisons with later Eurasian forms, such as *Eomellivora* and *Mellivora*. Given the poor condition of the holotype, she did not draw definitive system-

atic conclusions, except placing it in the family Mustelidae.

Pyctis also shares some resemblance to certain oligobunines (a group of basal musteloids) in the late Oligocene through early Miocene of North America (Baskin, 1998a), such as *Oligobunis* and *Megalictis*, which also have a highly hypercarnivorous lower carnassial and reduced posterior accessory cusp on p4. On the other hand, *Ischyrictis* and *Hoplictis* from early to middle Miocene of Europe also exhibit tendencies toward hypercarnivory (Ginsburg and Morales, 1992). The systematic status of *Pyctis* will remain uncertain without additional materials, particularly its upper teeth.

Comments on Chinese Basal Ursoids

Huang (1993) described a right ramal fragment with p4–m1 (IVPP V10527.1) and a left ramal fragment with m1 (IVPP V10527.2) from the early Oligocene Ulantatal locality, Ulantatal Formation, Inner Mongolia (fig. 1). He tentatively referred it to? *Amphicynodon* sp. Huang considered the Chinese materials to have a broad m1 talonid and therefore similar to that of *A. teilhardi*. However, he was rightly cautious in his assignment of these jaw fragments to *Amphicynodon* because of the poor preservation of the materials. Indeed, our own examination of a cast of IVPP V10527.1 (fig. 15D–F) led us to the following observations that the Ulantatal materials do not compare well with known Asian species of *Amphicynodon* and *Amphicticeps*.

Contrary to Huang's description, the m1 talonid is not broad—it is substantially narrower than that of *Amphicynodon teilhardi*. Correlated to this narrow talonid, IVPP V10527.1 also has a relatively trenchant m1 talonid, that is, high crowned m1 hypoconid dominating over a low entoconid crest, and is in contrast to a flat, basin-like talonid in *A. teilhardi*, as well as in most known European species of *Amphicynodon*. Of the 10 species of *Amphicynodon* recognized by Cirot and Bonis (1992), only three European species are known to have a high hypoconid: *A. typicus* (FSP PC 46 from Pech Crabit, Cirot and Bonis, 1992: fig. 14), *A. gracilis* (MNHN QU 9192 in Cirot and Bonis, 1992: fig. 11), and *A. crassirostris* (personal observation on an uncataloged specimen of Musée de Gaillac). Another prominent feature of IVPP V10527.1 is its high-crowned p4 that lacks of a posterior accessory cusp, a character also relatively rare among known species of *Amphicynodon*. Only two European species of *Amphicynodon* approach this condition—*A. gracilis* and *A. speciosus* (Cirot and Bonis, 1992: figs. 7, 11) lost the posterior accessory cusp, and a third species, *A. velaunus*, has nearly lost this cusp (Cirot and Bonis, 1992: fig. 1). It thus appears that IVPP V10527.1 is best compared with *A. gracilis* in terms of the p4. Our own comparisons with a referred specimen of *A. gracilis* (MM 11, see Teilhard de Chardin, 1915: pl. VIII, fig. 2) further confirm the above observation, although this specimen is much smaller than the Inner Mongolian form. On the other hand, the overall morphology of the m1 of IVPP V10527.1 is closest to that of *Amphicticeps*, particularly in its narrowed talonid relative to the laterally bulging trigonid, a condition *Amphicynodon* does not have. Given the fragmentary nature of the Ulantatal materials, it is difficult to choose between a small but aberrant (in terms of the absence of a posterior accessory cusp of p4) form of the local *Amphicticeps* or a taxon close to the European *Amphicynodon gracilis*. What seems to be certain is that the Inner Mongolian form is not closely related to *A. teilhardi*.

Most recently, Wang and Qiu (2003a) described three species of ursoids, based also on rather poor materials, from the early Oligocene Saint Jacques locality (fig. 1), Wulanbulage Formation, Inner Mongolia. A left lower jaw with c–m2 (IVPP V12426) was named a new species, *Pachycynodon tedfordi*; a maxillary fragment with M1 (IVPP V12428) was referred to *Amphicynodon* sp.; and an isolated left M2 (IVPP V12429) was referred to *Cephalogale* sp. Of these, *P. tedfordi* has the best material available and is also the least similar to known forms in Asia. For one thing, it has a rather long m2, unlike any known Asian *Amphicynodon* or *Amphicticeps*, but is consistent with an elongated m2 talonid in *Pachycynodon*. However, *P. tedfordi* also has narrow and trenchant cheek teeth, in sharp contrast to European species

of *Pachycynodon* that tend to have broad premolars and molars. Such relatively hypercarnivorous features are also seen in certain European specimens of *Cephalogale*. In particular, a posteriorly expanded m2 hypoconid is frequently associated with a posteriorly oriented M2 postprotocrista, a diagnostic feature for *Cephalogale*. This long hypoconid occludes with the posteriorly opened trigon basin of the M1 due to the reorientation of its postprotocrista. IVPP V12426 is particularly close to *Cephalogale minor*. For example, FSP PFRA 32, from the Pech du Fraysse locality of the Quercy district in the late Oligocene (Paleogene biochronological level MP 28; BiochroM'97, 1997), has proportions very similar to the lower cheek teeth of IVPP V12426. *C. minor*, as currently conceived, shows substantial variation (Beaumont, 1965; Bonis, 1973). The possibility that IVPP V12426 and V12429 may be conspecific cannot be ruled out at the moment.

As for the M1 in IVPP V12428 (fig. 15G), it is larger and more robust than those of all species of *Amphicynodon* that have preserved upper teeth (e.g., *A. velaunus*, *A. leptorhynchus*, and *A. teilhardi*). Furthermore, its parastyle area is also better developed than those of all known species of *Amphicynodon*. In that sense, IVPP V12428 is closer to *Amphicticeps dorog* than to *Amphicynodon*. The locations of the M2 roots also indicate an M2 equivalent in size to that of *A. dorog*. Beside such tentative observations, however, a more definite judgment will have to await further discovery.

PHYLOGENETIC ANALYSIS

Concepts of Major Clades and Selections of Basal Taxa

Our phylogenetic analysis of the Arctoidea stems from observations that past studies of higher level relationships are often based on living taxa (crown groups) or those that belong to terminal clades. While such an approach has the benefit of completeness of information (morphological as well as molecular) and taxonomic clarity (memberships of living taxa are rarely in doubt), with the exception of a few ''living fossils'' (such as African palm civet *Nandinia*), living taxa too often are far removed from the initial divergence point where their respective clades originated, and possess many derived characters that tend to obscure true relationships. In Carnivora, a limited morphological repertoire in which a clade can vary ensures that few morphological characters are truly unique. The result is an overwhelming number of homoplasies that are difficult to distinguish from true synapomorphies whenever the subjects have diverged from the point of origin for a sufficiently long time.

A solution to such a problem seems to lie in the studies of basal members of major clades, where the addition of fossils can reveal relationships previously obscure (Gauthier et al., 1988). Close to the point of divergence, basal taxa did not undergo long periods of differentiation as the terminal members did, and thus are far less affected by homoplasies and more likely to reveal the true morphotypical status of the clade. The disadvantage in such an approach, however, is that basal members are often small, generalized forms that commonly have poor fossil records, a problem that usually eases somewhat over time as fossil records improve. Such is the case in the basal arctoids as afforded by recent additions in Hsanda Gol materials. However, even where the fossil records are becoming adequate, it is imperative to ascertain the memberships of the basal forms in the major clades. It is therefore a matter of considerable importance to make sure that our selections of basal taxa are truly representative of their clades, and the following discussion attempts to detail our concept of the basal taxa selected for analysis. Our classification scheme follows that by McKenna and Bell (1997).

Cynoidea: The infraorder Cynoidea contains living and fossil relatives of foxes, wolves, and jackals in the family Canidae. Derived from the archaic, paraphyletic family Miacidae, Canidae is the first to arise among living families of Carnivora and tends to have the most conservative morphology. The basal canids are represented by excellently preserved materials from the late Eocene to early Oligocene of North America, and a common basal taxon, *Hesperocyon*, serves as an ideal outgroup for the present analysis both in terms of its primitive morphology and its closeness to the basal di-

chotomy of the Cynoidea and Arctoidea (Tedford, 1978; Wang, 1994; Wang and Tedford, 1994, 1996; Tedford et al., 1995).

Arctoidea: The infraorder Arctoidea represents the largest group of predators, with 211 extinct and 56 living genera (McKenna and Bell, 1997). It includes living families of bears (Ursidae), seals, sea lions, and walrus (Phocoidea = Pinnipedia), red pandas (Ailuridae), raccoons (Procyonidae), weasels, badgers, and otters (Mustelidae), as well as the extinct bear dogs (Amphicyonidae). Arctoids feature an unsurpassed diversity of terrestrial and aquatic adaptations and the widest extremes of dental specializations. Perhaps because of these extremes in morphological and ecological variations, arctoid relationships have been highly controversial and consistent resolutions have proven elusive so far. Attempts at phylogenetic synthesis are usually confined to forms that are well defined enough within a clade, often leaving the critically important basal forms unattended. We will include most early arctoid genera in our analysis (see below).

Ursida (= *Ursoidea*): Within the infraorder Arctoidea, parvorders Ursida and Mustelida represent two first-order dichotomous clades. Ursida includes the living Ursidae and the aquatic Phocoidea (= Pinnipedia), as well as the extinct bear-dogs (Amphicyonidae). The early Oligocene *Amphicynodon* is probably one of the most primitive members of Ursida known, and it plays a critical role in anchoring the Ursida clade. A North American group of basal Ursida includes the genera *Parictis*, *Subparictis*, and *Nothocyon* from the Chadronian to early Arikareean (late Eocene to late Oligocene; Clark and Guensburg, 1972; Wang and Tedford, 1992; Baskin and Tedford, 1996). Placed in a small clade of its own, Subparictidae (Baskin and Tedford, 1996) is still too poorly known to be included in this analysis.

Ursidae: Living members of the ursids are morphologically well defined by their hypocarnivorous dentitions. Fossil ursids, however, include some rather hypercarnivorous taxa but have never achieved the extreme hypercarnivory seen in mustelids (Hunt, 1998c). The mesocarnivorous *Cephalogale* is widely regarded as the most primitive ursid (e.g., Beaumont, 1965; Bonis, 1973; Ginsburg and Morales, 1995; Hunt, 1998c) and is ideally suited as a representative basal taxon for the family. Even among its primitive species, such as *C. minor* from the French Quercy phosphate fissures, such ursid synapomorphies as posteriorly oriented M2 postprotocrista, elongated m2, and reduction of premolars are already recognizable.

Phocoidea (= *Pinnipedia*): Extreme aquatic adaptations in the pinnipeds tend to obscure the primitive conditions of ancestral forms. Nowhere is this more apparent than in the secondarily undifferentiated teeth of living pinnipeds, which bear practically no resemblance to those of terrestrial arctoids. It is not surprising that pinniped relationships have been the most controversial among arctoids. Controversies still exist regarding the monophyletic versus diphyletic origins of the pinnipeds (e.g., Mitchell and Tedford, 1973; Tedford, 1976; Wiig, 1983; Wyss, 1987, 1988; Berta and Wyss, 1994; Flynn and Nedbal, 1998; Berta and Adam, 2001) or whether pinnipeds arose from ursoids or musteloids (e.g., Wolsan, 1993; Hunt and Barnes, 1994). For the present analysis, we assume the terrestrial *Pachycynodon* and its sister taxon *Allocyon* to be stem groups in the pinniped clade (Tedford et al., 1994), although the aquatic *Potamotherium* has been argued to play a role in the origin of the pinnipeds (e.g., Tedford, 1976; Wolsan, 1993) or not (Wyss, 1991). We also include *Potamotherium* in this analysis.

Amphicyonidae: Traditionally thought to be closely related to canids, mostly due to their conservative dental morphology (e.g., Matthew, 1924; Kuss, 1965), amphicyonids (bear-dogs) have a rather arctoid basicranium (Hough, 1948; Hunt, 1974, 1977, 1996a, 1998a). More specifically, many amphicyonids share with ursids a greatly enlarged inferior petrosal sinus that houses a double-looped internal carotid artery, presumably a counter current exchange mechanism for the cooling of the brain. It has become increasingly accepted that amphicyonids are arctoids and may be closely related to the ursids (Flynn et al., 1988; Viranta, 1996; Ginsburg, 1999). The most primitive amphicyonids appear to be the late Eocene *Daphoenus* of North America and *Cynodictis* of Europe; both gave rise to later clades in their respec-

tive continents (Kotsakis, 1980; Hunt, 1996a, 1998a, 2001). Unfortunately, the basicranial systems of these basal forms have not been studied adequately, and we exclude them from our analysis.

Mustelida (= *Musteloidea*): Outside the clades represented by Mustelidae and Procyonidae lie the basal musteloids, which, lacking all or parts of the derived features, do not fit neatly in any particular pattern and presumably occupy a place in a basal bush (Wolsan, 1993). This loosely defined musteloid stem group includes the archaic *Amphictis*, *Mustelictis*, *Bavarictis*, *Stromeriella*, and *Plesictis* from the Oligo–Miocene of Europe, in addition to some less well known taxa. Recent attempts to resolve relationships of these forms have met with limited success (Schmidt-Kittler, 1981; Cirot and Bonis, 1993; Wolsan, 1993), because of the increasing realization that nearly all characters traditionally thought to be consistent and reliable are subject to homoplasies of greater or lesser degrees. In North America, a similar group of archaic musteloids occurs in the Arikareean through Barstovian time (late Oligocene to middle Miocene). Referred to here as the Oligobuninae (Baskin, 1998a), it includes *Promartes*, *Oligobunis*, *Aelurocyon*, *Megalictis*, *Zodiolestes*, and *Brachypsalis*. Riggs (1945) proposed a linear transformation series from the primitive *Promartes*, through the intermediate *Oligobunis*, to the hypercarnivorous *Aelurocyon* and *Megalictis*. *Brachypsalis* is derived in its own peculiar way (presence of a P4 parastyle, enlarged M2, broadened lower molars, etc.), and its relationship with respect to Riggs' phylogenetic framework is unclear. *Zodiolestes*, on the other hand, has a deeply excavated suprameatal fossa and lacks a posterior crest on the mastoid process, and has been argued to be a procyonid (Hough, 1948; Schmidt-Kittler, 1981).

Another part of the basal musteloid radiation leads to an aquatic form, *Potamotherium*, in Eurasia and North America (Semantorinae Orlov, 1933). *Potamotherium* (see Savage, 1957, for a detailed description) is sometimes cited as a primitive pinniped, and thus is a contentious taxon in the controversy on monophyletic/diphyletic origin(s) of the Phocoidea. While study of a sister-group relationship (e.g., McLaren, 1960; Tedford, 1976; Muizon, 1982; Wolsan, 1993) or lack of it (e.g., Wyss, 1991) between *Potamotherium* and phocid pinnipeds is out of the scope of this paper, recent morphological and molecular studies seem mostly in favor of a monophyletic Pinnipedia with an ursoid origin (see Berta and Wyss, 1994, for a recent summary), and *Potamotherium* may thus be decoupled from discussions about pinniped phylogeny (Wyss, 1991), that is, aquatic adaptations in *Potamotherium* are hypothesized to be derived independently (but see Wolsan, 1993, for an alternative argument).

A very primitive musteloid, *Mustelavus*, from the late Eocene (Chadronian) to early Oligocene (Orellan) of North America, apparently occupies the most basal position in the Mustelida (see Baskin and Tedford, 1996). Although the original holotype skull was crushed, contributing to its relative obscurity since its original description, a new, undescribed skull is available in the AMNH collection that supplies important information in the present analysis. As shown in our phylogeny, *Mustelavus* occupies the most basal position of all Mustelida, and helps to establish its morphotypic status for the entire Mustelida clade.

Ailuridae: The highly derived and enigmatic Asiatic red (lesser) panda, *Ailurus* (and closely related *Parailurus*), and the related hypercarnivorous *Simocyon* form a small clade of their own, and their controversial phylogenetic position (e.g., Ginsburg, 1982; Wang, 1997) is increasingly pushed toward the base of the Arctoidea in recent studies of molecular phylogenies (Vrana et al., 1994; Flynn et al., 2000). Unfortunately, fossil records for Ailuridae are extremely rare and recent, with the exception of some dental fragments suggestive of red panda in the middle Miocene of Europe (Ginsburg et al., 2001), the earliest being the single tooth of *Pristinailurus* from the late Miocene or Pliocene of North America (Wallace and Wang, 2004) leaving a long gap of possibly ~30 My in the fossil record. We have no choice but to use the living genus *Ailurus* in the present analysis. However, its highly hypocarnivorous dentition is obviously far removed from the morphotypical condition of the ailurid clade. The Ailuridae is the only instance

in our analysis in which a basal taxon is not available, and our result cannot be completely free of the influence of homoplasies. Its sister group Simocyoninae has somewhat better fossil records, which go back to *Alopecocyon* in the middle Miocene of Eurasia (Viret, 1951; Ginsburg, 1961; Wang et al., 1998). *Alopecocyon* is mostly known by fragmentary materials. We thus use the terminal genus *Simocyon*, which is relatively better known (Wang, 1997).

Procyonidae: Although presently confined to North and South America, procyonids probably originated in the Old World (Baskin, 1982, 1989, 1998b; Wolsan, 1993). Living and most fossil procyonids can be diagnosed by an elongated m2 talonid and a modest suprameatal fossa (e.g., Schmidt-Kittler, 1981; Baskin, 1982, 1989, 1998b; Flynn et al., 1988; Wyss and Flynn, 1993). The most primitive forms of this clade appear to be the late Oligocene to early Miocene European *Pseudobassaris*, *Angustictis*, and *Broiliana* (Wolsan, 1993). We use *Broiliana* as a morphotypical synecdoche for the Procyonidae, which is agreed upon by recent workers (e.g., Baskin, 1982; Wolsan, 1993).

Mustelidae: Living members of the family Mustelidae constitute the largest and most diverse group of terrestrial arctoids. Most taxa can be diagnosed by a loss of a carnassial notch, ventrally enclosed suprameatal fossa, and loss of the M2 (e.g., Tedford, 1976; Schmidt-Kittler, 1981; Flynn et al., 1988; Bryant et al., 1993; Wyss and Flynn, 1993; Baskin, 1998a), although some homoplasies for these characters may have existed (Qiu and Schmidt-Kittler, 1982; Wolsan, 1993). The absence of the alisphenoid canal, shared by living members of mustelids and procyonids, is sometimes cited as a synapomorphy uniting the two families, although it may have been independently acquired (Wolsan, 1993; Wang, 1997). We follow Wolsan (1993) and accept that European early Miocene *Paragale* and *Plesiogale* represent the most primitive mustelids (mustelines of Wolsan, 1993). These genera, along with a recently discovered *Kinometaxia* from China (Wang et al., 2004), are included in the analysis.

Mephitidae: The skunks are traditionally treated as a subfamily in the Mustelidae (Schmidt-Kittler, 1981; Bryant et al., 1993; Wolsan, 1999), despite its apparently more primitive upper molars, bullar compositions, and brain morphology (Radinsky, 1973; Hunt, 1974; Wang and Qiu, 2004). Recent molecular studies (e.g., Ledje and Arnason, 1996a, 1996b; Dragoo and Honeycutt, 1997; Flynn and Nedbal, 1998), however, have increasingly indicated a more basal position for the skunks in the Mustelida or even Arctoidea, raising Mephitinae to family rank. Morphological studies, on the other hand, have not kept up with the apparent molecular advancement. However, a middle Miocene genus from Europe, *Palaeomephitis*, has been identified as the earliest mephitid (Wolsan, 1999). *Palaeomephitis* features a highly autapomorphous dental morphology (e.g., Fraas, 1870; Wegner, 1913; Wolsan, 1999), which almost certainly rules out its being in a basal position of the family. Until a more appropriate stem group is identified, we tentatively leave the mephitids aside, pending further investigations.

Character Analysis

Discrete morphological characters are coded to compile a 22 taxa $\times$ 39 characters data matrix (table 8) for parsimony analysis. Most characters used in this study have been mentioned by previous authors, although often in a different context and carrying different meanings. Our own contribution is mainly in the reexamination of the characters in a broader context, thus showing their relevance in the basal relationships of the arctoids. By necessity only cranial and dental characters, commonly the best preserved in fossil records, are used in this analysis. See Appendix 1 for a list of character descriptions and their states that correspond to those in the data matrix.

Parsimony Analysis of Basal Arctoids

Using *Miacis* and *Hesperocyon* as outgroups, we performed a maximum parsimony analysis on the 22 taxa $\times$ 39 characters data matrix compiled in the above Character Analysis using the computer program PAUP (Swofford, 1993). Searches using the ''Branch and Bound'' option yielded 36 shortest trees of 89 steps in length. A boot-

TABLE 8
A 22 Taxa × 39 Characters Data Matrix Used in the PAUP Analysis[a]

	1		2		3			
	12345	67890	12345	67890	12345	67890	12345	6789
Miacis	00000	0?000	00000	00000	00000	00000	?0000	0000
Hesperocyon	00000	0?000	01000	00000	00000	00001	10001	1110
Mustelavus	01000	??000	01000	?0000	01000	??101	?100?	??11
Amphictis	01001	0?000	02000	00031	01020	00001	?1001	1?11
Simocyon	01001	1?001	02000	31031	21021	11001	01101	1011
Ailurus	01001	00100	22000	30231	21221	11001	00001	1011
Broiliana	00112	00000	12000	30231	21200	00001	??001	1?1?
Stromeriella	00111	01001	12000	00031	01000	??001	?100?	??1?
Mustelictis	00002	00000	02010	00100	011?0	??001	?1001	1?11
Bavarictis	00001	00000	02000	00100	011??	?0001	??001	1?1?
Pseudobassaris	00011	00000	02000	00100	0110?	00001	0?001	101?
Plesictis	11112	00000	02000	10110	011?0	00001	??001	1?11
Promartes	01110	00000	01000	10110	11100	00101	?1001	1011
Potamotherium	01110	00001	11001	10110	11100	00101	01011	1011
Kinometaxia	11113	??110	0110?	2????	1?10?	??101	?100?	??11
Paragale	01113	0?010	0110?	21120	11100	00101	??01?	??11
Plesiogale	01113	01010	0110?	22120	111??	??101	??00?	??11
Amphicticeps	00001	0?000	01001	10010	10010	00101	?1011	1?11
Amphicynodon	00000	0?000	02000	00000	00010	00011	?1011	1?11
Cephalogale	00000	??001	02000	30030	20010	0?011	01111	1?11
Pachycynodon	01000	??001	12000	30000	2001?	?0011	01111	1011
Allocyon	01000	0?001	12000	30000	200?0	?00?1	01111	1?11

[a] Character numbers correspond to those listed in appendix 1.

strap analysis (fig. 16) shows relative support for individual nodes and a strict consensus of the 36 trees is shown in figure 17. Despite a relatively poor bootstrap support, many of the basal arctoids are well resolved in the consensus tree, except parts of the basal bush of the Mustelida, which have been difficult to resolve due to an unusually high diversity in the initial radiation of the Mustelida in the late Oligocene to early Miocene of Europe (see Wolsan, 1993).

Most of the major clades in our phylogeny (fig. 17) are supported by one or two derived characters. Such a small number of synapomorphies is not necessarily an indication of weak support for the respective clades. Instead, this is a reflection of the morphological closeness of all basal taxa analyzed (with the exception of *Ailurus*). Such a morphologically closely spaced array of taxa naturally yields few characters. We would argue that our use of basal taxa closely approximates the early divergence of arctoids and the strength of our phylogeny lies in the short morphological distance between taxa. Our phylogeny thus captures a sense of realism to reflect the early radiations, something that is not possible by studying terminal members of the clades. Such a sense of intimacy in observing early diversifications, as afforded by the richness of fossil record, is a strength of paleontology even in light of the increasingly large data set afforded to neontology.

The following paragraphs are brief narratives to highlight salient features of our phylogeny. As shown in the character optimizations in figure 17, the crown portion of the suborder Caniformia (Cynoidea + Arctoidea) is well differentiated from the archaic ''miacids'' by several derived characters: presence of an ossified bulla, a medially positioned internal carotid artery, reduction of M1 parastyle, and loss of M3. Infraorder Cynoidea is also well supported by autapomorphies that are unique to the canids, such as a type B bulla with enlarged caudal entotympanic and a semi-septum within the bullar chamber (Hunt, 1974; Wang and Tedford, 1994).

Infraorder Arctoidea is supported by two

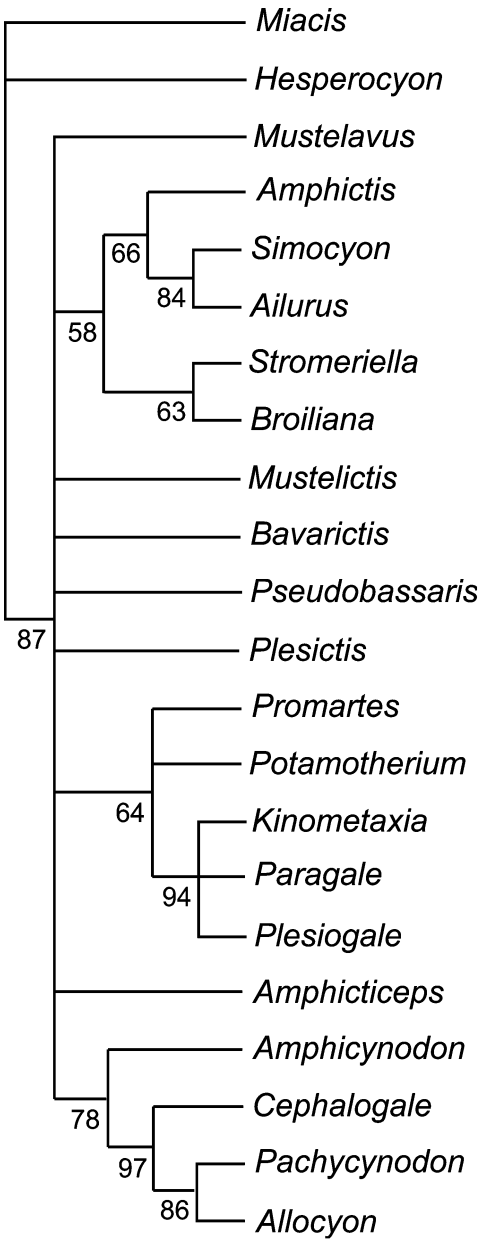

Fig. 16. Bootstrap analysis based on the data matrix in table 8. Numbers at the nodes indicate percent bootstrap support from heuristic search based on 100 replicates. Only groups with a frequency of greater than 50% are retained.

synapomorphies: a reduction or loss of posterior accessory cusps on premolars and a widening of the basioccipital between the bullae. Traditional phylogenetic assessments based on living taxa alone often list the loss of the alisphenoid canal and an elongated external auditory meatus as key synapomorphies for the arctoids (e.g., Flynn et al., 1988; Wyss and Flynn, 1993). These characters are almost certainly independently derived within various lineages of arctoids, when they are seen in the broader perspectives that include basal arctoids shown here.

Within the arctoids, the commonly accepted Ursida–Mustelida dichotomy is also reflected in our own phylogeny. The Mustelida includes all taxa that have lost the last lower molar (m3), as a commonly used synapomorphy (e.g., Tedford, 1976; Schmidt-Kittler, 1981). This loss of the last lower molars, which happens numerous times in mammals, was justifiably suspected to be a weak character (Schmidt-Kittler, 1981), and our demonstration in this study that *Amphicticeps* has independently lost its m3 adds further evidence of the homoplasticity of such a character. Nonetheless, it remains as the only derived character uniting the Mustelida. The North American *Mustelavus* is at the base of the entire Mustelida, and appears to be a stem taxon outside the mustelid–procyonid–ailurid clade.

European basal Mustelida are united by their possession of a small suprameatal fossa and reduced M1 parastyle, as demonstrated by Schmidt-Kittler (1981) and Wolsan (1993). A dichotomy between mustelids plus stem groups and procyonids plus stem groups (including ailurids) is supported by an enlarged m2 with an elongated talonid on the procyonid side, and a lingual notch in front of m1 entoconid and loss of M1 postprotocrista on the mustelid side. Presence of a suprameatal fossa has long been considered as a key synapomorphy for procyonids (Riggs, 1942, 1945; Segall, 1943; Hough, 1944, 1948), but this character has been further elaborated in the mustelids plus their stem groups to be the basis of a new phylogenetic scheme of the mustelids (Schmidt-Kittler, 1981; Wolsan, 1993). Elsewhere, Wang et al. (2004) explored the basal mustelid relationships in greater detail than is afforded here, including additional stem taxa not analyzed here.

Two derived characters help to push *Amphicticeps* toward the Ursida side: a dorso-

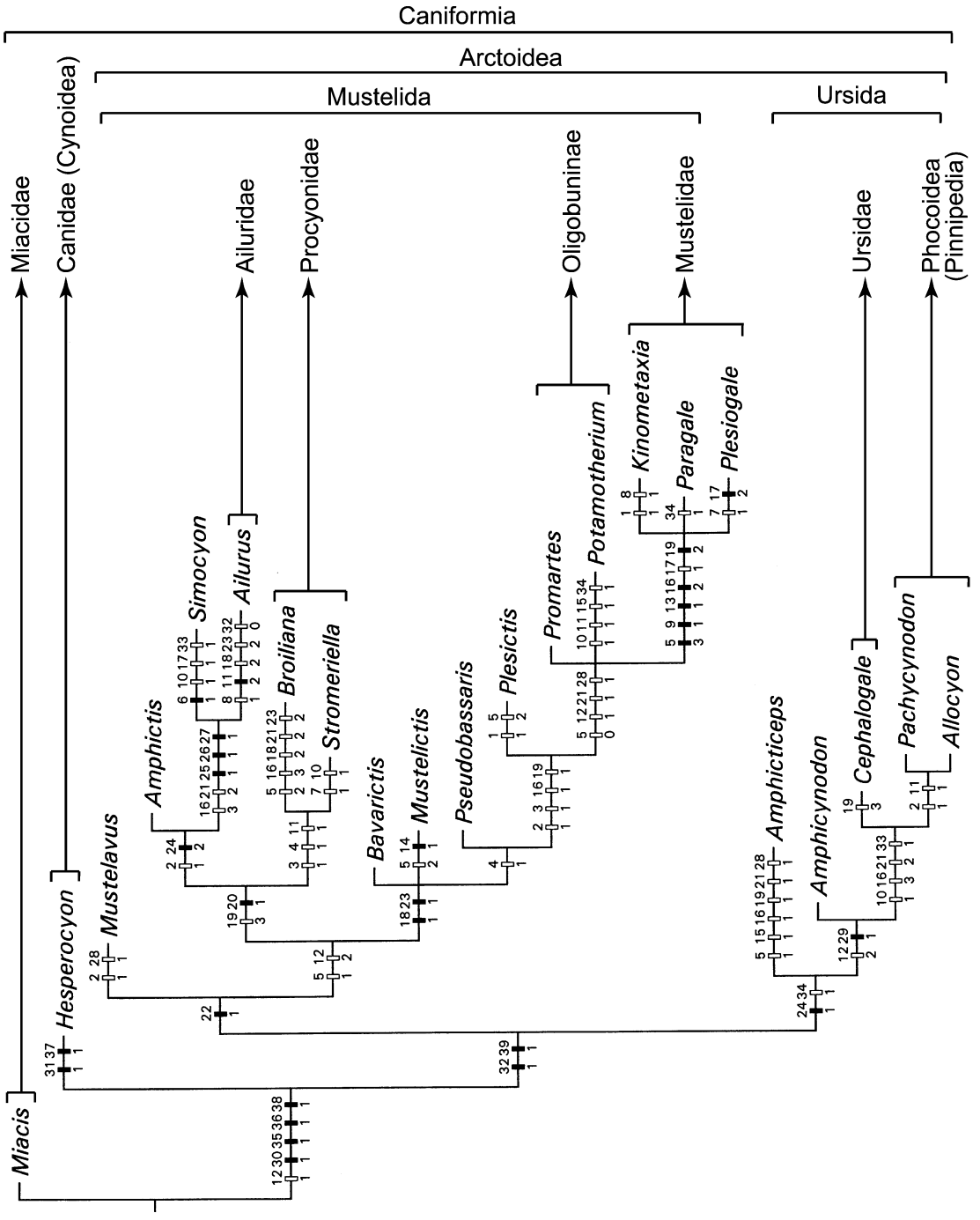

Fig. 17. Cladistic relationships of basal arctoids based on a strict consensus tree from 36 shortest trees (tree length = 89 steps) that were recovered from Branch and Bound method in the PAUP program (Swofford, 1993 version 3.1.1) on the 22 taxa × 39 characters data matrix (table 8). Character distributions are optimized using ClaDos program (version 1.2 by Kevin Nixon): solid bars are synapomorphies and open bars are homoplastic characters (parallelisms and reversals); numbers above the branches are character numbers and those below the branches are character states.

ventrally compressed, laterally expanded paroccipital process and a long distance between the postorbital process and the postorbital constriction. Such characters are often homoplastic and, in the present case, are not enough to withstand the bootstrap analysis (fig. 16). The highly autapomorphic *Amphicticeps* does not easily conform to any existing scheme of systematics, as shown by previous controversies (see above), and the present placement within the Ursida is also somewhat tentative. In favor of this placement, however, is a laterally expanded mastoid process in *Amphicticeps*, a character most prominently developed in the ursids and pinnipeds, but here treated as an autapomorphy by the parsimony program because of a relatively small mastoid process in *Amphicynodon*.

As recovered in the bootstrap analysis, undoubted Ursida starts at *Amphicynodon* with its incipient development of a posteriorly oriented postprotocrista of M1 and a very reduced parastyle, characters that are further elaborated in ursids. The position of *Cephalogale* as a basal ursid has been widely accepted (e.g., Beaumont, 1965; Bonis, 1973; Ginsburg and Morales, 1995; Hunt, 1998c). Its sister relationship to the phocoids is supported by a crestlike P4 protocone that is posteriorly positioned, enlarged M2, and enlarged mastoid process. These derived characters exclude *Amphicynodon* from being placed within the Ursidae–Phocoidea clade, and renders the Amphicynodontidae (Simpson, 1945; Cirot and Bonis, 1992; Baskin and Tedford, 1996; Hunt, 1996b) a paraphyletic group.

Here, we assume that the Phocoidea is monophyletic, based on recent morphological and molecular studies (Wyss, 1987; Wyss and Flynn, 1993; Berta and Wyss, 1994; Vrana et al., 1994; Flynn and Nedbal, 1998). The basal phocoid *Enaliarctos* has been demonstrated to be more ursoid than musteloid in its basicranium and dentition (Hunt and Barnes, 1994) and the terrestrial *Pachycynodon* and *Allocyon* are probably the closest stem taxa for the phocoids (Tedford et al., 1994). Under our phylogenetic scheme, *Potamotherium* must have acquired its aquatic adaptations independently from the phocoids.

RELATIONSHIPS WITHIN *AMPHICTICEPS*: Given the limitation of the fragmentary materials in two of the three recognized species of *Amphicticeps*, a comprehensive phylogenetic analysis using the full spectrum of cranial and basicranial characters listed above is not feasible. Instead, we tacitly assume that cranial and basicranial characters for *A. dorog* and *A. makhchinus* are similar to those of *A. shackelfordi* and that they mainly differ by dental morphology and size. Based on dental characters, relationships among species of *Amphicticeps* appear to fall in a linear progression, starting from the small *A. shackelfordi*, transitioning through the intermediate *A. dorog*, and ending in the large *A. makhchinus*.

Using *Miacis* and *Hesperocyon* as outgroups, character transformations within *Amphicticeps* can be deduced to show the following trends. A basal status for *A. shackelfordi* is indicated by such primitive characters as relatively less robust dentitions, small but high-crowned P4 protocone, large M1 parastyle, and the presence of an m3 in some individuals. *A. shackelfordi* may have one autapomorphy of its own: a reduced and lingually shifted M2, a condition that parallels that in the basal musteloid *Potamotherium*.

Amphicticeps dorog is obviously more derived than *A. shackelfordi* in the following characters: larger size and more robust dentitions and jaws, a more crestlike P4 protocone that is relatively lower crowned, a slightly more distinct P4 anterior cingulum, a reduced M1 parastyle (and consequently a larger angle between the labial borders of the P4 and M1), and the loss of an m3. *A. dorog* also has a larger and more labially positioned M2.

Amphicticeps makhchinus is apparently the most derived species of the genus. Compared to *A. shackelfordi* and *A. dorog*, *A. makhchinus* is the largest in size, has the broadest P3, possesses the lowest and most enlarged P4 protocone crest, and features the most reduced M1 parastyle, the largest M1 metaconule, and the greatest expansion of M1 lingual cingulum. *A. makhchinus* also hints at a relatively large and labially positioned M2. Most of the above derived characters in *A. makhchinus* suggest a modest

tendency toward hypocarnivory, paralleling some dental characters of the ursids.

ZOOGEOGRAPHIC COMMENTS

The theater of evolution for early arctoids centers around the northern continents (Holarctic region), at a time when southern continents are wholly or partially isolated from the northern continents. On the caniform side of the Carnivora, the archaic and paraphyletic family Miacidae, from which arctoids are presumably derived, was present in all three northern continents: Europe, Asia, and North America (Hunt, 1996b; McKenna and Bell, 1997). First to arise from the miacids is the Cynoidea (including family Canidae) from the Bridgerian and Uintan (middle Eocene) in the form of ''*Miacis*'' *sylvestris* and ''*Miacis*'' *gracilis* of North America (Wang and Tedford, 1994) followed by the true canids *Prohesperocyon* and *Hesperocyon* in the Duchesnean and Chadronian (late Eocene; Wang, 1994). The rest of canid history was mostly played in the North American continent until late Miocene, when some members finally crossed the Bering Strait to enter into Eurasia (Crusafont-Pairó, 1950), and later in the Pliocene, when canids crossed the Panamanian Isthmus to arrive in South America (Berta, 1987, 1988).

The case for the origin of arctoids is less clear. Almost all major clades of the arctoids (except pinnipeds) have their basal members first appearing in Europe, such as *Cynodictis* for basal amphicyonids, *Cephalogale* for basal ursids, *Broiliana* (and other genera) for basal procyonids, and *Plesiogale* (and others) for basal mustelids. However, North America also has several basal arctoids that may predate the European counterparts. On the Mustelida side, *Mustelavus* occupies the most basal position in the musteloids. Its first appearance in the Chadronian is probably earlier than most of the Quercy musteloids. On the Ursida side, the North American subparictines are comparable to European amphicynodontines in their stage of evolution, and their occurrence in the Chadronian may also predate the European counterparts (many of the classic Quercy fissure collections from France cannot be dated precisely and generally range from late Eocene to Oligocene). As for the more basal amphicyonids, North American *Daphoenus* is similar in stage of evolution to the European *Cynodictis*, and both of them first appear in the late Eocene (Hunt, 1996a, 1998a). Although some authors are inclined to treat the above North American basal arctoids as occasional immigrants from Eurasia (e.g., Hunt, 1996b), given that the North American forms are either more primitive and/or earlier in occurrence, a North American origin of the Arctoidea seems an equally likely scenario. In favor of such an argument is the sister relationship between cynoids and arctoids, and the former is undoubtedly North American in origin.

The three species of *Amphicticeps* apparently form an endemic clade confined to central Asia. Their zoogeographic origin is currently unknown. *Amphicynodon* has a much higher diversity in Europe than in Asia, and phylogenetically the Asian *A. teilhardi* seems to be nested within the European congeneric species, indicating an eastward dispersal for this group and linking the European ''Grande Coupure'' and the Asian ''Mongolian Reconstruction'' events as land connection began to form between Asia and Europe in the early Oligocene (Meng and McKenna, 1998).

ACKNOWLEDGMENTS

We are greatly indebted to Richard H. Tedford for his unfailing generosity of his time and his knowledge of carnivoran systematics. He served as an excellent sounding board for many ideas developed in this paper, and thoroughly critiqued several drafts of this paper. A preliminary draft of this paper was also reviewed by Louis de Bonis, Harold Bryant, and Mieczysław Wolsan. We are especially grateful to the latter two reviewers for their detailed criticisms and insightful comments. We have also benefited greatly from the critical reviews by two anonymous reviewers for the latest draft of this paper.

We thank Edward Pederson and Jane Shumsky of the AMNH for their skillful preparation and casting of the basicranium of the holotype of *Amphicticeps shackelfordi* and other relevant specimens. Howell Thomas, Theodore Conner, and Norman Rosenfeld of the Natural History Museum of Los An-

geles County made additional preparations and casting of many comparative materials. We thank the following individuals for their permission to access collections under their care: Louis de Bonis (Université du Poitiers), Burkart Engesser (Naturhistorisches Museum Basel), Meng Jin and Richard Tedford (American Museum of Natural History), Michael Morlo and Doris Nagel (joint Austrian–Mongolian collection in Museum of Natural History of Vienna), Qiu Zhanxiang and Wang Banyue (Institute of Vertebrate Paleontology and Paleoanthropology), Alexander Averianov (Institute of Paleontology, Russian Academy of Sciences), and Mieczysław Wolsan (Institute of Paleobiology, Polish Academy of Sciences).

Field work for securing the new materials and for the new synthesis of the stratigraphic relationships, by the joint Mongolian Academy of Sciences–American Museum of Natural History Paleontological Expeditions, was funded by the Frick Laboratory Endowment Fund of the AMNH, Philip McKenna Foundation, National Geographic Society, and by the National Science Foundation (DEB-9300770 to M. Novacek and others). We gratefully acknowledge funding for travels and research by X. Wang from the National Science Foundation (EAR-0446699, DEB-9420004, and DEB-9707555), Chinese National Natural Science Foundation (Nos. 40232023 and 40128004), and National Geographic Society (Nos. 6004–97 and 6771–00).

REFERENCES

Antón, M., M.J. Salesa, J.F. Pastor, I.M. Sánchez, S. Fraile, and J. Morales. 2004. Implications of the mastoid anatomy of larger extant felids for the evolution and predatory behaviour of sabretoothed cats (Mammalia, Carnivora, Felidae). Zoological Journal of the Linnean Society 140(2): 207–222.

Babbitt, C. 1999. *Pyctis inamatus*, gen. et sp. nov., a new mustelid from the Hsanda Gol Formation, Oligocene, Mongolia. Journal of Vertebrate Paleontology 19(4): 791–792.

Baskin, J.A. 1982. Tertiary Procyoninae (Mammalia: Carnivora) of North America. Journal of Vertebrate Paleontology 2(1): 71–93.

Baskin, J.A. 1989. Comments on New World Tertiary Procyonidae (Mammalia: Carnivora). Journal of Vertebrate Paleontology 9(1): 110–117.

Baskin, J.A. 1998a Mustelidae. *In* C.M. Janis, K.M. Scott, and L.L. Jacobs (editors), Evolution of Tertiary mammals of North America, Volume 1: Terrestrial carnivores, ungulates, and ungulatelike mammals: 152–173. Cambridge: Cambridge University Press.

Baskin, J.A. 1998b. Procyonidae. *In* C.M. Janis, K.M. Scott, and L.L. Jacobs (editors), Evolution of Tertiary mammals of North America, Volume 1: Terrestrial carnivores, ungulates, and ungulatelike mammals: 144–151. Cambridge: Cambridge University Press.

Baskin, J.A., and R.H. Tedford. 1996. Small arctoid and feliform carnivorans. *In* D.R. Prothero, and R.J. Emry (editors), The terrestrial Eocene—Oligocene transition in North America, Pt. II: Common vertebrates of the White River chronofauna: 486–497. Cambridge: Cambridge University Press.

Beaumont, G.d. 1964. Essai sur la position taxonomique des genres *Alopecocyon* Viret et *Simocyon* Wagner (Carnivora). Eclogae Geologicae Helvetiae 57: 829–836.

Beaumont, G.d. 1965. Contribution à l'Étude du genre *Cephalogale* Jourdan (Carnivora). Schweizerische Paläontologische Abhandlungen 82: 1–34.

Beaumont, G.d. 1968a. Note sur la région auditive de quelques carnivores. Archives des Sciences (Geneva) 21: 213–223.

Beaumont, G.d. 1968b. Note sur l'ostéologie crânienne de *Plesiogale* Pomel (Mustelidae, Carnivora). Archives des Sciences (Geneva) 21(1): 27–34.

Berggren, W.A., D.V. Kent, J.D. Obradovich, and C.C. Swisher, III. 1992. Toward a revised Paleogene geochronology. *In* D.R. Prothero, and W.A. Berggren (editors), Eocene–Oligocene climatic and biotic evolution: 29–45. Princeton, NJ: Princeton University Press.

Berkey, C.P., and W. Granger. 1923. Later sediments of the desert basins of central Mongolia. American Museum Novitates 77: 1–16.

Berkey, C.P., and F.K. Morris. 1927. Geology of Mongolia. Reconnaissance report based on the investigations of the years 1922–1923. Natural History of Central Asia, vol. II. New York: American Museum of Natural History, 475 pp.

Berta, A. 1987. Origin, diversification, and zoogeography of the South American Canidae. *In* B.D. Patterson and R.M. Timm (editors), Studies in Neotropical mammalogy: essays in honor of Philip Hershkovitz, Fieldiana Zoology, n. ser. 39: 455–471.

Berta, A. 1988. Quaternary evolution and biogeography of the large South American Canidae

(Mammalia: Carnivora). University of California Publications in Geological Science 132: 1–149.

Berta, A., and P.J. Adam. 2001. Evolutionary biology of pinnipeds. *In* J.-M. Mazin, and V.d. Buffrénil (editors), Secondary adaptation of tetrapods to life in water: 235–260. München: Verlag Dr. Friedrich Pfeil.

Berta, A., and A.R. Wyss. 1994. Pinniped phylogeny. *In* A. Berta and T.A. Deméré (editors), Contributions in marine mammal paleontology honoring Frank C. Whitmore, Jr., Proceedings of the San Diego Society of Natural History: 33–56.

BiochroM'97. 1997. Paleogene biochronology. *In* J.-P. Aguilar, S. Legendre, and J. Michaux (editors), Actes du Congrès BiochroM'97, Memoires et Travaux de l'EPHE 21: 769–805. Montpellier: Institut de Montpellier.

Bonis, L.d. 1971. Deux nouveaux carnassiers des Phosphorites du Quercy. Annales de Paléontologie 57: 117–127.

Bonis, L.d. 1973. Contribution à l'étude des Mammifères de l'Aquitanien de l'Agenais, rongeurs-carnivores-perissodactyles. Mémoires du Muséum National d'Histoire Naturelle Nouvelle Série 28: 1–192.

Bonis, L.d. 1997. Précisions sur l'âge géologique et les relations phylétiques de *Mustelictis oliveri* nov. sp. (Carnivora, Mustelidae), carnassier de l'Oligocène inférieur (MP 22) des Phosphorites du Quercy (France). Geobios 20: 55–60.

Bryant, H.N., A.P. Russell, and W.D. Fitch. 1993. Phylogenetic relationships within the extant Mustelidae (Carnivora): appraisal of the cladistic status of the Simpsonian subfamilies. Zoological Journal of the Linnean Society 108: 301–334.

Bryant, J.D., and M.C. McKenna. 1995. Cranial anatomy and phylogenetic position of *Tsaganomys altaicus* (Mammalia, Rodentia) from the Hsanda Gol Formation (Oligocene), Mongolia. American Museum Novitates 3156: 1–42.

Cirot, E. 1992. Étude phylogénétique de quelques genres d'Arctoidea de l'Oligocène Eurasiatique, comparaison des données morphologiques et moléculaires. Ph.D. thesis, Université de Poitiers, Poitiers, 152 pp.

Cirot, E., and L.d. Bonis. 1992. Révision du genre *Amphicynodon*, carnivore de l'Oligocène. Palaeontographica Abteilung A 220: 103–130.

Cirot, E., and L.d. Bonis. 1993. Le crâne d'*Amphictis ambiguus* (Carnivora, Mammalia): son importance pour la compréhension de la phylogénie des mustéloïdes. Comptes Rendus de l'Académie des Sciences Paris 316: 1327–1333.

Clark, J. 1937. The stratigraphy and paleontology of the Chadron Formation in the Big Badlands of South Dakota. Annals of Carnegie Museum 25: 261–350.

Clark, J., and T.E. Guensburg. 1972. Arctoid genetic characters as related to the genus *Paractis*. Fieldiana Geology 26(1): 1–71.

Crusafont-Pairó, M. 1950. El primer representante del género *Canis* en el Pontiense eurasiatico (*Canis cipio* nova sp.). Boletin de la Real Sociedad Española de Historia Natural Seccion Geologica 48: 43–51.

Dalrymple, G.B. 1979. Critical tables for conversion of K-Ar ages from old to new constants. Geology 7: 558–560.

Dashzeveg, D. 1996. Some carnivorous mammals from the Paleogene of the eastern Gobi Desert, Mongolia, and the application of Oligocene carnivores to stratigraphic correlation. American Museum Novitates 3179: 1–14.

Daxner-Höck, G. 2000. *Ulaancricetodon badamae* n. gen., n. sp. (Mammalia, Rodentia, Cricetidae) from the Valley of Lakes in Central Mongolia. Paläontologische Zeitschrift 74(1/2): 215–225.

Daxner-Höck, G. 2001. New zapodids (Rodentia) from Oligocene–Miocene deposits in Mongolia, Part 1. Senckenbergiana Lethaea 81(2): 359–389.

Daxner-Höck, G., V. Höck, D. Badamgarav, G. Furtmüller, W. Frank, O. Montag, and H.P. Schmid. 1997. Cenozoic stratigraphy based on a sediment-basalt association in central Mongolia as requirement for correlation across central Asia. *In* J.-P. Aguilar, S. Legendre, and J. Michaux (editors), Actes du Congrès BiochroM'97, Memoires et Travaux de l'EPHE, 21: 163–176. Montpellier: Insitut de Montpellier.

Daxner-Höck, G., and W.-y. Wu. 2003. *Plesiosminthus* (Zapodidae, Mammalia) from China and Mongolia: migrations to Europe. *In* J.W.F. Reumer, and W. Wessels (editors), Distribution and migration of Tertiary mammals in Eurasia. A volume in honour of Hans de Bruijn, Deinsea 10: 127–151.

Dayan, M., D. Simberloff, E. Tchernov, and Y. Yom-Tov. 1992. Canine carnassials: character displacement in the wolves, jackals, and foxes of Israel. Biological Journal of Linnean Society 45: 315–331.

Dayan, M., E. Tchernov, Y. Yom-Tov, and D. Simberloff. 1989. Ecological character displacement in Saharo-Arabian Vuples: outfoxing Bergmann's rule. Oikos 55: 263–272.

Dehm, R. 1950. Die Raubtiere aus dem Mittel-Miocän (Burgidalium) von Wintershof-West bei Eichstätt in Bayern. Bayerische Akademie der Wissenschaften Mathematisch-Naturwis-

senschaftliche Klasse Abhandlungen, N. F. 58: 1–141.

Dragoo, J.W., and R.L. Honeycutt. 1997. Systematics of mustelid-like carnivores. Journal of Mammalogy 78(2): 426–443.

Ducrocq, S. 1993. Mammals and stratigraphy in Asia: is the Eocene–Oligocene boundary at the right place? Comptes Rendus de l'Académie des Sciences Paris 316: 419–426.

Erbajeva, M.A., and G. Daxner-Höck. 2001. Paleogene and Neogene lagomorphs from the Valley of Lakes, Central Mongolia. Lynx (Prague), n. s. 32: 55–65.

Evans, H.E., and G.C. Christensen. 1979. Miller's anatomy of the dog. Philadelphia: W. B. Saunders, 1181 pp.

Evernden, J.F., D.E. Savage, G.H. Curtis, and G.T. James. 1964. Potassium-argon dates and the Cenozoic mammalian chronology of North America. American Journal of Science 262: 145–198.

Flynn, J.J., and M.A. Nedbal. 1998. Phylogeny of the Carnivora (Mammalia): congruence vs. incompatibility among multiple data sets. Molecular Phylogenetics and Evolution 9(3): 414–426.

Flynn, J.J., M.A. Nedbal, J.W. Dragoo, and R.L. Honeycutt. 2000. Whence the Red Panda. Molecular Phylogenetics and Evolution 17(2): 190–199.

Flynn, J.J., N.A. Neff, and R.H. Tedford. 1988. Phylogeny of the Carnivora. *In* M.J. Benton (editor), The phylogeny and classification of the tetrapods, vol. 2: Mammals, Systematics Association Special Volume 35B: 73–116. Oxford: Clarendon Press.

Fraas, O. 1870. Die Fauna von Steinheim. Mit Rüchsicht auf die Miocänen Säugethier- und Vogelreste des Steinheimer Beckens. Jahreshefte des Vereins für Vaterländische Naturkunde in Württemberg 26: 145–306.

Gabuniya, L.K.E.V.D., and M.M. Rubinshtein. 1975. Data on the absolute age of Cenozoic continental deposits of Asia and their biostratigraphic significance. Doklady Akademii Nauk SSSR 225(4): 895–898.

Gauthier, J.A., A.G. Kluge, and T. Rowe. 1988. Amniote phylogeny and the importance of fossils. Cladistics 4: 105–209.

Geisler, J.H. 2004. Humeri of *Oligoscalops* (Proscalopidae, Mammalia) from the Oligocene of Mongolia. *In* G.C. Gould and S.K. Bell (editors), Tributes to Malcolm C. McKenna: his students, his legacy. Bulletin of the American Museum of Natural History 285: 166–176.

Ginsburg, L. 1961. La faune des carnivores Miocènes de Sansan (Gers). Mémoires du Muséum National d'Histoire Naturelle Série C Geologie 9: 1–187.

Ginsburg, L. 1982. Sur la position systématique du petit panda, *Ailurus fulgens* (Carnivora, Mammalia). Geobios Mémoire Spécial 6: 247–258.

Ginsburg, L. 1999. Order Carnivora. *In* G.E. Rössner and K. Heissig (editors), The Miocene land mammals of Europe: 109–148. München: Verlag Dr. Friedrich Pfeil.

Ginsburg, L., O. Maridet, and P. Mein. 2001. Un Ailurinae (Mammalia, Carnivora, Ailuridae) dans le Miocène moyen de Four (Isère, France). Geodiversitas 23(1): 81–85.

Ginsburg, L., and J. Morales. 1992. Contribution à la connaissance des Mustélidés (Carnivora, Mammalia) du Miocène d'Europe *Trochictis* et *Ischyrictis*, genres affines et genres nouveaux. Comptes Rendus de l'Académie des Sciences 315(2): 111–116.

Ginsburg, L., and J. Morales. 1995. *Zaragocyon daamsi* n. gen. sp. nov., Ursidae primitif du Miocène inférieur d'Espagne. Comptes Rendus de l'Académie des Sciences 321: 811–815.

Helbing, H. 1930. Zwei oligocaene Musteliden (*Plesictis genettoïdes* Pomel. *Palaeogale angustifrons* Pomel). Abhandlungen der Schweizerischen Palaeontologischen Gesellschaft 50(3): 1–36.

Höck, V., G. Daxner-Höck, H.P. Schmid, D. Badamgarav, W. Frank, G. Furtmüller, O. Montag, R. Barsbold, Y. Khand, and J. Sodov. 1999. Oligocene–Miocene sediments, fossils and basalts from the Valley of Lakes (Central Mongolia), An integrated study. Mitteilungen der Österreichischen Geologischen Gesellschaft 90(1997): 83–125.

Hough, J.R. 1944. The auditory region in some Miocene carnivores. Journal of Paleontology 22: 573–600.

Hough, J.R. 1948. The auditory region in some members of the Procyonidae, Canidae, and Ursidae. Bulletin of the American Museum of Natural History 92: 73–118.

Huang, X.-s. 1993. Note on some carnivorous remains from the middle Oligocene of Ulantatal, Nei Mongol. Vertebrata PalAsiatica 31(4): 294–303.

Hunt, R.M., Jr. 1974. The auditory bulla in Carnivora: an anatomical basis for reappraisal of carnivore evolution. Journal of Morphology 143: 21–76.

Hunt, R.M., Jr. 1977. Basicranial anatomy of *Cynelos* Jourdan (Mammalia: Carnivora), an Aquitanian amphicyonid from the Allier Basin, France. Journal of Paleontology 51: 826–843.

Hunt, R.M., Jr. 1996a. Amphicyonidae. *In* D.R. Prothero and R.J. Emry (editors), The terrestrial

Eocene–Oligocene transition in North America: 476–485. Cambridge: Cambridge University Press.

Hunt, R.M., Jr. 1996b. Biogeography of the Order Carnivora. *In* J.L. Gittleman (editor), Carnivore behavior, ecology, & evolution 2: 485–541. Ithaca, NY: Cornell University Press.

Hunt, R.M., Jr. 1998a. Amphicyonidae. *In* C.M. Janis, K.M. Scott, and L.L. Jacobs (editors), Evolution of Tertiary mammals of North America, Volume 1: Terrestrial carnivores, ungulates, and ungulatelike mammals: 196–227. Cambridge: Cambridge University Press.

Hunt, R.M., Jr. 1998b. Evolution of the aeluroid Carnivora: diversity of the earlier aeluroids from Eurasia (Quercy, Hsanda-Gol) and the origin of felids. American Museum Novitates 3252: 1–65.

Hunt, R.M., Jr. 1998c Ursidae. *In* C.M. Janis, K.M. Scott, and L.L. Jacobs (editors), Evolution of Tertiary mammals of North America, Volume 1: Terrestrial carnivores, ungulates, and ungulatelike mammals: 174–195. Cambridge: Cambridge University Press.

Hunt, R.M., Jr. 2001. Small Oligocene amphicyonids from North America (*Paradaphoenus*, Mammalia, Carnivora). American Museum Novitates 3331: 1–20.

Hunt, R.M., Jr., and L.G. Barnes. 1994. Basicranial evidence for ursid affinity of the oldest pinnipeds. *In* A. Berta and T.A. Deméré (editors), Contributions in marine mammal paleontology honoring Frank C. Whitmore, Jr., Proceedings of the San Diego Society of Natural History: 57–67. San Diego.

Hunt, R.M., Jr., and R.H. Tedford. 1993. Phylogenetic relationships within the aeluroid Carnivora and implications of their temporal and geographic distribution. *In* F.S. Szalay, M.J. Novacek, and M.C. McKenna (editors), Mammal phylogeny: Placentals: 52–73. New York: Springer-Verlag.

Janovskaja, N.M. 1970. New cynodictines from the middle Oligocene of Mongolia and Kazakhstan and the evolution of Carnivora of the subfamily Canidae. Materialy po Evolyutsii Nazemnykh Pozvonochnikh: 71–84.

Kellner, A.W.A., and M.C. McKenna. 1996. A leptictid mammal from the Hsanda Gol Formation (Oligocene), central Mongolia, with comments on some Palaeoryctidae. American Museum Novitates 3168: 1–13.

Kotsakis, T. 1980. Revisione sistematica e distribuzione stratigrafica e geografica del genere *Cynodictis* Bravard & Pomel (Carnivora, Mammalia). Bolletino della Società Paleontologica Italiana 19(2): 259–273.

Kowalski, K. 1974. Results of the Polish-Mongolian Palaeontological Expeditions—Part V. Middle Oligocene rodents from Mongolia. Palaeontologia Polonica 30: 147–178.

Kuss, S.E. 1965. Revision der europäischen Amphicyoninae (Canidae, Carnivora, Mamm.) ausschließlich der voroberstampischen Formen. Sitzungsberichte der Heidelberger Akademie der Wissenschaften 1: 1–168.

Lange-Badré, B. 1970. *Mustelictis piveteaui*, mustélidé nouveau des Phosphorites du Quercy. Annales de Paléontologie (Vertébrés) 56: 73–91.

Lange-Badré, B., and D. Dashzeveg. 1989. On some Oligocene carnivorous mammals from Central Asia. Acta Palaeontologica Polonica 34: 125–148.

Ledje, C., and U. Arnason. 1996a. Phylogenetic analyses of complete cytochrome *b* genes of the order Carnivora with particular emphasis on the Caniformia. Journal of Molecular Evolution 42: 135–144.

Ledje, C., and U. Arnason. 1996b. Phylogenetic relationships within caniform carnivores based on analyses of the mitochondrial 12S rRNA gene. Journal of Molecular Evolution 43: 641–649.

Lévêque, F. 1993. Correlating the Eocene–Oligocene mammalian biochronological scale from SW Europe with the marine magnetic anomaly sequence. Journal of the Geological Society, London 150: 661–664.

Li, C.-k., and S.-y. Ting. 1983. The Paleogene mammals of China. Bulletin of Carnegie Museum of Natural History 21: 1–98.

Matthew, W.D. 1924. Third contribution to the Snake Creek fauna. Bulletin of the American Museum of Natural History 50: 59–210.

Matthew, W.D., and W. Granger. 1924. New Carnivora from the Tertiary of Mongolia. American Museum Novitates 104: 1–9.

McKenna, M.C. 1995. Biostratigraphy of the type Hsanda Gol Formation, Oligocene of Mongolia. Journal of Vertebrate Paleontology 15(suppl. 3): 42A.

McKenna, M.C., and S.K. Bell. 1997. Classification of mammals above the species level. New York: Columbia University Press.

McKenna, M.C., D. Dashzeveg, and J.D. Bryant. MS. Hsanda Gol Formation and Loh Formation, Oligocene and Miocene, Valley of Lakes, Mongolia.

McLaren, I.A. 1960. Are the Pinnipedia biphyletic? Systematic Zoology 9: 18–28.

Mellett, J.S. 1968. The Oligocene Hsanda Gol Formation, Mongolia: a revised faunal list. American Museum Novitates 2318: 1–16.

Meng, J., and M.C. McKenna. 1998. Faunal turn-

overs of Palaeogene mammals from the Mongolian Plateau. Nature 394: 364–367.
Mitchell, E., and R.H. Tedford. 1973. The Enaliarctinae a new group of extinct aquatic Carnivora and a consideration of the origin of the Otariidae. Bulletin of the American Museum of Natural History 151: 203–284.
Mödden, C. 1991. *Bavarictis gaimersheimensis* n. gen. n. sp., ein früher Mustelide aus der oberoligozänen Spaltenfüllung Gaimersheim bei Ingolstadt. Mitteilungen der Bayerischen Staatssammlung für Paläontologie und Historische Geologie 31: 125–147.
Muizon, C.d. 1982. Les relations phylogénétiques des Lutrinae (Mustelidae, Mammalia). Geobios Mémoire Spécial 6: 259–277.
Nagel, D., and M. Morlo. 2001. The endemic carnivorous fauna from the Oligocene of Taatsiin Gol—Creodonta and Carnivora. Conference on Distribution and Migration of Tertiary Mammals in Eurasia in Honor of Hans de Buijn: 38.
Nagel, D., and M. Morlo. 2003. Guild structure of the carnivorous mammals (Creodonta, Carnivora) from the Taatsiin Gol area, Lower Oligocene of Central Mongolia. *In* J.W.F. Reumer, and W. Wessels (editors), Distribution and migration of Tertiary mammals in Eurasia. A volume in honour of Hans de Bruijn, Deinsea 10: 419–429.
Orlov, Y.A. 1933. *Semantor macrurus* (Ordo Pinnipedia, Fam. Semantoridae fam. nova) aus den Neogen-Ablagerungen Westsibiriens. Travaux de l'Institut Paléozoologique, Académie des Sciences, URSS 2: 165–268.
Petter, G. 1967. *Paragale hürzeleri* nov. gen., nov. sp., Mustélidé nouveau de l'Aquitanien de l'Allier. Bulletin de la Société Géologique de France, Série 7, 9: 19–23.
Piveteau, J. 1961. Traité de paléontologie, Tome VI, Vol. I, L'origine des mammifères et les aspects fondamentaux de leur évolution. Paris: Brodard-Taupin Imprimeur-Relieur, 1138 pp.
Prothero, D.R., and C.C. Swisher, III. 1992. Magnetostratigraphy and geochronology of the terrestrial Eocene–Oligocene transition in North America. *In* D.R. Prothero and W.A. Berggren (editors), Eocene–Oligocene climatic and biotic evolution: 46–73. Princeton, NJ: Princeton University Press.
Qiu, Z.-x., and N. Schmidt-Kittler. 1982. On the phylogeny and zoogeography of the leptarctines (Carnivora, Mammalia). Paläontologische Zeitschrift 56: 131–145.
Radinsky, L. 1973. Are stink badgers skunks? Implications of neuroanatomy for mustelid phylogeny. Journal of Mammalogy 54(3): 585–593.
Riggs, E.S. 1942. Preliminary description of two lower Miocene carnivores. Field Museum of Natural History Geological Series 7: 59–62.
Riggs, E.S. 1945. Some early Miocene carnivores. Field Museum of Natural History Geological Series 9(3): 69–114.
Russell, D.E., and R.-j. Zhai. 1987. The Paleogene of Asia: mammals and stratigraphy. Mémoires du Muséum National d'Histoire Naturelle, Série C, Sciences de la Terre 52: 1–488.
Savage, R.J.G. 1957. The anatomy of *Potamotherium*, an Oligocene lutrine. Proceedings of the Zoological Society of London 129: 151–244.
Schmidt-Kittler, N. 1981. Zur Stammesgeschichte der marderverwandten Raubtiergruppen (Musteloidea, Carnivora). Eclogae Geologicae Helvetiae 74: 753–801.
Schmidt-Kittler, N. 1989. A biochronologic subdivision of the European Paleogene based on mammals—report on results of the Paleogene Symposium held in Mainz in February 1987. *In* E.H. Lindsay, V. Fahlbusch, and P. Mein (editors), European Neogene mammal chronology, NATO (Advanced Science Institute) Series A: Life Sciences 180: 47–50. New York: Plenum Press.
Scott, W.B., and G.L. Jepsen. 1936. The mammalian fauna of the White River Oligocene. Princeton University Bulletin 28: 1–980.
Segall, W. 1943. The auditory region of the arctoid carnivores. Field Museum of Natural History Zoological Series 29(3): 33–59.
Simpson, G.G. 1945. The principles of classification and a classification of mammals. Bulletin of the American Museum of Natural History 8: 1–350.
Story, H.E. 1951. The carotid arteries in the Procyonidae. Fieldiana: Zoology 32: 477–557.
Swisher, C.C., III, and D.R. Prothero. 1990. Single-crystal 40Ar/39Ar dating of the Eocene–Oligocene transition in North America. Science 249: 760–762.
Swofford, D.L. 1993. Phylogenetic analysis using parsimony (PAUP), version 3. 1.1. Urbana: Illinois Natural History Survey.
Tedford, R.H. 1976. Relationship of pinnipeds to other carnivores (Mammalia). Systematic Zoology 25: 363–374.
Tedford, R.H. 1978. History of dogs and cats: a view from the fossil record. Nutrition and Management of Dogs and Cats: chap. M23. St. Louis: Ralston Purina Co.
Tedford, R.H., L.G. Barnes, and C.E. Ray. 1994. The early Miocene littoral ursoid carnivoran Kolponomos: systematics and mode of life. *In* A. Berta and T.A. Deméré (editors), Contributions in marine mammal paleontology honoring Frank C. Whitmore, Jr.: 11–32. San Diego: San Diego Society of Natural History.

Tedford, R.H., B.E. Taylor, and X. Wang. 1995. Phylogeny of the Caninae (Carnivora: Canidae): the living taxa. American Museum Novitates 3146: 1–37.

Teilhard de Chardin, P. 1915. Les carnassiers des Phosphorites du Quercy. Annales de Paléontologie 9: 101–191.

Tsubamoto, T., M. Takai, and N. Egi. 2004. Quantitative analyses of biogeography and faunal evolution of middle to late Eocene mammals in East Asia. Journal of Vertebrate Paleontology 24(3): 657–667.

Viranta, S. 1996. European Miocene Amphicyonidae—taxonomy, systematics and ecology. Acta Zoologica Fennica 204: 1–61.

Viret, J. 1951. Catalogue critique de la faune des mammifères miocènes de la Grive Saint-Alban. Nouvelles Archives du Muséum d'Histoire Naturelle de Lyon 3: 1–104.

Vislobokova, I.A., and G. Daxner-Höck. 2002. Oligocene–early Miocene ruminants from the Valley of Lakes (Central Mongolia). Annalen des Naturhistorischen Museums in Wien 103(A): 213–235.

Vrana, P.B., M.C. Milinkovitich, J.R. Powell, and W.C. Wheeler. 1994. Higher level relationships of the arctoid Carnivora based on sequence data and ''total evidence''. Molecular Phylogenetics and Evolution 3: 47–58.

Wallace, S.C., and X. Wang. 2004. Two new carnivores from an unusual late Tertiary forest biota in eastern North America. Nature 431: 556–559.

Wang, B.-y. 1992. The Chinese Oligocene: a preliminary review of mammalian localities and local faunas. *In* D.R. Prothero and W.A. Berggren (editors), Eocene–Oligocene climatic and biotic evolution: 529–547. Princeton, NJ: Princeton University Press.

Wang, B.-y. 2001. On Tsaganomyidae (Rodentia, Mammalia) of Asia. American Museum Novitates 3317: 1–32.

Wang, B.-y., and Z.-x. Qiu. 2003a. Notes on early Oligocene ursids (Carnivora, Mammalia) from Saint Jacques, Nei Mongol, China. *In* L.J. Flynn (editor), Vertebrate fossils and their context: contributions in honor of Richard H. Tedford. Bulletin of the American Museum of Natural History 279: 116–124.

Wang, X. 1994. Phylogenetic systematics of the Hesperocyoninae (Carnivora: Canidae). Bulletin of the American Museum of Natural History 221: 1–207.

Wang, X. 1997. New cranial material of *Simocyon* from China, and its implications for phylogenetic relationship to the red panda (*Ailurus*). Journal of Vertebrate Paleontology 17: 184–198.

Wang, X., and Z.-x. Qiu. 2003b. A primitive leptarctine (Carnivora: Mustelidae) from the early Miocene of western Gansu, China and zoogeography of early mustelids. Journal of Vertebrate Paleontology 23(suppl. 3): 107A.

Wang, X., and Z.-x. Qiu. 2004. Late Miocene *Promephitis* (Carnivora, Mephitidae) from China. Journal of Vertebrate Paleontology 24(3): 721–731.

Wang, X., Z.-x. Qiu, and B.-y. Wang. 2004. A new leptarctine (Carnivora: Mustelidae) from the early Miocene of the northern Tibetan plateau and implications of the phylogeny and zoogeography of basal mustelids. Zoological Journal of the Linnean Society 142: 405–421.

Wang, X., and R.H. Tedford. 1992. The status of genus *Nothocyon* Matthew, 1899 (Carnivora): an arctoid not a canid. Journal of Vertebrate Paleontology 12: 223–229.

Wang, X., and R.H. Tedford. 1994. Basicranial anatomy and phylogeny of primitive canids and closely related miacids (Carnivora: Mammalia). American Museum Novitates 3092: 1–34.

Wang, X., and R.H. Tedford. 1996. Canidae. *In* D.R. Prothero and R.J. Emry (editors), The terrestrial Eocene–Oligocene transition in North America, Pt. II: Common vertebrates of the White River Chronofauna: 433–452. Cambridge: Cambridge University Press.

Wang, X., R.H. Tedford, and B.E. Taylor. 1999. Phylogenetic systematics of the Borophaginae (Carnivora: Canidae). Bulletin of the American Museum of Natural History 243: 1–391.

Wang, X., J. Ye, J. Meng, W.-y. Wu, L.-p. Liu, and S.-d. Bi. 1998. Carnivora from middle Miocene of northern Junggar Basin, Xinjiang Autonomous Region, China. Vertebrata PalAsiatica 36(3): 218–243.

Wegner, R.N. 1913. Tertiaer und umgelagerte Kreide bei Oppeln (Oberschlesien). Palaeontographica 60: 175–272.

Werdelin, L., and N. Solounias. 1991. The Hyaenidae: taxonomy, systematics and evolution. Fossils and Strata 30: 1–104.

Wiig, O. 1983. On the relationship of pinnipeds to other carnivores. Zoologica Scripta 12(3): 225–227.

Wolsan, M. 1993. Phylogeny and classification of early European Mustelida (Mammalia: Carnivora). Acta Theriologica 38: 345–384.

Wolsan, M. 1999. Oldest mephitine cranium and its implications for the origin of skunks. Acta Palaeontologica Polonica 44(2): 223–230.

Wyss, A.R. 1987. The walrus auditory region and the monophyly of pinnipeds. American Museum Novitates 2871: 1–31.

Wyss, A.R. 1988. On ''retrogression'' in the evolution of the Phocinae and phylogenetic affini-

ties of the monk seals. American Museum Novitates 2924: 1–38.

Wyss, A.R. 1991. What, then, is *Potamotherium* (Mammalia, Carnivora)? Journal of Vertebrate Paleontology 11(suppl.): 63A.

Wyss, A.R., and J.J. Flynn. 1993. A phylogenetic analysis and definition of the Carnivora. *In* F.S. Szalay, M.J. Novacek, and M.C. McKenna (editors), Mammal phylogeny: placentals: 32–52. New York: Springer.

APPENDIX 1

Characters Scored in the Character Matrix (table 8) for PAUP Analysis

Most of these characters have been discussed and illustrated previously (e.g., Hunt, 1974; Wolsan, 1993; Wang and Tedford, 1994), although we may code them differently.

1. **Temporal crest**: 0, converge to sagittal crest; 1, parallel without a merged sagittal crest.
2. **Posterior border of palatine**: 0, short and anterior to posterior border of last upper molars; 1, elongated and posterior to posterior border of last upper molars.
3. **Alisphenoid canal**: 0, present; 1, absent.
4. **Posterior carotid foramen**: 0, within fossa for posterior lacerate foramen; 1, anterior to the fossa.
5. **Suprameatal fossa**: 0, absent or a mere depression on squamosal; 1, small; 2, dorsally deep; 3, partially covered anteriorly.
6. **Epitympanic recess**: 0, not reduced; 1, reduced.
7. **Postlateral sulcus of brain**: 0, absent; 1, present.
8. **P1**: 0, present; 1, absent.
9. **Carnassial notch on P4**: 0, present; 1, absent.
10. **P4 protocone**: 0, conical; 1, crescent.
11. **P4 lingual cingulum**: 0, absent or small; 1, enlarged; 2 enlarged to form a hypocone.
12. **M1 parastyle**: 0, large; 1, reduced.
13. **M1 anterior and posterior borders**: 0, not parallel anterior and posterior borders; 1, parallel anterior and posterior borders.
14. **M1 anterior and posterior cingula**: 0, continuous; 1, discontinuous.
15. **M2 position relative to M1**: 0, buccal; 1, lingual.
16. **M2 size**: 0, three-rooted and small; 1, reduced; 2, absent; 3, enlarged.
17. **Metaconid on m1**: 0, equal or higher than paraconid; 1, lower than paraconid; 2, absent.
18. **Entoconid on m1**: 0, poorly developed; 1, presence of a lingual notch; 2, cuspidate.
19. **Size of m2**: 0, not enlarged or reduced; 1, reduced; 2, lost; 3, enlarged.
20. **Talonid of m2**: 0, short; 1, elongated.
21. **Mastoid process**: 0, small; 1, laterally expanded; 2, ventrally expanded.
22. **Reduction of m3**: 0, m3 not reduced; 1, m3 reduced or absent.
23. **M1 postprotocrista**: 0, present; 1, absent; 2, enlarged metaconule.
24. **Paroccipital process**: 0, rodlike; 1, dorsoventrally compressed; 2, laterally compressed.
25. **Ascending ramus**: 0, reclined; 1, anteriorly inclined.
26. **Zygomatic arch**: 0, horizontally flat; 1, dorsally arched.
27. **Posterior promontorium process**: 0, absent, 1, present.
28. **M1 anteroposterior length**: 0, not shortened; 1, shortened.
29. **M1–2 postprotocrista**: 0, laterally oriented; 1, posteriorly oriented.
30. **Bullar ossification**: 0, unossified; 1, ossified bony bulla.
31. **Bullar composition of Hunt** (1974): 0, type A; 2, type B.
32. **Premolar accessary cusps**: 0, well developed; 1, absent or poorly developed.
33. **P4 protocone**: 0, anterorly positioned; 1, posteriorly positioned.
34. **Posterior orbital constriction**: 0, short; 1, long.
35. **Position of internal carotid artery**: 0, transpromontorial; 1, medial.
36. **Petrosal**: 0, isolated from basioccipital and basisphenoid; 1, medially expanded to fuse with basioccipital and basisphenoid.
37. **Semi-septum of bulla**: 0, absent; 1, present.
38. **M3**: 0, present; 1, absent.
39. **Basioccipital**: 0, not broadened; 1, broadened between bullae.

Complete lists of all issues of the *Novitates* and the *Bulletin* are available at World Wide Web site http://library.amnh.org/pubs. Inquire about ordering printed copies via e-mail from scipubs@amnh.org or via standard mail from: American Museum of Natural History, Library—Scientific Publications, Central Park West at 79th St., New York, NY 10024. TEL: (212) 769-5545. FAX: (212) 769-5009.

♾ This paper meets the requirements of ANSI/NISO Z39.48-1992 (Permanence of Paper).